Universidade de Aveiro
Ano 2012/2013

Departamento de Eletrónica,
Telecomunicações e Informática

Gustavo Miranda Castilho dos Anjos

MIMO Processing Techniques for 4G Systems

Técnicas de Processamento MIMO para Sistemas 4G

Universidade de Aveiro
Ano 2012/2013

Departamento de Eletrónica,
Telecomunicações e Informática

Gustavo Miranda Castilho dos Anjos

MIMO Processing Techniques for 4G Systems

Técnicas de Processamento MIMO para Sistemas 4G

Dissertação apresentada à Universidade de Aveiro para cumprimento dos requisitos necessários à obtenção do grau de Mestre em Engenharia Eletrónica e Telecomunicações, realizada sob a orientação científica do Doutor Adão Paulo Soares da Silva, Professor auxiliar do Departamento de Eletrónica, Telecomunicações e Informática da Universidade de Aveiro; e do Doutor Atílio Manuel da Silva Gameiro, Professor associado do Departamento de Eletrónica, Telecomunicações e Informática da Universidade de Aveiro.

A todos aqueles cuja influência me ajudou a chegar até aqui

o júri

presidente

Prof. DoutorRui Luis Andrade Aguiar
professor associado c/agregação da Universidade de Aveiro

Prof. Doutor Carlos Miguel Nogueira Gaspar Ribeiro
professor adjunto do Instituto Politécnico de Leiria

Prof. Doutor Adão Paulo Soares da Silva
professor auxiliar da Universidade de Aveiro

agradecimentos

Em primeiro lugar aos meus pais pelo apoio e orientação dados ao longo da vida.

Em segundo, ao professor Adão Silva pela orientação, disponibilidade e interesse que sempre demonstrou ao longo do trabalho.

Ao José Assunção do Instituto de Telecomunicações pela ajuda prestada durante o desenvolvimento da plataforma de simulação.

A todos os professores pelos ensinamentos dados durante a minha formação, desde a entrada na escola primária até á finalização do mestrado.

palavras-chave

4G, LTE, MIMO, Diversidade, Multiplexagem Espacial, Beamforming, OFDM, Propagação Multipercurso, Correlação Espacial, Pré-Codificação e Equalização.

resumo

O tema deste trabalho de dissertação visa uma das tecnologias chave especificada nos últimos standards 4G para o sector das comunicações móveis, que são os sistemas MIMO. Neste contexto, o acrónimo MIMO é usado para referenciar um sistema de comunicação que faz uso de múltiplas antenas, assim, usando este tipo de sistemas conjuntamente com técnicas de processamento de sinal apropriadas, podemos usar a dimensão espacial de forma a gerar ganhos de multiplexagem, diversidade e beamforming.

O objetivo deste trabalho é mostrar que tipo de processamento de sinal deve ser feito de forma a gerar cada um dos ganhos acima referidos, assim como as condições de canal em que estes podem ser maximizados. Para além da apresentação dos fundamentos teóricos relacionados com este tipo de técnicas, iremos apresentar os modos de transmissão MIMO especificados para o 4G-LTE, tendo não só como objectivo observar o tipo de constrangimentos prácticos inerentes a uma implementação real, mas também observar o tipo de soluções usadas para fazer face a esses mesmos constrangimentos.

Na parte final do trabalho é apresentada uma plataforma de simulação implementada para um dos modos de multiplexagem espacial especificados no LTE, ou seja o modo 4. Os resultados numéricos obtidos permitiram constatar a vantagem em usar equalizadores SIC em modos de transmissão multi-camada, assim como também nos permitiu observar as limitações de performance inerentes á transmissão através de um canal com elevada correlação espacial. Usando várias matrizes de pré-codificação especificadas no LTE para este modo, conseguimos perceber a importância que a escolha de uma correcta pré-codificação tem no melhoramento de desempenho da transmissão neste tipo de canais. Para além das observações referidas acima, também podemos verificar o custo em termos de diversidade inerente ao aumento do ganho de multiplexagem.

keywords 4G, LTE, MIMO, Diversity, Spatial Multiplexing, Beamforming, OFDM, Multipath Propagation, Spatial Correlation, Precoding, and Equalization

abstract

The theme of this dissertation work is focused in one of the key technologies specified in the last 4G cellular standards, which are the MIMO systems. In this context, the MIMO (Multiple Input Multiple Output) acronym is used to define a communication system where multiple antennas are used, therefore using this type of systems jointly with specific signal processing techniques, we can use the spatial dimension in order to generate multiplexing, diversity and beamforming gains.

The aim of this work is to show the type of signal processing techniques that must be applied in order to achieve the gains referenced above, as well the optimal channel conditions in which these gains are maximized.Therefore, beyond the presentation of the theoretical background related with these type of techniques, we will present the MIMO transmission modes specified on 4G-LTE, having not only the aiming of show the type of practical constraints verified in a practical implementation, but also present the solutions used to solve that kind of constraints.

In the last part of this work is presented a simulation platform implemented for one of the spatial multiplexing modes specified on LTE, which is the mode 4. The numerical results obtained allowed to see the advantage in the use of SIC (Successive Interference Cancelation) equalizers for multi-layer transmission modes, as well as the performance limitations related with the transmission through a channel where high spatial correlation conditions are verified. With the use of multiple precoding matrices, we understand the importance of perform a correct precoding selection in order to improve the transmission through a channel with this type of conditions.Beyond the observations referred above, we also saw the diversity cost related with the increase of spatial multiplexing gain.

Table of Contents

List of Acronyms

AWGN Added White Gaussian Noise

AUC Authentication Center

ARQ Automatic Repeat Request

BER Bit Error Rate

CS Circuit Switch

CSI Channel State Information

CRS Cell specific Reference Signal

CQI Channel Quality Indicator

CDMA Code Division Multiple Access

DAC Digital Analogue Converter

DFT Discrete Fourier Transform

DW Downlink

ETSI European Telecommunications Standards Institute

EGC Equal Gain Combining

E-UTRA Evolved UTRA

E-UTRAN Evolved UTRAN

EPC Evolved Packet System

FDD Frequency Division Duplexing

FEC Forward Error Correcting

FSTD Frequency Shift Transmit Diversity

FDMA Frequency Division Multiple Access

GSM Global System Mobile communications

GPRS General Packet Radio Service

HSPA High Speed Packet Access

HSS Home Subscriber Server

H-ARQ Hybrid ARQ

IRC Interference Rejection Combining

ITU-R International Telecommunications Union – Radio sector

IMT-A International Mobile Telecommunications – Advanced

IFFT Inverse Fast Fourier Transform

IDFT Inverse Discrete Fourier Transform

IP Internet Protocol

LD-CDD Large Delay-Cyclic Delay Diversity

MIMO Multiple Input Multiple Output

MU-MIMO Multiuser MIMO

MRC Maximum Ratio Combining

MF Match Filter

MCS Modulation Coding Scheme

MMSE Minimum Mean Square Error

MME Mobility Management Entity

MAC Medium Access Control

MBFSN Multimedia Broadcast Single Frequency Network

NAS Non Access Stratum

OFDM Orthogonal Division Multiplexing

OFDMA Orthogonal Frequency Multiple Access

PS Packet Switch

PSD Power Spectral Density

PCRF Policy Charging Rules Function

PDCP Packet Data Convergence Protocol

PDSCH Physical Downlink Shared Channel

PDU Packet Data Unity

PCCC Parallel Concatenated Convolutional Code

PMI Precoding Matrix Index

QoS Quality of Service

QPP Quadrature Polynomial Permutation

QPSK Quadrature Phase Shift Key

QAM Quadrature Amplitude Modulation

RAN Radio Access Network

RNC Radio Network Controller

RLC Radio Link Control

RB Resource Block

RE Resource Element

RSC Recursive Systematic Convolutional

RM Rate Match

RV Redundancy Version

RI Rank Indicator

SVD Singular Value Decomposition

SU-MIMO Single User – MIMO

SISO Single Input Single Output

SNR Signal to Noise Ratio

SFBC Space Frequency Block Code

STBC Space Time Block Code

SC Select Combining

SIC Successive Interference Cancelation

SM Spatial Multiplexing

SAE System Architecture Evolution

SDU Service Data Unity

TDMA Time Division Multiple Access

TSTD Time Shift Transmit Diversity

TM Transmission Mode

TDD Time Division Duplexing

UE User Equipment

UTRAN Universal Terrestrial Radio Access Network

UP Uplink

UMTS Universal Mobile Telecommunication System

ULA Uniform Linear Array

ZF Zero Forcing

3GPP 3rd Generation Partnership Project

List of Figures

List of Tables

1. Introduction

1.1. Continuous Evolution of 3GPP Cellular Standards

In the last years the cellular systems have been shaped by the 3GPP/ETSI standards, starting with the 2G-GSM until the present 3.9G/4G-LTE standard. The 3rd Generation Partnership Project (3GPP) is an association of several regional specification groups, which are responsible by selection and development of the technologies that will meet the requirements of a given technological family, like 2G, 3G or 4G for instance. In this work thesis we discuss the technology that is strongly integrated in one of the last 3GPP cellular standards, therefore in this point an overview of the 3GPP standards evolution is presented.

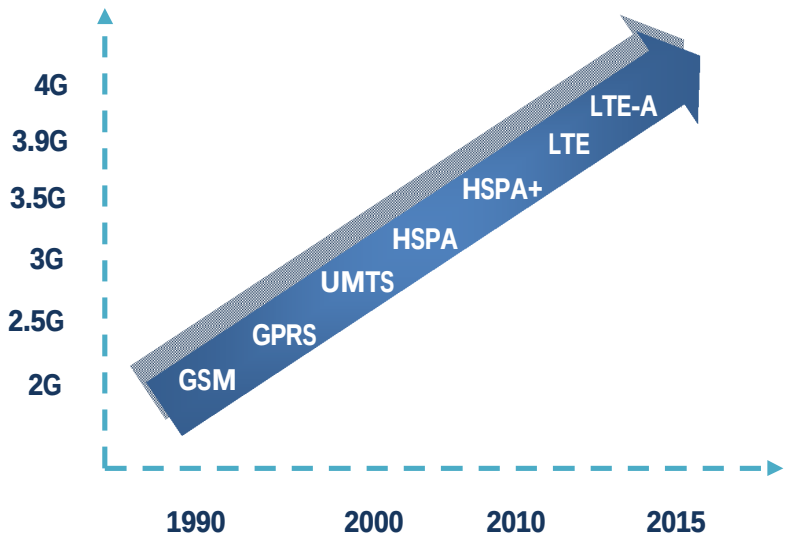

Figure 1. 1 - 3GPP Family Evolution

The first and the most succeeded cellular standard of all time was the 2G-GSM/GPRS system, specified by European Telecommunications Standards Institute (ETSI) in Europe. The Global System for Mobile Communications (GSM) was designed just for voice service support, being the core network fully circuit switched oriented, and the sharing of radio spectrum between User Equipments (UEs) performed via TDMA/FDMA techniques. The Time Division Multiple Access/Frequency Division Multiple Access (TDMA/FDMA) gives to each User Equipment (UE) a particular band of the spectrum at a given time, and in GSM case this band is switched from time slot to time slot for the same UE. The next evolution phase of GSM was based on the introduction of a Packet Switch (PS) domain in parallel with the Circuit Switch (CS) domain inside the core network, so the core network starts the trend to evolve for a fully packet switch domain based on IP transport. This add-on was called General Packet Radio Service (GPRS), and was the base for the first release of 3GPP 3G Universal Mobile Telecommunication System (UMTS) system.

With the increasing demand for mobile data services, a quick upgrade of the available 2G networks was necessary; therefore several performance requirements were defined for the next generation of cellular networks, which result in the 3G family. One of the standards that fulfill the requirements to be recognized as a 3G technology was UMTS from 3GPP specification group. Due the necessity of perform a quick upgrade, the UMTS standard was designed to run over the actual GSM/GPRS system, being the first releases of UMTS composed by simple add-ons to the present GSM system. The first release of UMTS defined only a new Radio Access Network (RAN) called Universal Terrestrial Radio Access Network (UTRAN), which it was specified to be used in parallel with the actual GSM RAN (GERAN), therefore UMTS system remains the same of 2G, with the difference of this new parallel RAN. The following UMTS upgrades resulted in the specification of High Speed Packet Access (HSPA), which defines a high speed channel of 14.4 Mbps for the downlink, and a 5.76 Mbps channel for the uplink. Finally, the last 3G/3.5G release of 3GPP was the HSPA+, which introduces a direct tunnel between the Base Station (BS) and the gateway to the external networks; hence a reduction of latency delays imposed by some intermediate network nodes was achieved. Another important feature of UMTS/HSPA is the use of Code Division Multiple Access (CDMA) as the channel access technique, allowing UEs to be mapped in the same time-frequency resources using orthogonal sequences to code the information of those UEs. Note that with CDMA, the information of each UE is orthogonal to other UEs information, allowing each UE separate without interference their information from the other UEs information.

The evolution of the UMTS/HSPA+ standards towards 4G continued with the specification of LTE, which it was approved as a 3.9G/4G system. Although LTE comprises some of the paradigms used in the latter releases of 3G, the overall LTE system design was made from the

root, not being the result of an upgrade or a small specific change of UMTS/HSPA+ system. The main distinct changes in LTE were made in the following parts of the network: radio interface level, radio access network level and core network. At the radio interface level we can underline Multiple Input Multiple Output (MIMO) systems and Orthogonal Frequency Division Multiple Access (OFDMA) as being the most important upgrades for the spectral efficiency performance boost verified. Also a reduction of latency delays was achieved with a specification of a simpler flat architecture for the radio access and core networks, being the last composed by a fully IP packet switched network [1][2][3].

1.2. MIMO Overview and Motivations

The evolution verified in the last years in fixed wired networks was drive by the emergence of a new set of services, applications and devices, which start to become an important part of people business and personal daily life. The dependence of these services and applications increase in such a form, that subscribers now demands for access to these services and applications from anywhere, at anytime, over any circumstances, which led to the emergence of new mobile broadband systems. The growth of subscriber's number and the high requirements of these new applications and services, allied with limited radio spectral resources, make necessary an improvement of the actual mobile broadband technologies. These improvements are related with an increase of spectral efficiency, peak data rates, reduced latency delays, set-up times, and so on. These goals can only be achieved with MIMO technology. Therefore, this technology has an important role in the current 4G cellular systems and it is expected to be a key technology for the future cellular systems.

The MIMO systems use multiple antennas at the radio interface level to add a new spatial dimension beyond the time and frequency domain, thus with this spatial domain we can improve some communication metrics like capacity, user throughput, spectral efficiency and coverage area, without an increase of time-frequency resources used. The cost of MIMO systems is the necessity of install multiple antennas and applies complex signal processing techniques. Before we proceed, is important refer that it is common look to a MIMO system as a communication link where multiple antennas are needed at both the transmitter and receiver, but this is not the most correct definition of MIMO, the MIMO word is used in a widest sense, enclosing the Single Input Multiple Output (SIMO) and also Multiple Input Single Output (MISO) systems, where multiple antennas are available just in one side of the communication link. The improvement of performance metrics referred above is accomplished using specific MIMO mechanisms like diversity, beamforming and spatial multiplexing (SM). Each one of

these mechanisms is used to improve specific performance metrics according the transmission scenario circumstances, like we will see when we discuss the LTE transmission modes.

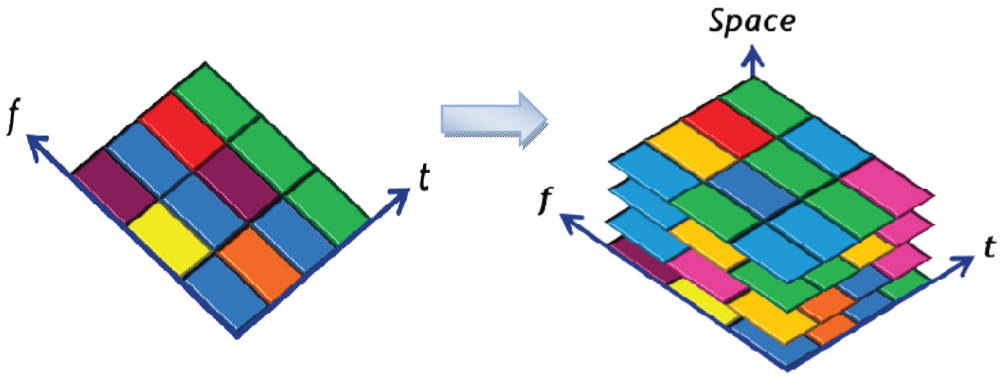

Figure 1. 2 - MIMO resource domains [11]

The correct working of these 3 mechanisms is strongly dependent of the instantaneous channel conditions, and also of the precise knowledge of these channel conditions in the BS and/or UE, in order to do a correct precoding at transmitter and/or correct equalization at receiver.
In Table1 is presented the aim of each one of the MIMO mechanisms, as well the antenna separation conditions required for the correct working of each one of these 3 MIMO mechanisms.

MIMO Mechanism	Aim	Antenna Separation
Diversity	Reliability	Medium
Beamforming	Coverage	Low
Spatial Multiplexing	Throughput	High

Table 1 - MIMO mechanisms

MIMO can be implemented in a single user context, referred as Single-User MIMO (SU-MIMO) techniques, where only one UE is served; or in a multi-user context, referred as Multi-User MIMO (MU-MIMO) techniques, where more than one UE share the same time-frequency resources. As we will see along this work, the changing in the processing techniques when we pass from a SU-MIMO to a MU-MIMO system are very little, but sometimes the channel conditions are better to perform a MU-MIMO than a SU-MIMO.
The use of optimal processing techniques to create several independent MIMO channels is dependent of available channel knowledge at both transmitter and receiver. With this channel knowledge, a signal processing technique named Singular Value Decomposition (SVD)

decomposition is applied over the estimated channel in order to compute optimum precoding and equalization matrices. We will see later, when present the LTE transmission modes, that there are some practical constraints that change the form of done the precoding (codebook basis) in relation to the optimal way [2][4][5][6][11].

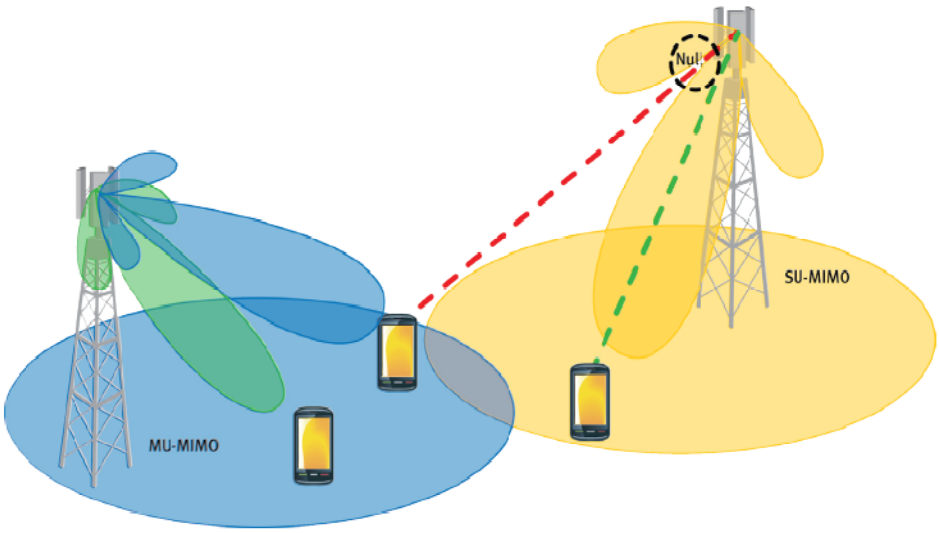

Figure 1. 3 - MU-MIMO and SU-MIMO schemes [11]

1.3. Thesis Objectives

As discussed, MIMO is the key technology of the current and future cellular systems to achieve high spectral efficiency. The objective of this thesis is to study, implement and evaluate MIMO techniques under the LTE specifications. We start by presenting the theoretical fundaments of some MIMO strategies. Then, we present the different types of MIMO techniques, i.e. the different transmission modes considered in LTE 4G cellular standard.

In this thesis we implemented the transmission mode 4 of LTE, which is a spatial multiplexing mode used in a closed loop configuration. At the transmitter side we implement several transmit precoders considering different ranks for 2 and 4 antenna configurations. At the receiver side, and to efficiently separate the data streams, we derive and implement a multi-symbol Successive Interference Cancellation (SIC) Minimum Mean Square Error (MMSE), SIC-MMSE, and SIC Zero Forcing (SIC-ZF) based equalizers. The results are compared with conventional linear multi-symbol MMSE and ZF equalizers. It is well known that the performance of the MIMO schemes strongly depends on the correlation between the different channels. In practical

systems, and in some scenarios, may be difficult to have uncorrelated antenna channels. Thus, we evaluate the implemented schemes under both uncorrelated and correlated antenna channels.

1.4. Thesis Structure

From this point forward, the thesis structure is organized in the following form:

In chapter 2 we will give an overview of the different physical phenomena which affects the radio channel response, as well the concept of correlation between radio channels. The capacity of the different MIMO channel configurations will also be discussed in this chapter.

In chapter 3 we will start to discuss the three types of MIMO mechanisms, such as diversity, beamforming and multiplexing. Then, we will present some transmission and receive diversity schemes. Finally, we discuss the different types of algorithms used in SU/MU MIMO spatial multiplexing modes.

In chapter 4 we will give an overview of the most important aspects related with LTE, hence we will start to present the overall network architecture and performance results for several evaluation metrics. Then, we will focus on some of the main physical layer subjects, starting with the presentation of LTE time-frequency signal structure, reference signals, OFDM modulation concept, and lastly we will see the layers that compose the full physical chain in LTE.

In chapter 5 is presented the different MIMO transmission modes specified for the downlink of LTE, therefore we will present for some modes the signal processing structure performed by the MIMO layers within the physical chain. Besides the signal processing presentation, we will try to understand the MIMO principles related with each one of these transmission modes.

In chapter 6 we will present the developed simulation platform of LTE transmission mode 4, considering 2x2 MIMO and 4x4 MIMO configurations. Hence, we will start to detail all the MIMO signal processing performed at transmission and reception in each one of these configurations. Then, we will present and analyze the Bit Error Rate (BER) results obtained by simulations.

In chapter 7 we will finish with the conclusion, and we will also discuss future work and trends for the future MIMO systems.

2. Radio Channel Propagation

The use of the radio channel in a wireless transmission makes the signal vulnerable to the effect of several physical phenomena, which will result in distortion and signal attenuation. The performance of a radio interface technology is dependent of the capacity in adapt the communication to the radio channel behavior; therefore the anticipation of all physical effects on the transmitted signal is crucial. In order to model these effects in all typical communication scenarios, several mathematical models based on empirical ground measurements campaigns were developed. Note that the accuracy of these models is crucial to assess the technology performance during the standard development, and thus perform the correct technology choice. We can identify 3 main phenomena which affects wireless transmissions, which are: propagation path-loss, shadow and multipath fading. The effect of these 3 phenomena in the received power P_R is presented in Figure 2.1.

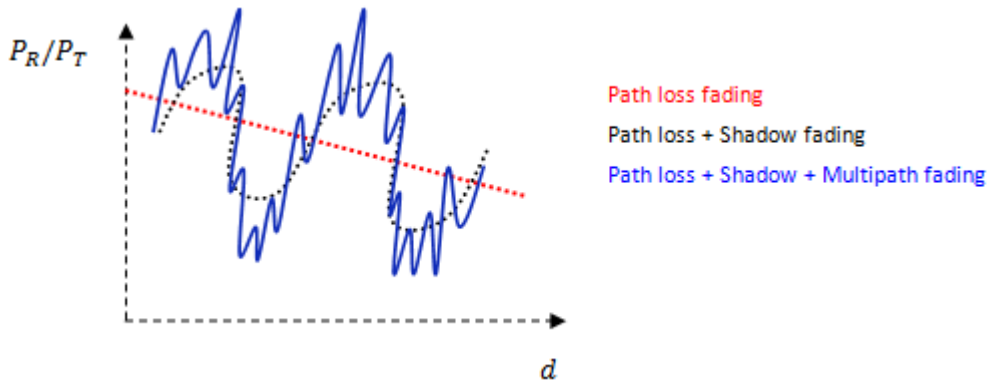

Figure 2. 1 - Power variation due path loss, shadowing and multipath

In this section we analyze in detail each one of the phenomena that affect the received power P_R in a wireless transmission.

2.1. Path Loss

The path loss attenuation is the result of the natural wave expansion along the signal propagation. The receiver sees the path loss phenomena as the average power around which the received power varies due to the shadowing and multipath fading effects. Of all the 3 phenomena the path loss is the one that presents the slowest received power variation with the distance during the movement. The slow power variation due path-loss is represented by the red line in Figure 2.1.

The simplest model used to represent the path-loss power attenuation is a function of the distance d between BS and UE, like is shown below.

$$P_{R_{PL}}(d) = P_T G_T G_R p_L(d) \qquad (2.1)$$

$$P_{R_{PL}}(d) = P_T G_T G_R \left[\frac{d_0}{d}\right]^{\rho}$$

The value of the attenuation exponent ρ and also d_0 depends on the type of environment, while G_T and G_R are transmit and receive antenna gains respectively. Beyond this model, some other empirical frequency dependent models like Okumura, Okumura-Hata, Cost 136 and Walfish/Bertoni were developed [7][8].

2.2. Shadowing

The shadow effect is the result of signal path blocking by terrestrial objects (buildings, mountains, walls, trucks, trees) during the UE movement. The received power variation due to this type of fading is modeled as a Gaussian random variable$x$ with zero mean (relative to the path loss value) and variance σ^2 in dB, where the different values of σ^2 normally varies between 6 to 10 dB depending on the environment features.

The Gaussian fdp that defines the probability of the received power variation x (dB) being within a given interval, is defined by the following expression.

$$f_{SH}(x) = \frac{e^{-\frac{x^2}{2\sigma^2}}}{\sqrt{2\pi\sigma^2}} \qquad (2.2)$$

Considering the path-loss plus shadowing effect, the received power (dB) along the distance, is modeled by expression 2.3.

$$P_{R_{PL,SH}}(dB) = x + 10\log_{10}(P_T) + 10\log_{10}(G_T G_R) + 10\log_{10}(p_L) \quad (2.3)$$

This kind of fading is called as large scale fading due the fact that their variation is spread along distances in the order of the tens to the hundreds of meters [7][8].

2.3. Multipath fading

The multipath fading effect causes a random variation on the amplitude of the received signal due the constructive/destructive interference between multiple copies of the original signal that arrive the receptor. The multiple paths are created due reflections, diffraction and scattering in typical urban objects. For each main path, several subpaths with random amplitude and phase are generated when the signal cross scattering clusters, like is shown in Figure 2.2.

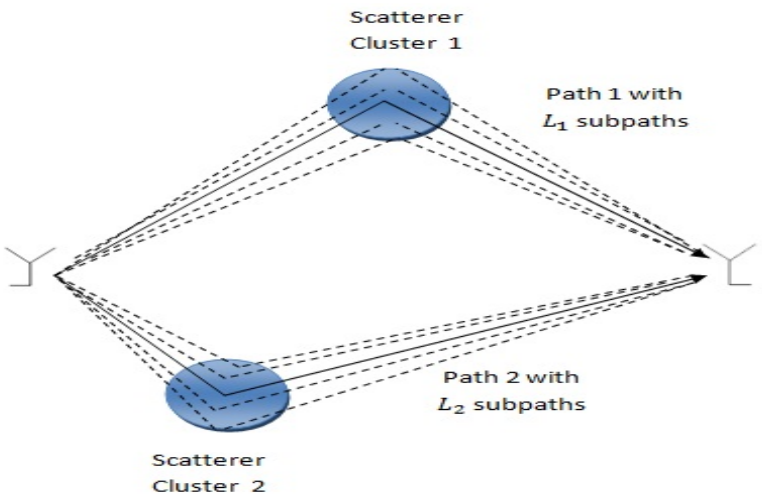

Figure 2. 2 - Multipath illustration with the several subpaths for each main path

The multipath channel can be model as,

$$h(\tau, t) = \sum_{n=1}^{L(t)} \alpha_n(t) e^{-j\phi_n(t)} \delta(\tau - \tau_n(t)) \quad (2.4)$$

Where $L(t)$, $\alpha_n(t)$, $\phi_n(t)$, and $\tau_n(t)$ represent the number of paths, the amplitude, the phase and the delay of the nth path at instant t respectively.

The amplitude α_n of each path can be modeled by a Rayleigh or a Ricean distribution. In scenarios with Line of Sight (LOS), with a path stronger than the others, the amplitude is modeled by a Ricean distribution. In scenarios without LOS, where there is not a path much

stronger that the other, the amplitude is modeled by a Rayleigh distribution. The phase ϕ_n can be modeled as random uniform distribution between [0, 2π].

The fdp of a Rayleigh distribution is the following,

$$f_{MP}(\alpha) = \frac{\alpha}{\sigma^2} e^{-\alpha^2/2\sigma^2} \qquad \alpha > 0 \tag{2. 5}$$

As discussed, the multiple paths are modeled as a set of time domain taps, with each one representing a delayed copy of the transmitted signal, like is shown in Figure 2.3. The number, the position and the relative power of the taps, changes according the scenario environment, hence some channel models like EPA, EVA and ETU, were created by ITU organization in order simulate typical channel environments for the development of 4G wireless technologies.

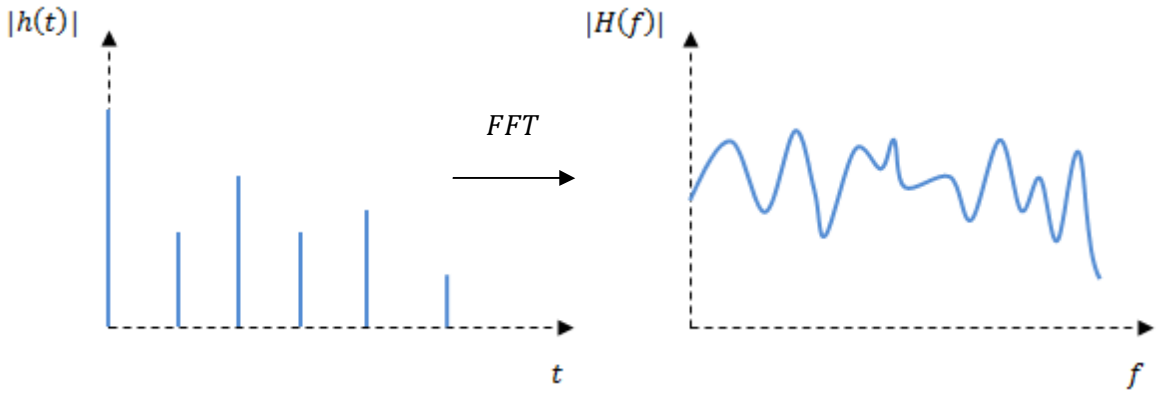

Figure 2. 3 - Time domain and frequency domain model for channel response

It is important refer that the time domain received signal is obtained performing the convolution operation between the time domain transmitted signal and the channel response $h(t)$; while in the frequency domain, the received signal is computed making the product between the transmitted signal in the frequency domain, with the channel response $H(f)$. Note that working in the frequency domain is simpler than in the time domain, therefore is usual all the signal processing being performed in the frequency domain.

Depending on the relative delays between the multiple copies, and the period T of the transmitted signal, we can define narrowband or wideband channels. In narrowband channels, the delays between the multiple copies are too small compared with the transmitted signal period T, therefore interference between symbols transmitted consecutively is avoided, and just constructive/destructive interference fading occurs. In the case of wideband channels, the delays between the multiple copies are of the same order of the signal period, therefore copies will overlap with consecutive transmitted signals, and then, interference between the symbols and attenuation will occur. In the frequency domain we can see the narrowband channel as a non-frequency selective channel, where the signal bandwidth B is smaller than the channel

coherence bandwidth B_C, which is defined as the range of frequencies where the channel has a flat frequency response. For the wideband case, the signal bandwidth is larger than the channel coherence bandwidth, so frequency selective response is verified.

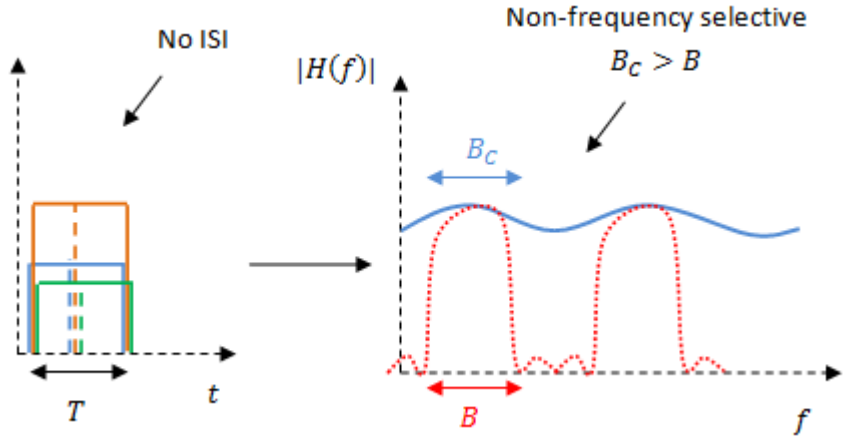

Figure 2. 4 - Narrowband channel

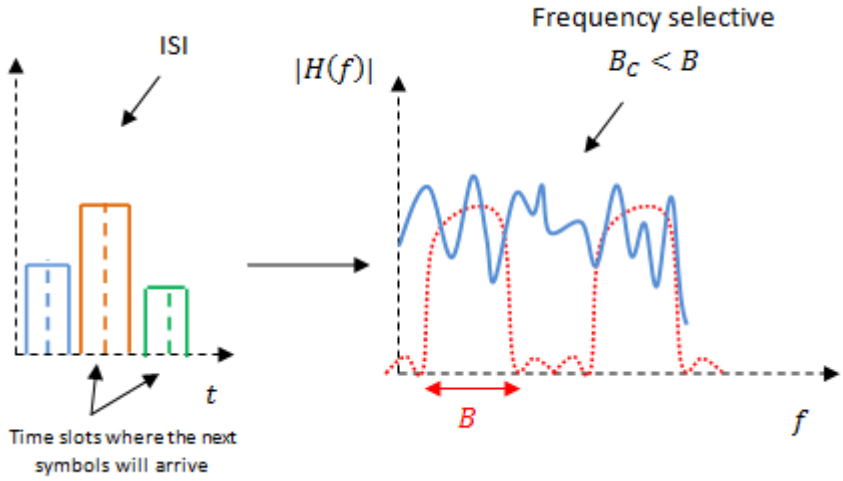

Figure 2. 5 - Wideband channel

So, according the spread of delayed copies, we are able to take information relative to the channel frequency domain variation (B_C) in a fixed local area, which is approximate by the bellow expression,

$$B_C \approx \frac{1}{5\sigma_\tau} \tag{2. 6}$$

Looking to the above expression we can see that the coherence bandwidth of the channel is inversely proportional to the r.m.s. time delay spread σ_τ. Another important channel feature is the time coherence T_C, which is the time domain version of B_C. The time coherence is defined as the range of time that the channel is invariant, while the UE is in movement. Depending on the velocity of this movement, a proportional difference between the original transmitted frequency and the received frequency will occur, which is defined as the frequency Doppler

spread f_D. This spectral shift caused by Doppler effect is related with T_C according the following expression [7][8][9].

$$T_C = \sqrt{\frac{9}{16\pi f_D^2}} \quad (2.7)$$

2.4. Spatial Channel Correlation in MIMO Systems

The performance of the different MIMO mechanisms, briefly presented in chapter 1, is strongly dependent of spatial antenna correlation. While spatial multiplexing and diversity mechanisms require a low level of spatial correlation to achieve full multiplexing gain and diversity order respectively, the beamforming mechanism might work under high correlation level between the channels. The channel correlation is a way of measure the amount of difference between the several radio channels in a MIMO system, therefore low correlation between channels means that the channels varies in opposite directions, thus achieving a high degree of difference between them; while high correlation between channels means a high degree of similarity between them.

In Figure 2.6 is presented the frequency response of 2 radio channels generated by a MIMO system composed by 2 antennas at the transmitter, and 1 antenna at the receiver. We can see from Figure 2.6 the low/high level of similarity verified in low/high correlation condition between the channels frequency response. The degree of correlation between the channels in a MIMO system is influenced by 2 aspects: the level of scattering in the urban environment, and antenna spacing. In order to achieve low correlation levels, a rich scattering environment and high distance spacing between antennas at both transmit and receiver is necessary.

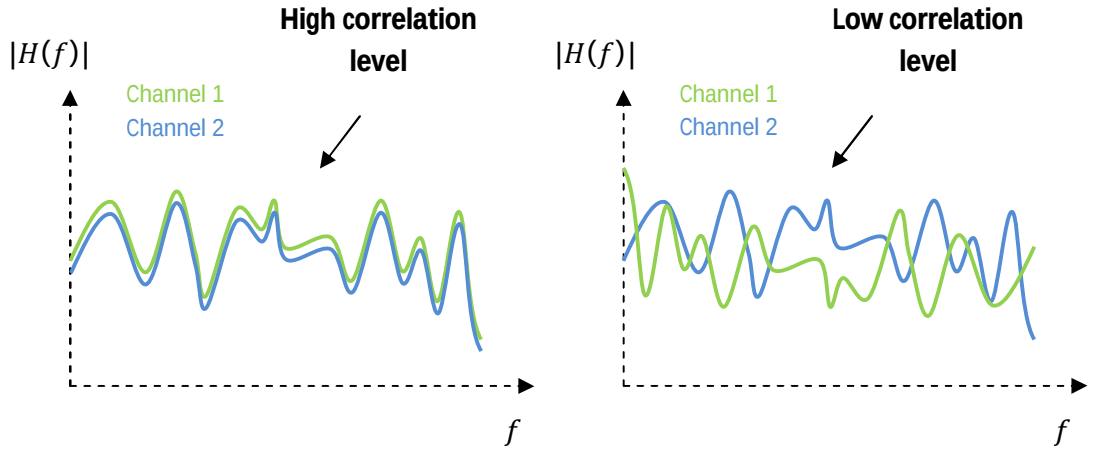

Figure 2. 6 - Frequency response of 2 channels in low/high correlation condition

According the level of scattering, the full set of paths transmitted from the antenna array (ULA), will departure/arrive to the BS/UE with a given angle spread in an average direction. In rich scattering environments the value of this angle spread for both signal departure and signal arrive increases, allowing that the multiple paths travel with sufficient direction separation to vary independently.

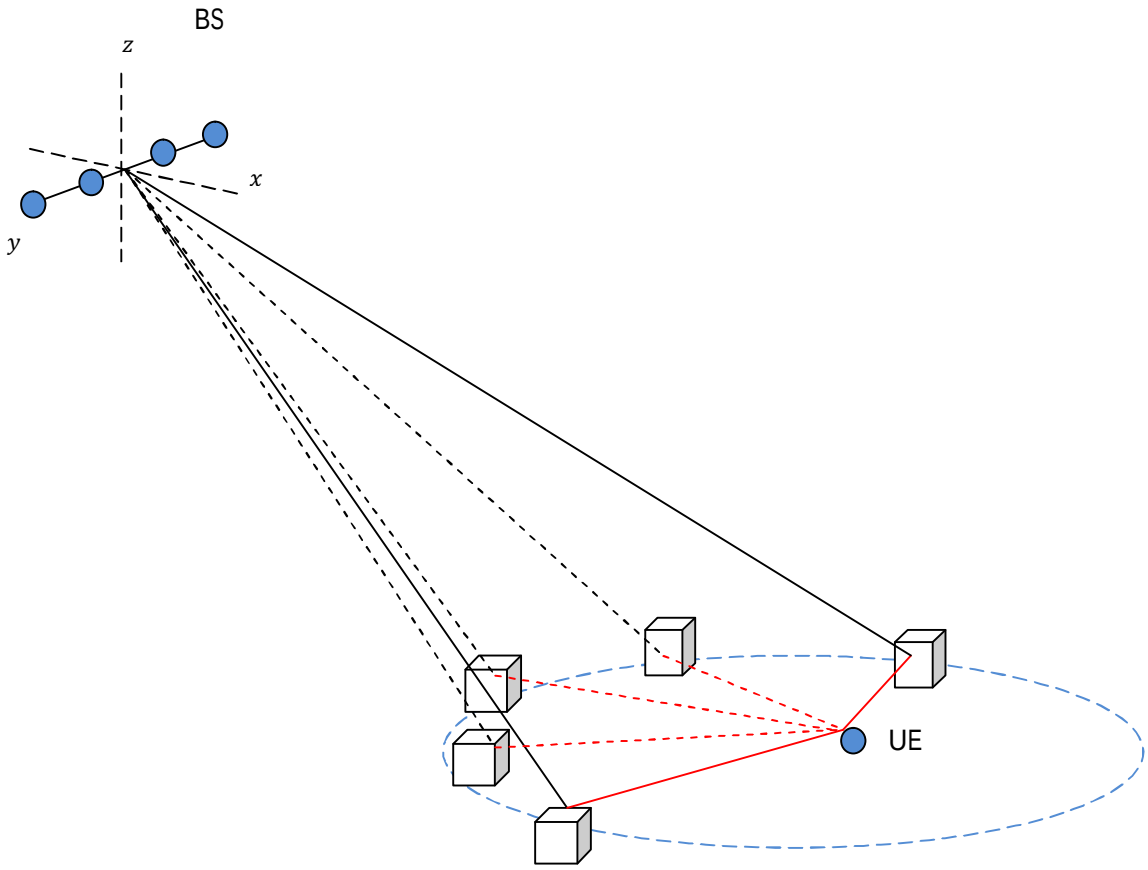

Figure 2. 7 - Multipath scenario

In figure 2.7 we can see a typical multipath scenario where a 4 antenna array transmits a signal for a single antenna UE surrounded by urban objects. Note that due the urban objects are located closely the UE, the spreading of the multipath is larger around the UE than in the BS, allowing lower correlation conditions for UE. Due this spatial context, the BS must to use a higher antenna separation to achieve the same level of spatial correlation verified in UE.

In figure 2.8 is presented the downlink azimuth geometrical configuration of spread and average angles used to model spatial correlation. At the left side of Figure 2.8 we can see the azimuth domain average angle of departure $\bar{\Phi}_{AoD}$, and also the spread angle of departure σ_{AoD}; while at

the right side is shown the geometrical configuration for the azimuth average angle of arrive $\bar{\Phi}_{AoA}$ and the spread angle of arrive σ_{AoA}.

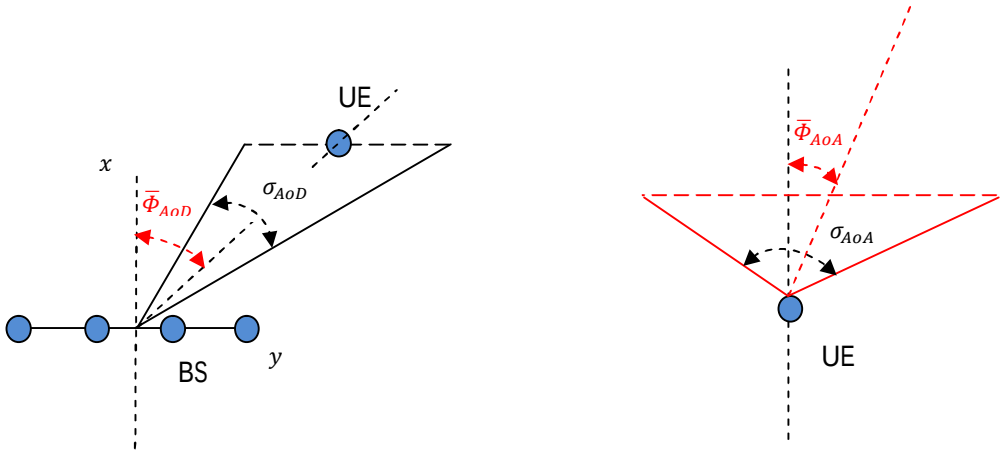

Figure 2. 8 - Geometric configuration of spread and average angles

In chapter 6 we will use this geometrical configuration to present the channel correlation model used in the practical work.

We will see latter, when present the simulation BER results of the implemented spatial multiplexing mode specified in LTE, that the number of parallel data streams that we can transmit over a MIMO channel is limited by the level of correlation between these channels [10][11].

2.5. Capacity in MIMO channels

In this point is present the several MIMO channel configurations, as well the capacity provided by each one of those MIMO configurations.

2.5.1. AWGN Channel

In Additive White Gaussian Noise (AWGN) channel it is consider that we have a Single Input Single Output (SISO) link without channel multipath fading, path loss or shadowing. Therefore, just the original signal x arrives at the receiver, resulting in a h coefficient of 1. The only perturbation in this channel is the white noise n (AWGN) with a Gaussian distribution of mean 0. The white noise has a constant Power Spectral Density (PSD), so we will consider that constant equals N_0 watts/Hz.

The signal model in a SISO AWGN channel is the following,

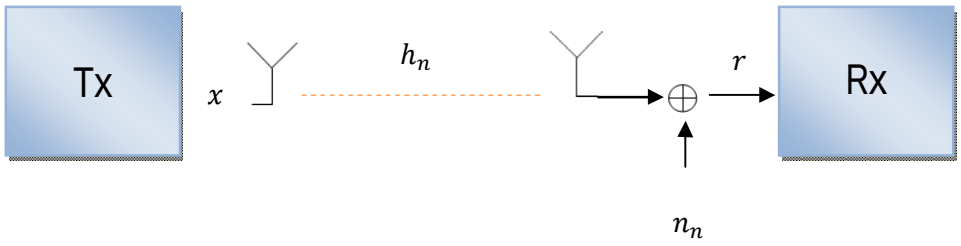

Figure 2. 9 - SISO Channel signal model

$$r = x + n \tag{2. 8}$$

The channel capacity limit for a SISO configuration (for lower BER) was defined by Shannon using the following expression.

$$C_{AWGN} = W \log_2\left(1 + \frac{P}{N_0 W}\right) bits/s \tag{2. 9}$$

$$C_{AWGN} = W \log_2(1 + SNR) bits/s$$

Where P, W, and N_0 are the transmitted power (watts), the bandwidth (Hz) and noise PSD (watts/Hz)[8][9].

2.5.2. SISO Channel

Now we consider that the received signal is not only affected by AWGN noise at the receiver antenna, but also by the multipath channel fading, resulting in a h coefficient different from 1. The signal model is the same presented in figure 2.9,

$$r = h_n x + n_n \tag{2. 10}$$

Now, we can intuitively see that the Signal to Noise Ratio (SNR) will be affected by the channel response h. We consider n as the index of the nth random channel realization.

$$SNR = |h_n|^2 \frac{P}{N_0} \tag{2. 11}$$

Therefore the expression for channel capacity is the following,

$$C_n = \log_2\left(1 + |h_n|^2 \frac{P}{N_0}\right) bits/s/Hz \quad (2.12)$$

The capacity of the SISO channel will be the expected $E\{C_n\}$ of all C_n realizations [8][9].

2.5.3. SIMO and MISO Channel

In the SIMO case, we will use an Maximum Ratio Combining (MRC) combining technique to align all the N_R channel coefficients in order maximize the received SNR.

The signal model for a SIMO system with N_R antennas at the receiver is presented in Figure 2.10.

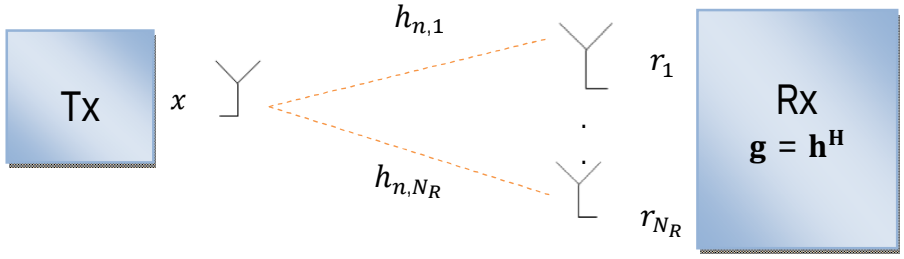

Figure 2. 10 - Overall SIMO signal model

In a matrix notation the received signal **r** is the following,

$$\mathbf{r} = \mathbf{h}x + \mathbf{n} \quad (2.13)$$

$$\begin{bmatrix} r_1 \\ \vdots \\ r_{N_R} \end{bmatrix} = \begin{bmatrix} h_{n,1} \\ \vdots \\ h_{n,N_R} \end{bmatrix} x + \begin{bmatrix} n_{n,1} \\ \vdots \\ n_{n,N_R} \end{bmatrix}$$

Using an MRC $\mathbf{g} = \mathbf{h}^H$ combiner the received signal estimation $\hat{x}$ is the following,

$$\hat{x} = \mathbf{g}\mathbf{r} \quad (2.14)$$

$$\hat{x} = \mathbf{h}^H\mathbf{h}x + \mathbf{h}^H\mathbf{n}$$

$$\hat{x} = [h_{n,1}^* \quad \dots \quad h_{n,N_R}^*] \begin{bmatrix} h_{n,1} \\ \vdots \\ h_{n,N_R} \end{bmatrix} x + \tilde{\mathbf{n}}$$

$$\hat{x} = \sum_{k=1}^{N_R} |h_{n,k}|^2 x + \tilde{\mathbf{n}}$$

Latter, we will see in detail how the MRC (Matched Filter) combining work.

The SIMO channel capacity using an MRC combiner at the receiver is the following,

$$C_i = \log_2 \left(1 + \sum_{k=1}^{N_R} |h_{n,k}|^2 \frac{P}{N_0} \right) bits/s/Hz \quad (2.\ 15)$$

Note that we achieve greater channel capacity than the SISO and AWGN cases. This SNR improvement is done maintaining the transmission power P constant. The capacity of the SIMO channel will be the expected value $E\{C_n\}$ of all C_n realizations [8][9].

In the case of a MISO system composed by N_T transmit antennas; the signal model is presented in Figure 2.11.

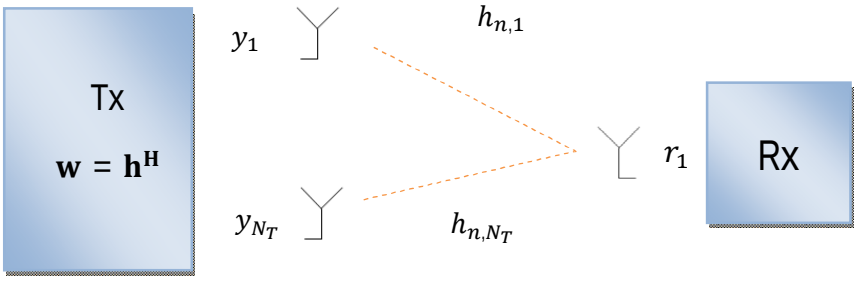

Figure 2. 11 - Overall MISO signal model

In MISO transmission case with Channel State Information (CSI) available at the transmitter, and also using MRC precoding, the channel capacity is the same of SIMO case.
When we don't have CSI at the transmitter, and we have to use some kind of diversity transmission scheme, the capacity decreases. For instance, the channel capacity for a MISO 2x1 using Alamouti Space Frequency Block Code/Space Time Block Code (SFBC/STBC) is the following,

$$C_i = \log_2 \left(1 + \frac{\sum_{k=1}^{2} |h_{n,k}|^2}{2} \frac{P}{N_0} \right) bits/s/Hz \quad (2.\ 16)$$

Latter we discuss the Alamouti SFBC/STBC diversity scheme.

2.5.4. MIMO Channel

The adopted MIMO signal model is composed by N_T antennas at the transmitter (BS) and N_R antennas at the receiver (UE). The h_{ji} coefficient is the frequency channel response from transmit antenna i to receive antenna j. At each receive antenna, it will be added noise n_j with a Gaussian distribution. In this part we will not present the index n of a specific channel realization.

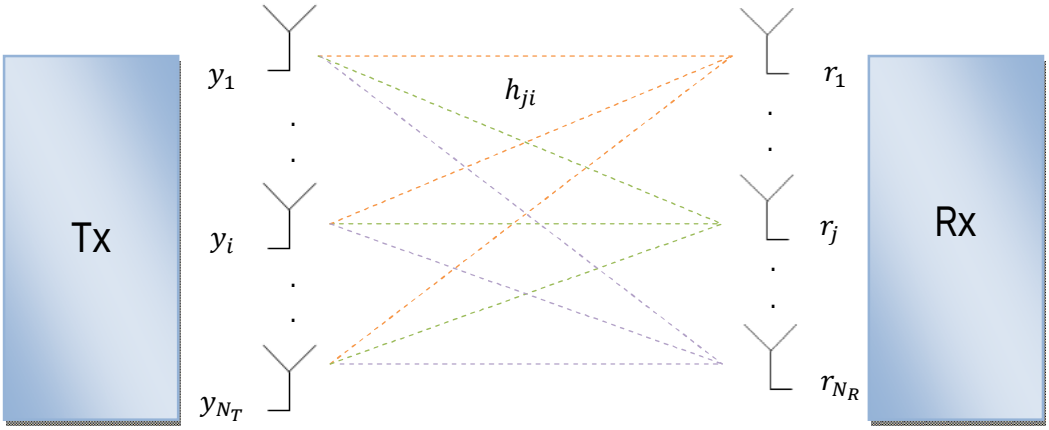

Figure 2. 12 - Overall MIMO signal model

In a matrix notation the received signal **r** is the following,

$$\mathbf{r} = \mathbf{H}\mathbf{y} + \mathbf{n} \tag{2. 17}$$

$$\begin{bmatrix} r_1 \\ \vdots \\ r_{N_R} \end{bmatrix} = \begin{bmatrix} h_{11} & \dots & h_{1N_T} \\ \vdots & \ddots & \vdots \\ h_{N_R1} & \dots & h_{N_RN_T} \end{bmatrix} \begin{bmatrix} y_1 \\ \vdots \\ y_{N_T} \end{bmatrix} + \begin{bmatrix} n_1 \\ \vdots \\ n_{N_R} \end{bmatrix}$$

Considering a $N_T \times N_R$ MIMO channel **H**, and full CSI only at the receiver, the channel capacity is given by the following expression,

$$C_n = \log_2 \left[\det \left(\mathbf{I}_N + \frac{P}{N_T N_0} \mathbf{H}_n \mathbf{H}_n{}^H\right)\right] \tag{2. 18}$$

$$C_n = \log_2 \left[\det \left(\mathbf{I}_N + \frac{SNR}{N_T} \mathbf{H}_n \mathbf{H}_n{}^H\right)\right]$$

The capacity of the MIMO channel will be the expected value $E\{C_n\}$ of all C_n realizations for a given SNR. In the above expression $\mathbf{I}_N$ is a size N identity matrix, being $N = \min(N_T, N_R)$. We can figure that MIMO channel capacity increases with the minimum value between the number of transmit and receive antennas, and the ideal maximum channel capacity for a defined

antenna configuration is obtained when $\mathbf{H}_n$ is a unitary matrix, i.e., $\mathbf{H}_n\mathbf{H}_n^H = \mathbf{H}_n^H\mathbf{H}_n = \mathbf{I}$. We also should refer that when the channels within matrix **H** are strongly correlated, the channel capacity in the above expression decreases for the same MIMO channel.

In this subchapter the aim was see that with multiple antenna systems we are able to multiply the capacity of a SISO channel [8][9].

3. MIMO Systems

In this chapter we start by presenting an overall explanation related with spatial multiplexing, beamforming and diversity mechanisms used in MIMO systems. Then, we will focus on the presentation and development of specific MIMO schemes used within diversity and spatial multiplexing mechanisms. So, the aim of this Chapter is discuss all the signal processing related with specific MIMO schemes, presenting how these schemes can eliminate interferences between received symbols, and also increase the SNR for each received symbol.

3.1. MIMO Mechanisms

3.1.1. Diversity

The aim of diversity is combat the multipath fading channel sending the same symbol across several independent paths. Then, the receiver using some processing techniques combines all the independent paths together to increase the SNR of that symbol. Depending of the multiple antenna configuration used (SISO, SIMO, MISO or MIMO) is possible create independent fading channels in time, frequency and space.

In an intuitive way we can see that if multipath fading varies in a different and fully random form, the probability that some symbol transmitted across all these paths experiment high fading in all of the paths is very little. Therefore, increasing the number of independent paths across which we repeat the information symbol, we increase the received SNR, and consequently we decrease the error probability, resulting in BER curves that tend to AWGN BER, which is characterized by just affect the link with noise. This means that in ideal high diversity scenario,

multipath fading is almost canceled, and an improvement in the reliability of the link communication is verified [2][8][9].

- **SISO Diversity**

In a SISO system the only diversity that can be used, is provided repeating the symbols in time and frequency domains, using a time/bandwidth separation between the symbol copies greater than the channel coherence time/bandwidth.

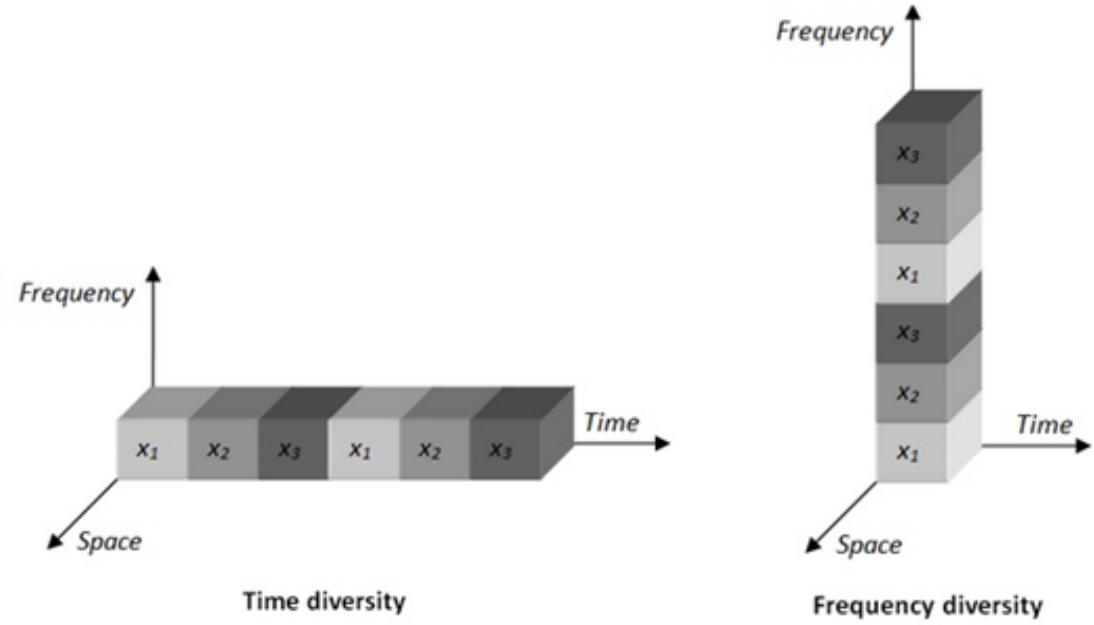

Figure 3. 1 - Time and Frequency Diversity [35]

At the receiver we can use a Matched Filter (MF) filter (MRC) that knowing the channel response aligns the phases of the channel coefficients where the symbol is repeated, in order to increase the SNR. In this case, increase diversity means increase the used bandwidth in frequency case; and in time case, means increase the number of time slots to transmit a fixed set of symbols, thus reducing the data rate. This type of diversity doesn't make part of typical MIMO diversity schemes, where the space dimension is used, so we will not go into more details.

- **SIMO Diversity**

The use of multiple antennas at the receiver can be used to add spatial diversity antenna at reception in order to decrease the influence of the multipath channel effect; thus we can use not only time and frequency diversity but also spatial diversity. In this case, independent paths could be created using the spatial separation in the receiver antennas, thus we are able to increase diversity order without increasing bandwidth or reducing the data rate.

Combining techniques like Maximum Ratio Combining (MRC), Equal Gain Combining (EGC), Select Combining (SC) and Interference Rejection Combining (IRC) used at the receiver, will not be detailed here.

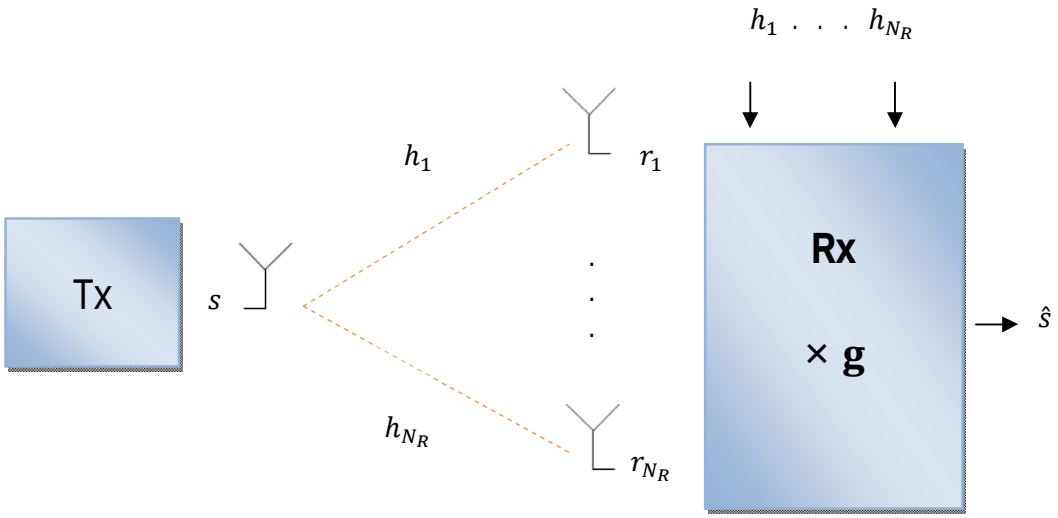

Figure 3. 2 - SIMO signal model

The general signal model in this case is the following,

$$\begin{bmatrix} r_1 \\ \vdots \\ r_{N_R} \end{bmatrix} = \begin{bmatrix} h_1 \\ \vdots \\ h_{N_R} \end{bmatrix} s + \begin{bmatrix} n_1 \\ \vdots \\ n_{N_R} \end{bmatrix} \quad (3.\ 1)$$

After applying the selected combining technique the result is,

$$\hat{s} = [g_1 \quad \cdots \quad g_{N_R}] \begin{bmatrix} h_1 \\ \vdots \\ h_{N_R} \end{bmatrix} s + [g_1 \quad \cdots \quad g_{N_R}] \begin{bmatrix} n_1 \\ \vdots \\ n_{N_R} \end{bmatrix} \quad (3.\ 2)$$

- **MISO Diversity**

Diversity in a MISO system is divided in 2 different scenarios, the scenario where CSI is available at the transmitter (beamforming), and the scenario where CSI is not available at transmitter. In the first scenario (beamforming) the symbol is repeated with a phase shift across the space, and in the second scenario the symbol diversity is provided across space-time/frequency. Although these 2 different scenarios can be considered as diversity forms, the diversity term is normally just used to define the scenario where no CSI is available at the transmitter, being the first scenario commonly referred as a beamforming mechanism. In this point we will overview the diversity scenario where no CSI is available at the transmitter; hence we will present next, space-time/frequency coding techniques.

Without channel information at transmitter, the diversity could be provided using Space Time Block Codes (STBC) or Space Frequency Block Codes (SFBC). In a STBC/SFBC, spatial dimension is combined together with time or frequency in order to send each symbol of the block across several independent channels.

In SFBC/STBC the symbols are coded in blocks, and each symbol of the block is repeated in different time/frequency-space, thus a copy of a symbol never share time/frequency and space resources with the original symbol, so in each time or frequency resource, each antenna transmits a different symbol, which will create an interference problem. To cancel this interference, orthogonal designs between the set of symbols sent in each antenna are computed doing phase shifts in some symbols. A very popular SFBC/STBC is Alamouti coding, used to transmit blocks of 2 symbols across 2 transmit antennas. The Alamouti coding is a fully orthogonal code, which allows the transmission of each symbol across 2 independent channels in a non-interfering way, like we will see in detail in another sub-chapter.

We will see next that Alamouti orthogonal codes are only available for 2 transmit antennas, thus in cases of more than 2 antennas, the possibilities are: use quasi-orthogonal codes (ABBA code), or use a code rate lower than 1 (Tarohk code).

3.1.2. Beamforming

Instead of use STBC/SFBC diversity to increase the SNR in the target UE, we can use beamforming if CSI is available at transmitter. With this CSI and using an array of antennas, we can precode one information symbol in order to create a pattern of constructive interference in the direction of the UE, and destructive interference in other directions. The beamforming mode can be used to improve cell coverage in situations of UEs located at the cell edges, without creating interference to other UEs.

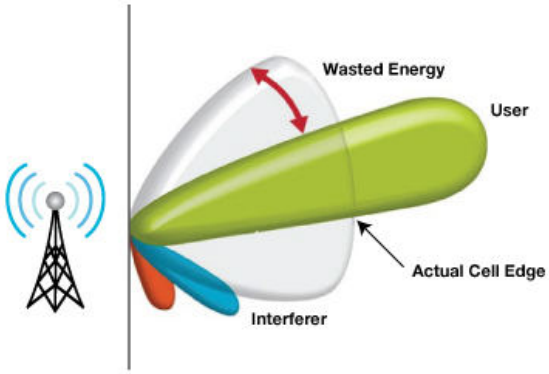

Figure 3. 3 - Single layer beamforming [14]

In beamforming precoding we use an array of antennas, and in each antenna we send the same symbol doing a phase shift according the CSI. When CSI is not available at the transmitter,

other techniques based on computing Direction of Arrive (DoA) at the uplink are considered in order to get the UE direction.

The signal model is the following,

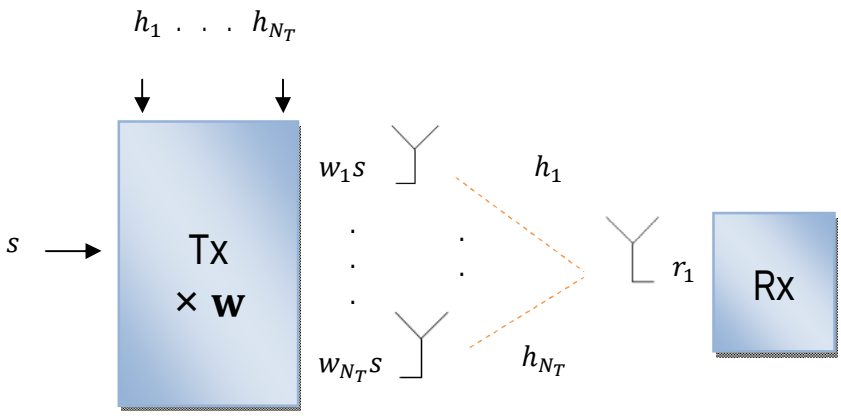

Figure 3. 4 - Beamforming signal model

The received signal in matrix notation is the following,

$$r_1 = [w_1 \quad \dots \quad w_{N_R}] \begin{bmatrix} h_1 \\ \vdots \\ h_{N_R} \end{bmatrix} s + n_1 \tag{3. 3}$$

- **Beamforming fundamentals**

Let's make a short revision of some basic technical aspects around signal beamforming and antennas. Like we said before, beamforming allow us direct the signal power into one specific direction instead perform an omnidirectional transmission. To perform a directional transmission a set of equal spaced antennas is used to shape the beam of the signal; this antenna set is defined as Uniform Linear Array (ULA).

Let's see the following horizontal radiation diagrams that will help us figure out some important technical aspects. At the left side of Figure 3.5 we have one omnidirectional antenna that radiates the same power in all azimuth directions; then, we add in the same axis another omnidirectional antenna spaced of 0.5 wavelength, and feed with the same signal; the result is the formation of a beam in the direction of 0 azimuth degrees.

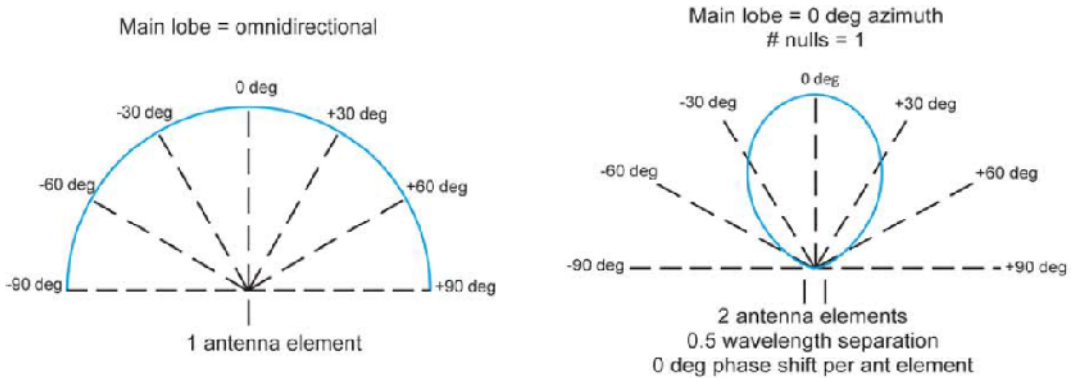

a) b)

Figure 3. 5 - Radiation Diagrams for 1 and 2 antennas [13]

Is important refer that in the case of one array composed by 2 antennas, each antenna is fed with the same signal of the omnidirectional case, but with a power decrease of 3dB (half) in order to use the same power in the 2 configurations; the power gain of 2 antennas ULA in the 0 azimuth direction is 3dB higher relatively to omnidirectional case.

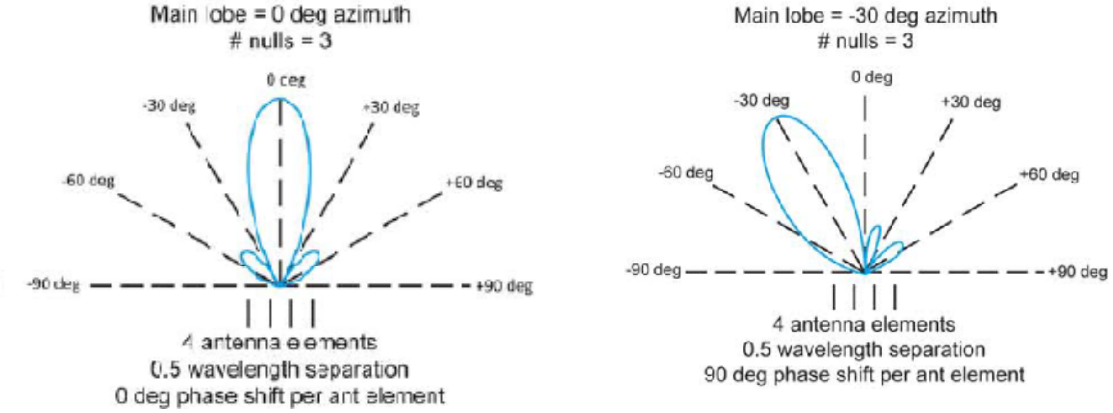

a) b)

Figure 3. 6 - Radiation Diagrams for 4 antennas [13]

Looking to Figure 3.6 a), we can see that after a third and fourth antenna have been added, and fed using the same input signal (just power reduction) , the selectivity of the main lobe increase, and 3 nulls were created in approximately +30, -30 azimuth directions, and one in the axis line. The conclusion here is that increasing the number of antennas we increase the selectivity and the number of null directions. In Figure 3.6 b) we direct the beam for -30 degrees in the azimuth direction applying a phase shift of 90 degrees between the signals in each antenna. So, instead of move mechanically the ULA in the azimuth domain, we direct the beam using phase shifts

[13]. To perform the 90 degree phase shift, and considering s symbol for transmission, the following signal precoding is done in each antenna,

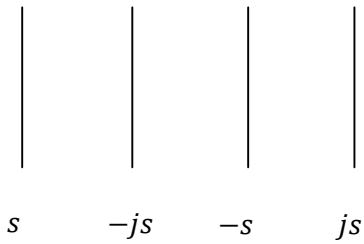

Figure 3. 7 - 90 degrees phase shift across 4 antennas

3.1.3. Spatial Multiplexing

Spatial Multiplexing allow us increase the data throughput without an increase of frequency resource elements used, therefore in certain channel conditions we are able to decompose the MIMO channel in several logic non-interfering channels (pipes). We will see latter, that while OFDM modulation allow us separate the symbols transmitted in a set of frequency subcarriers, the spatial multiplexing schemes allow us the separation of a set of symbols transmitted in the same frequency subcarrier. Therefore a spectral efficiency improvement is achieved using spatial multiplexing techniques.

The number of parallel data-streams or layers per subcarrier that is possible send in a MIMO channel is limited by the number of antennas at the transmitter and receiver; this limit is equal to min(N_T,N_R), so if we want to perform for instance a layer 2 transmission, at least both the transmitter and receiver must have 2 antennas. Another important aspect that must be verified to achieve high spatial multiplexing gain is low correlation channel conditions, thus a high degree of difference between the channels is needed to perform the separation of multiple layers without interference.

Figure 3. 8-Logic channel pipes [11]

Using optimal SVD decomposition, we are able to assess the capacity of each channel pipe in order to select the best pipes to adapt the transmission. This adaptation is done performing a power allocation according the singular values computed using SVD decomposition. With SVD we also obtain the optimum signal precoding to perform at the transmitter, and the necessary information for ideal equalization at the receiver, so that we are able to create the non-interfering channels/pipes. Note that CSI must be available at both transmitter and receiver, but sometimes just the receiver has precise channel information, therefore in these cases the solution to decode the signal is just based in an equalization scheme (ZF, MMSE, SIC) performed at the receiver.

SVD decomposition is the signal process theoretical basis for creation of non-interfering channel pipes, and so is reference in MIMO processing techniques, even sometimes not being possible implement it in a fully way. We will see later in detail how optimal SVD channel decomposition is done [2][8][9].

3.2. Transmission Diversity Schemes

As discussed, when channel knowledge is not available at the transmitter, the solution to reduce the multipath fading channel effect and increase the SNR at the receiver, is using a transmission diversity scheme. In this point we present some important diversity techniques for 2 and 4 transmit antennas. Later when we present LTE Transmission Modes we will discuss Alamouti SFBC and SFBC-FSTD, which are the frequency version of STBC and STBC-TSTD presented in this chapter, so we will not talk about them in here.

3.2.1. STBC Alamouti

Space-Time diversity can be provided in the case of 2 transmit antennas using Alamouti coding. The aim of Alamouti coding is give orthogonal feature to data-stream, allowing symbol separation in the receiver. We should refer that in here, we will consider a single time domain tap for each channel during t_0 and t_1 time slots, therefore h_1 and h_2 will be the single channel tap amplitude for each antenna during t_0 and t_1 (single tap invariant channel during t_0 and t_1 is considered).The Alamouti coding works in blocks of 2 symbols that are send in 2 OFDM consecutive symbols in each one of the antennas, like is shown in Figure 3.9.

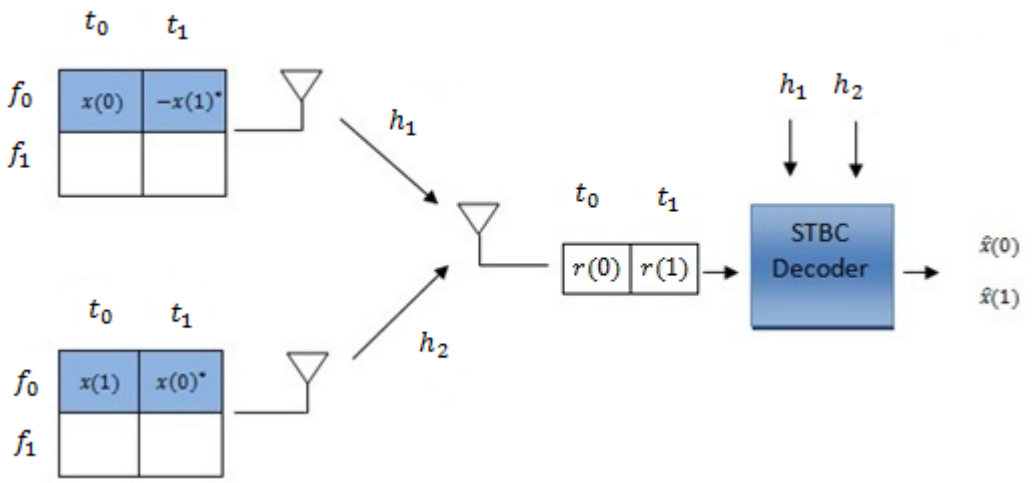

Figure 3. 9 - STBC Alamouti Tx-Rx

In the first antenna, the symbol $x(0)$ is sent in the subcarrier f_0 of the first OFDM symbol, and $-x(1)^*$ is sent also in the subcarrier f_0 but in the second OFDM symbol. In the second antenna happens the same thing of antenna 1. So in each antenna are generated 2 OFDM symbols.

We can figure out that the 2 sets of coded symbols are orthogonal,

$$x(0)x(1) - x(0)^*x(1)^* = 0 \tag{3. 4}$$

After Alamouti coding, the received signal is,

$$r(t_0) = h_1x(0) + h_2x(1) + n(0) \tag{3. 5}$$

$$r(t_1) = -h_1x(1)^* + h_2x(0)^* + n(1) \tag{3. 6}$$

Then, the receiver computes the complex conjugate version of the received $r(t_1)$ signal. Note that with $r(t_1)^*$ we can see the rearranged received signal in the following form,

$$\tilde{\mathbf{r}} = \mathbf{H_{eq}}\mathbf{x} + \tilde{\mathbf{n}} \tag{3. 7}$$

$$\begin{bmatrix} r(t_0) \\ r(t_1)^* \end{bmatrix} = \begin{bmatrix} h_1 & h_2 \\ h_2^* & -h_1^* \end{bmatrix} \begin{bmatrix} x(0) \\ x(1) \end{bmatrix} + \begin{bmatrix} n(0) \\ n(1)^* \end{bmatrix}$$

With channel knowledge available at the receiver, we will decode the symbols $\hat{\mathbf{x}}$, using $\tilde{\mathbf{r}}$ and the matched filter version of $\mathbf{H_{eq}}$.

$$\mathbf{H_{eq}^H} = \begin{bmatrix} h_1^* & h_2 \\ h_2^* & -h_1 \end{bmatrix} \tag{3. 8}$$

The estimated symbols will be,

$$\hat{\mathbf{x}} = \mathbf{H}_{\mathbf{eq}}^{\mathrm{H}}\tilde{\mathbf{r}} \tag{3. 9}$$

$$\hat{\mathbf{x}} = \mathbf{H}_{\mathbf{eq}}^{\mathrm{H}}\mathbf{H}_{\mathbf{eq}}\mathbf{x} + \mathbf{H}_{\mathbf{eq}}^{\mathrm{H}}\tilde{\mathbf{n}}$$

Using a matrix notation, the symbols estimation is the following,

$$\begin{bmatrix}\hat{x}(0)\\ \hat{x}(1)\end{bmatrix} = \begin{bmatrix}h_1^* & h_2\\ h_2^* & -h_1\end{bmatrix}\begin{bmatrix}h_1 & h_2\\ h_2^* & -h_1^*\end{bmatrix}\begin{bmatrix}x(0)\\ x(1)\end{bmatrix} + \begin{bmatrix}h_1^* & h_2\\ h_2^* & -h_1\end{bmatrix}\begin{bmatrix}n(0)\\ n(1)^*\end{bmatrix}$$

$$\begin{bmatrix}\hat{x}(0)\\ \hat{x}(1)\end{bmatrix} = \begin{bmatrix}h_1h_1^* + h_2h_2^* & 0\\ 0 & h_2^*h_2 + h_1^*h_1\end{bmatrix}\begin{bmatrix}x(0)\\ x(1)\end{bmatrix} + \begin{bmatrix}h_1^* & h_2\\ h_2^* & -h_1\end{bmatrix}\begin{bmatrix}n(0)\\ n(1)^*\end{bmatrix}$$

$$\hat{x}(0) = (|h_1|^2 + |h_2|^2)x(0) + h_1^*n(0) + h_2n(1)^*$$

$$\hat{x}(1) = (|h_1|^2 + |h_2|^2)x(1) + h_2^*n(0) - h_1n(1)^*$$

Looking to $\hat{\boldsymbol{x}}$ we can see that is possible separate the signals without interference between them, we also should note that the channel response must be stable during 2 symbols periods. In this case we receive the 2 symbols across 2 independent channel paths; therefore we achieve a full diversity order of 2. Using M antennas at the receiver, we achieve diversity order of $2M$.

The above Alamouti STBC scheme is only available for 2 antennas at the transmitter. One possible solution of apply Alamouti coding in the case of 4 antennas transmission is performing a time and space shift of Alamouti blocks using a STBC-Time Shift Transmit Diversity (STBC-TSTD) scheme, like is shown in Figure 3.10.

The space-time mapping of STBC-TSTD is presented in Figure 3.10.

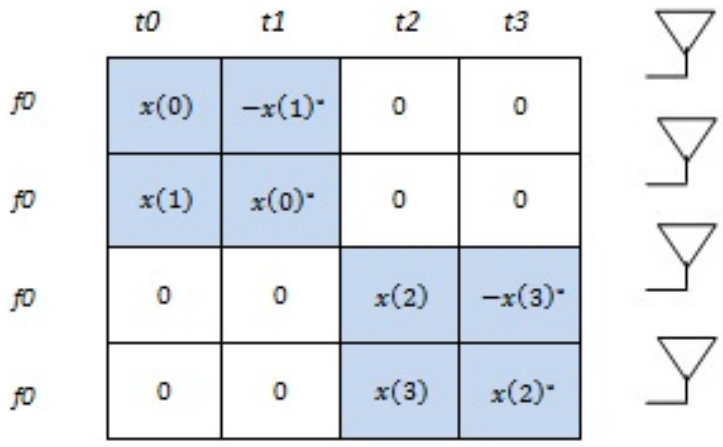

Figure 3. 10 - STBC-TSTD mapping

We can see in the above figure that in practice STBC-TSTD is the normal Alamouti scheme for 2 antennas, the only difference is the exchange of the pair of transmit antennas between consecutive code blocks. Therefore, we continue to achieve the same diversity level, but now we have the liberty of switch the antennas used in each time block. The decoding process of STBC-TSTD is similar of SFBC-FSTD, which we will compute later in the chapter of LTE transmission modes [8][9].

The OFDM mapping of STBC-TSTD is shown below.

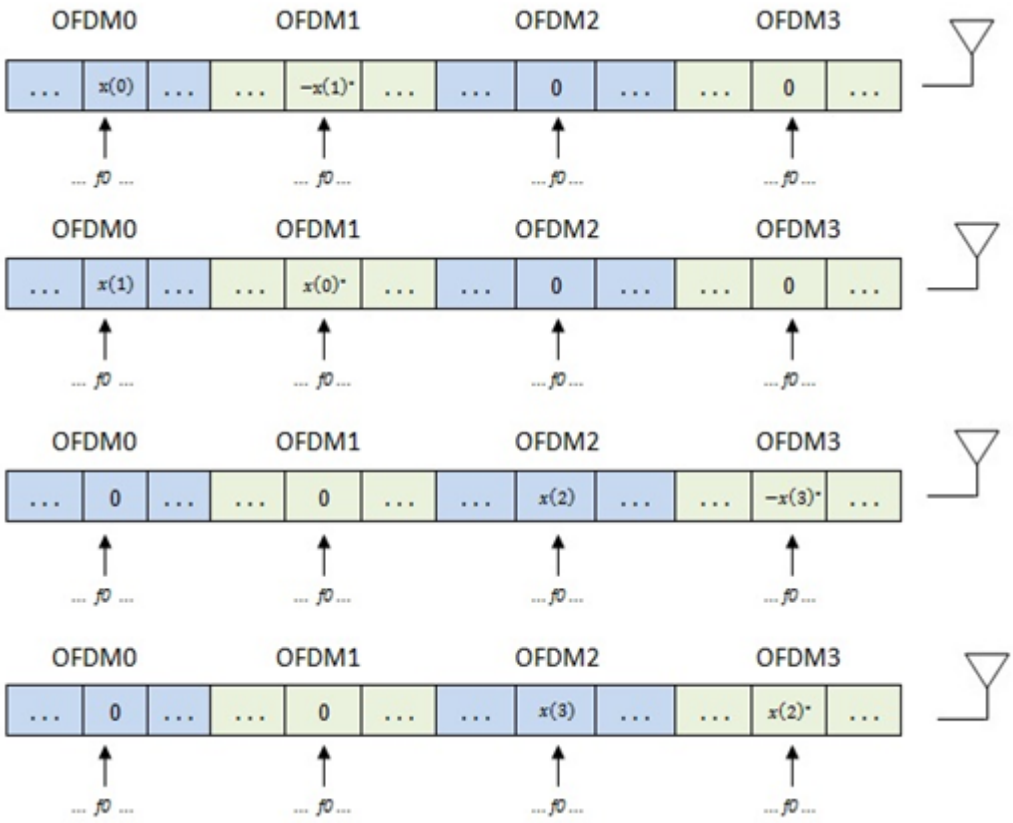

Figure 3. 11 - STBC-TSTD OFDM mapping

3.2.2. ABBA Coding

The ABBA coding is quasi-orthogonal block code that can be used in the case of 4 transmit antennas. Due to the fact that ABBA coding doesn't allow full orthogonality between the antenna data streams, the receiver will be unable to separate the symbols without interference between them.

From this point forward we will consider in all processing schemes where frequency subcarriers are used, that the channel frequency response where each OFDM subcarrier is located, has a flat response. We will also assume that the symbols are separate without interference across the frequency subcarriers using OFDM demodulation.

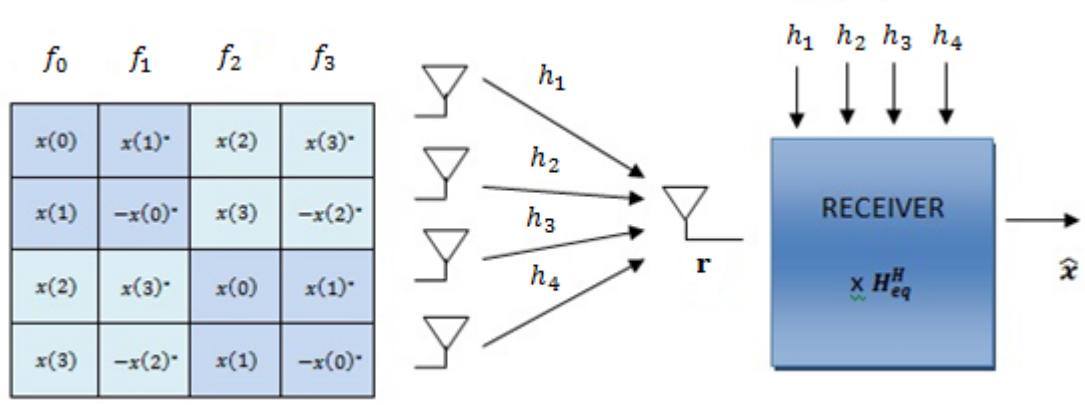

Figure 3. 12 - ABBA coding mapping

$$\mathbf{ABBA} = \begin{bmatrix} \mathbf{A} & \mathbf{B} \\ \mathbf{B} & \mathbf{A} \end{bmatrix} \qquad \mathbf{A} = \begin{bmatrix} x(0) & x(1)^* \\ x(1) & -x(0)^* \end{bmatrix} \qquad \mathbf{B} = \begin{bmatrix} x(2) & x(3)^* \\ x(3) & -x(2)^* \end{bmatrix}$$

The ABBA coding uses blocks of 4 symbols to make the coding in space-time/frequency. In Figure 3.12 is shown the mapping of the ABBA coding in space-frequency, so we can see that ABBA coding transmits 4 symbols in one time slot using 4 subcarriers (1 OFDM/antenna). We should note that now it was considered a constant frequency flat channel across 4 subcarriers in each antenna.

The received signal is the following,

$$\mathbf{r} = \mathbf{Xh} + \mathbf{n} \tag{3. 10}$$

$$\begin{bmatrix} r(f_0) \\ r(f_1) \\ r(f_2) \\ r(f_3) \end{bmatrix} = \begin{bmatrix} x(0) & x(1) & x(2) & x(3) \\ x(1)^* & -x(0)^* & x(3)^* & -x(2)^* \\ x(2) & x(3) & x(0) & x(1) \\ x(3)^* & -x(2)^* & x(1)^* & -x(0)^* \end{bmatrix} \begin{bmatrix} h_1 \\ h_2 \\ h_3 \\ h_4 \end{bmatrix} + \begin{bmatrix} n(f_0) \\ n(f_1) \\ n(f_2) \\ n(f_3) \end{bmatrix}$$

Then, the receiver performs the complex conjugate of $r(f_1)$ and $r(f_3)$, which after rearranged can be seen in the following form,

$$\tilde{\mathbf{r}} = \mathbf{H}_{\mathbf{eq}_{\mathbf{ABBA}}}\mathbf{x} + \tilde{\mathbf{n}} \tag{3. 11}$$

$$\begin{bmatrix} r(f_0) \\ r(f_1)^* \\ r(f_2) \\ r(f_3)^* \end{bmatrix} = \begin{bmatrix} h_1 & h_2 & h_3 & h_4 \\ -h_2^* & h_1^* & -h_4^* & h_3^* \\ h_3 & h_4 & h_1 & h_2 \\ -h_4^* & h_3^* & -h_2^* & h_1^* \end{bmatrix} \begin{bmatrix} x(0) \\ x(1) \\ x(2) \\ x(3) \end{bmatrix} + \begin{bmatrix} n(f_0) \\ n(f_1)^* \\ n(f_2) \\ n(f_3)^* \end{bmatrix}$$

Based on the above matrix treatment and with channel knowledge available, the receiver will use $\tilde{\mathbf{r}}$ and a MF (Matched Filter) version of $\mathbf{H}_{\mathbf{eq}_{\mathbf{ABBA}}}$ to decode the received signal $\mathbf{r}$.

$$\hat{\mathbf{x}} = \mathbf{H}_{\mathbf{eq}_{\mathbf{ABBA}}}^{\mathbf{H}} \tilde{\mathbf{r}} \tag{3. 12}$$

$$\hat{\mathbf{x}} = \mathbf{H}_{\mathbf{eq}_{\mathbf{ABBA}}}^{\mathbf{H}} \mathbf{H}_{\mathbf{eq}_{\mathbf{ABBA}}} \mathbf{x} + \mathbf{H}_{\mathbf{eq}_{\mathbf{ABBA}}}^{\mathbf{H}} \tilde{\mathbf{n}}$$

We can see the estimated symbols in the following matrix notation,

$$\begin{bmatrix} \hat{x}(0) \\ \hat{x}(1) \\ \hat{x}(2) \\ \hat{x}(3) \end{bmatrix} = \begin{bmatrix} h_1^* & -h_2 & h_3^* & -h_4 \\ h_2^* & h_1 & h_4^* & h_3 \\ h_3^* & -h_4 & h_1^* & -h_2 \\ h_4^* & h_3 & h_2^* & h_1 \end{bmatrix} \begin{bmatrix} h_1 & h_2 & h_3 & h_4 \\ -h_2^* & h_1^* & -h_4^* & h_3^* \\ h_3 & h_4 & h_1 & h_2 \\ -h_4^* & h_3^* & -h_2^* & h_1^* \end{bmatrix} \begin{bmatrix} x(0) \\ x(1) \\ x(2) \\ x(3) \end{bmatrix} + \begin{bmatrix} \tilde{n}_0 \\ \tilde{n}_1 \\ \tilde{n}_2 \\ \tilde{n}_3 \end{bmatrix}$$

$$\begin{bmatrix} \hat{x}(0) \\ \hat{x}(1) \\ \hat{x}(2) \\ \hat{x}(3) \end{bmatrix} = A \begin{bmatrix} 1 & 0 & X & 0 \\ 0 & 1 & 0 & X \\ X & 0 & 1 & 0 \\ 0 & X & 0 & 1 \end{bmatrix} \begin{bmatrix} x(0) \\ x(1) \\ x(2) \\ x(3) \end{bmatrix} + \begin{bmatrix} \tilde{n}_0 \\ \tilde{n}_1 \\ \tilde{n}_2 \\ \tilde{n}_3 \end{bmatrix}$$

$$A = |h_1|^2 + |h_2|^2 + |h_3|^2 + |h_4|^2 \tag{3. 13}$$

Looking to the above result we can figure out that symbol $x(2)$ interferes with $x(0)$, $x(3)$ interferes with $x(1)$, $x(0)$ with $x(2)$ and $x(1)$ with $x(3)$[9].

3.2.3. Tarohk Codes

Another solution beyond the quasi-orthogonal codes, is the use of code rates lower than 1. An example of such codes is the Tarohk case, which can be used for transmit diversity across 4 antennas using a code rate of 1/2. The advantage of use code rates lower than 1, is that we can achieve full orthogonality between the streams in each antenna, making full diversity order possible; the cost is the necessity of increase the bandwidth used, or else, decrease the transmission rate. Note that due the code rate be 1/2, we will need 8 frequency subcarriers or 8 time slots to transmit only 4 symbols [8][9].

$$\mathbf{x_{in}} = [x(0) \quad x(1) \quad x(2) \quad x(3)]^T$$

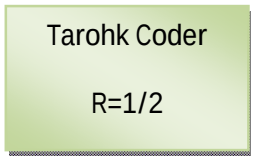

$$\mathbf{X} = \underbrace{\begin{bmatrix} x(0) & -x(1) & -x(2) & -x(3) & x(0)^* & -x(1)^* & -x(2)^* & -x(3)^* \\ x(1) & x(0) & x(3) & -x(2) & x(1)^* & x(0)^* & x(3)^* & -x(2)^* \\ x(2) & -x(3) & x(0) & x(1) & x(2)^* & -x(3)^* & x(0)^* & x(1)^* \\ x(3) & x(2) & -x(1) & x(0) & x(3)^* & x(2)^* & -x(1)^* & x(0)^* \end{bmatrix}}_{\text{8 Slots/Subcarriers}}$$

Using 4 antennas in transmission and 1 antenna at the receiver, and considering that the frequency channel response is constant across the 8 subcarriers, the received signal $r(f_k)$ in each k subcarrier will be the following,

$$\mathbf{r} = \mathbf{X^T h} + \mathbf{n} \tag{3. 14}$$

$$\begin{bmatrix} r(f_0) \\ r(f_1) \\ r(f_2) \\ r(f_3) \\ r(f_4) \\ r(f_5) \\ r(f_6) \\ r(f_7) \end{bmatrix} = \mathbf{X^T} \begin{bmatrix} h_0 \\ h_1 \\ h_2 \\ h_3 \end{bmatrix} + \begin{bmatrix} n_0 \\ n_1 \\ n_2 \\ n_3 \\ n_4 \\ n_5 \\ n_6 \\ n_7 \end{bmatrix}$$

$$r(f_0) = h_0x(0) + h_1x(1) + h_2x(2) + h_3x(3) + n_0$$

$$r(f_1) = -h_0x(1) + h_1x(0) - h_2x(3) + h_3x(2) + n_1$$

$$r(f_2) = -h_0x(2) + h_1x(3) + h_2x(0) - h_3x(1) + n_2$$

$$r(f_3) = -h_0x(3) - h_1x(2) + h_2x(1) + h_3x(0) + n_3$$

$$r(f_4) = h_0x(0)^* + h_1x(1)^* + h_2x(2)^* + h_3x(3)^* + n_4$$

$$r(f_5) = -h_0x(1)^* + h_1x(0)^* - h_2x(3)^* + h_3x(2)^* + n_5$$

$$r(f_6) = -h_0x(2)^* + h_1x(3)^* + h_2x(0)^* - h_3x(1)^* + n_6$$

$$r(f_7) = -h_0x(3)^* - h_1x(2)^* + h_2x(1)^* + h_3x(0)^* + n_7$$

The receiver performs the complex conjugate of signals $r(f_4)$, $r(f_5)$, $r(f_6)$ and $r(f_7)$, which we can be seen in the following form,

$$\tilde{\mathbf{r}} = \tilde{\mathbf{H}}\mathbf{x} + \tilde{\mathbf{n}} \tag{3. 15}$$

$$\begin{bmatrix} r(f_0) \\ r(f_1) \\ r(f_2) \\ r(f_3) \\ r(f_4)^* \\ r(f_5)^* \\ r(f_6)^* \\ r(f_7)^* \end{bmatrix} = \begin{bmatrix} h_0 & h_1 & h_2 & h_3 \\ h_1 & -h_0 & h_3 & -h_2 \\ h_2 & -h_3 & -h_0 & h_1 \\ h_3 & h_2 & -h_1 & -h_0 \\ h_0^* & h_1^* & h_2^* & h_3^* \\ h_1^* & -h_0^* & h_3^* & -h_2^* \\ h_2^* & -h_3^* & -h_0^* & h_1^* \\ h_3^* & h_2^* & -h_1^* & -h_0^* \end{bmatrix} \begin{bmatrix} x(0) \\ x(1) \\ x(2) \\ x(3) \end{bmatrix} + \begin{bmatrix} n_0 \\ n_1 \\ n_2 \\ n_3 \\ n_4^* \\ n_5^* \\ n_6^* \\ n_7^* \end{bmatrix}$$

Then, with the channel knowledge available at the receiver, $\tilde{\mathbf{H}}^{\mathrm{H}}$ is computed in order to estimate the received symbols.

$$\tilde{\mathbf{H}}^{\mathrm{H}} = \begin{bmatrix} h_0^* & h_1^* & h_2^* & h_3^* & h_0 & h_1 & h_2 & h_3 \\ h_1^* & -h_0^* & -h_3^* & h_2^* & h_1 & -h_0 & -h_3 & h_2 \\ h_2^* & h_3^* & -h_0^* & -h_1^* & h_2 & h_3 & -h_0 & -h_1 \\ h_3^* & -h_2^* & h_1^* & -h_0^* & h_3 & -h_2 & h_1 & -h_0 \end{bmatrix} \tag{3. 16}$$

Thus the estimated symbols $\hat{\boldsymbol{x}}$ are obtained performing the follow operation,

$$\hat{\mathbf{x}} = \tilde{\mathbf{H}}^{\mathrm{H}}\tilde{\mathbf{r}} \tag{3. 17}$$

$$\hat{\mathbf{x}} = \tilde{\mathbf{H}}^{\mathrm{H}}\tilde{\mathbf{H}}\mathbf{x} + \tilde{\mathbf{H}}^{\mathrm{H}}\tilde{\mathbf{n}}$$

$$\begin{bmatrix} \hat{x}(0) \\ \hat{x}(1) \\ \hat{x}(2) \\ \hat{x}(3) \end{bmatrix} = \begin{bmatrix} A & 0 & 0 & 0 \\ 0 & A & 0 & 0 \\ 0 & 0 & A & 0 \\ 0 & 0 & 0 & A \end{bmatrix} \begin{bmatrix} x(0) \\ x(1) \\ x(2) \\ x(3) \end{bmatrix} + \begin{bmatrix} \tilde{n}_0 \\ \tilde{n}_1 \\ \tilde{n}_2 \\ \tilde{n}_3 \end{bmatrix}$$

$$A = 2\sum_{n=1}^{4} |h_n|^2 \tag{3. 18}$$

3.3. Receive Diversity Schemes

With multiple antennas at the receiver, we can decrease the influence of the multipath channel effect using spatial diversity antenna reception. Therefore we can use not only time and frequency diversity, but also spatial diversity at the reception.

The use of N_R antennas at the receiver will allow the reception of the symbols across N_R channels. Then, we can use different processing combination techniques to improve the SNR

performance at the receiver. The aim of these type of combination schemes is to use the N_R copies of the signal that arrive at each one of the receiver antennas, and then, combine them together like is shown in Figure 3.13 [3][8].

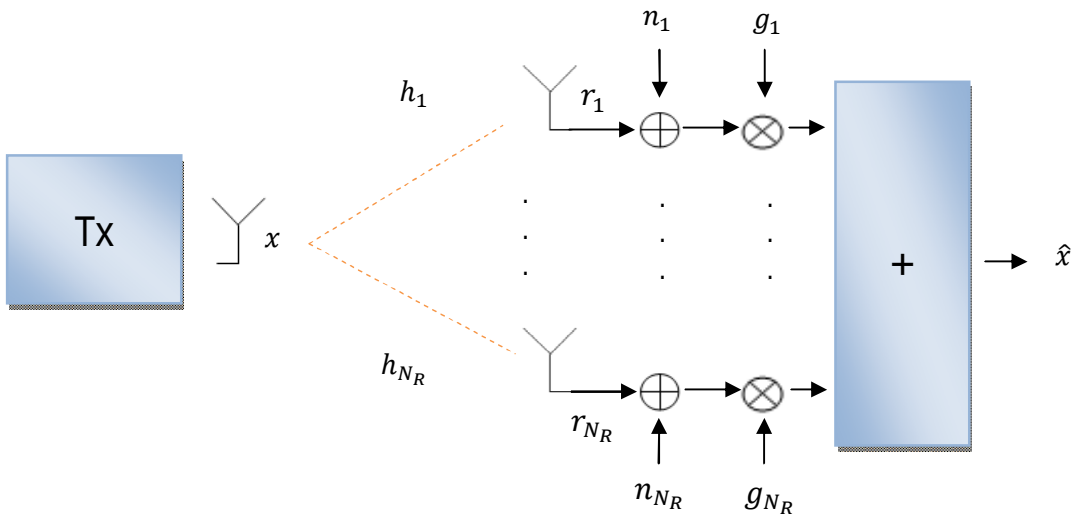

Figure 3. 13 - Spatial receive antenna diversity

The overall signal model for the received symbol will be the following,

$$\begin{bmatrix} r_1 \\ \vdots \\ r_{N_R} \end{bmatrix} = \begin{bmatrix} h_1 \\ \vdots \\ h_{N_R} \end{bmatrix} x + \begin{bmatrix} n_1 \\ \vdots \\ n_{N_R} \end{bmatrix} \tag{3. 19}$$

The estimated symbols will be,

$$\hat{x} = [g_1 \quad \cdots \quad g_{N_R}] \begin{bmatrix} r_1 \\ \vdots \\ r_{N_R} \end{bmatrix} \tag{3. 20}$$

$$\hat{x} = [g_1 \quad \cdots \quad g_{N_R}] \begin{bmatrix} h_1 \\ \vdots \\ h_{N_R} \end{bmatrix} x + [g_1 \quad \cdots \quad g_{N_R}] \begin{bmatrix} n_1 \\ \vdots \\ n_{N_R} \end{bmatrix}$$

3.3.1. MRC combining

The Maximum Ratio Combining (MRC) is used when he we want maximize the SNR in order to eliminate bad noise conditions at the reception. Hence, the g_i coefficients computed, are equal to the conjugate transpose $(.)^H$ of the channel instantaneous coefficients vector.

$$\mathbf{g} = \mathbf{h}^{\mathbf{H}} \tag{3. 21}$$

$$g_i = h_i^*, \quad i = 1, \ldots, N_R$$

Therefore, with accurate channel knowledge **h** at the receiver, we can compute the MRC weights.

The MRC combining at the receiver output will be:

$$\hat{x} = \sum_{i=1}^{N_R} |h_i|^2 x + \sum_{i=1}^{N_R} h_i^* n_i \quad \text{(3. 22)}$$

Note that MRC maximizes SNR aligning the phases of all N_R channel coefficients, and also giving more weight to the best channels h_i with $|h_i|^2$. The antenna gain achieved with this combining technique is equal N_R.

3.3.2. EGC combining

The Equal Gain Combining scheme just rotates the phases of the arrived signals at each antenna. Therefore, the weights that will be given at each branch are complex numbers with unitary amplitude and 180° phase shift relative to the phase θ_i of channel response $h_i = |h_i|e^{j\Theta_i}$.

$$g_i = \frac{h_i^*}{|h_i|} = \frac{|h_i|e^{-j\Theta_i}}{|h_i|} = e^{-j\Theta_i}, \quad i = 1, \dots, N_R \quad \text{(3. 23)}$$

We can see from the above expression that the amplitude weights are equal for all the N_R antennas. At the receiver output the estimated symbol is,

$$\hat{x} = \sum_{i=1}^{N_R} h_i g_i x + \sum_{i=1}^{N_R} g_i n_i \quad \text{(3. 24)}$$

$$\hat{x} = \sum_{i=1}^{N_R} \frac{|h_i|e^{j\Theta_i}}{e^{j\Theta_i}} x + \sum_{i=1}^{N_R} e^{-j\Theta_i} n_i$$

$$\hat{x} = \sum_{i=1}^{N_R} |h_i| x + \sum_{i=1}^{N_R} e^{-j\Theta_i} n_i$$

In this case the antenna gain A_g will be smaller than the MRC case,

$$A_g = 1 + \frac{\pi}{4}(N_R - 1) \quad \text{(3. 25)}$$

3.3.3. SC combining

The Selection Combining receiver only uses the antenna with the highest channel amplitude of all the receiver antennas, thus the received signals in the other $N_R - 1$ antennas are ignored. Therefore the receiver must to seek the antenna with best channel conditions.

$$|h_{max}| = \max\left[|h_i|\right], \quad i = 1, \dots, N_R \tag{3. 26}$$

$$g_{max} = h_{max}^* \tag{3. 27}$$

$$\hat{x} = g_{max}(h_{max}x + n_{max}) \tag{3. 28}$$

$$\hat{x} = h_{max}h_{max}^* x + h_{max}^* n_{max}$$

$$\hat{x} = |h_{max}|^2 x + h_{max}^* n_{max}$$

In relation to A_g, we will not develop the demonstration process, and thus only the result is presented in expression 3.30.

$$A_g = \sum_{i=1}^{N_R} \frac{1}{i} \tag{3. 29}$$

So we can see that in SC scheme A_g keeps growing with the receiver antenna number, but in a non-linear way, and lesser than in MRC case and EGC case.

3.3.4. IRC combining

In MRC case the target is to improve the reception under bad noise conditions, now the aim is to remove dominant intercellular/intracellular interference sources. Thus the choice is to use IRC (Interference Rejection Combining) for the receiver.

If we consider **r** the received vector signal affected by the interference of x_I symbol transmitted over the $\mathbf{h_I}$ channel, we can figure out (looking at the below expression) that the interference of x_I will be cancelled if we choose a weight vector **g** that verifies the condition 3.31. Note that to compute **g**, channel knowledge of the interference source $\mathbf{h_I}$ must be available at the receiver, hence some kind of feedback scheme between the base stations, or directly between the interfering BS and the receiver, must be performed in order to acquire this information.

$$\mathbf{r} = \mathbf{h}x + \mathbf{h_I}x_I + \mathbf{n} \tag{3. 30}$$

$$\begin{bmatrix} r_1 \\ \vdots \\ r_{N_R} \end{bmatrix} = \begin{bmatrix} h_1 \\ \vdots \\ h_{N_R} \end{bmatrix} x + \begin{bmatrix} h_{I,1} \\ \vdots \\ h_{I,N_R} \end{bmatrix} x_I + \begin{bmatrix} n_1 \\ \vdots \\ n_{N_R} \end{bmatrix}$$

$$\mathbf{g}.\mathbf{h_I} = 0 \tag{3. 31}$$

In Figure 3.14 is presented a situation where a single antenna BS2, interferes with BS1 during the transmission to a UE with 2 antennas.

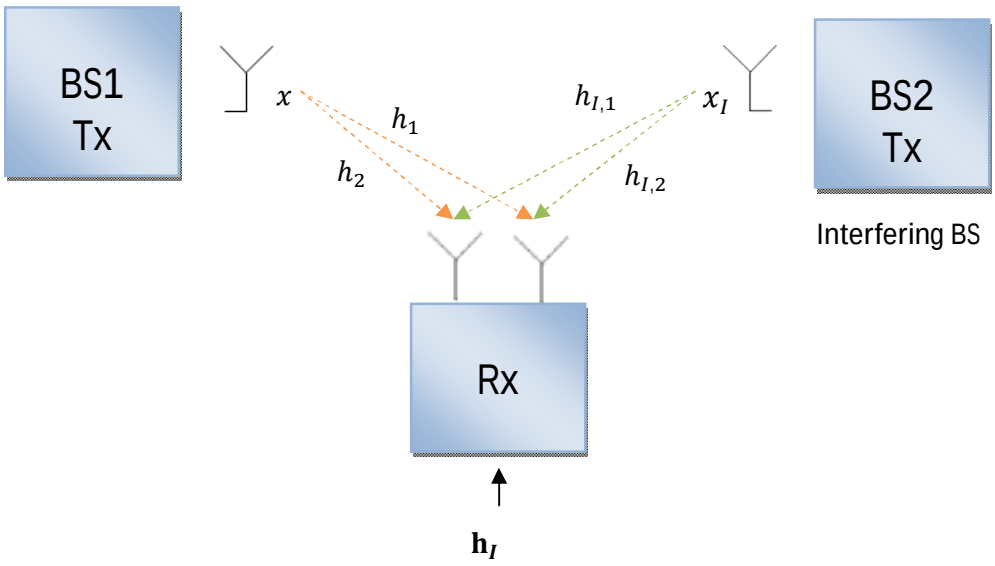

Figure 3. 14 - Intercellular interference situation

3.4. SU-MIMO Techniques for Spatial Multiplexing

3.4.1. SU-MIMO with CSI known at both Tx and Rx

In the earlier chapters we present in a quick way the MIMO spatial multiplexing mechanism, and we said that the optimal signal processing technique used to generate the non-interfering channels, were based in SVD decomposition of the channel matrix **H**. Remember that transmit precoding and receive beamforming via SVD requires full and precise CSI at both sides of the link, so we will consider that CSI is available at both BS and UE. In this part we will show how this processing technique is used to create the channel pipes [2][8].

Let's assume the transmission of r parallel data streams ($r \leq \min(N_R, N_T)$) over a $N_R \times N_T$ MIMO channel in a given subcarrier i, like is presented in Figure 3.15.

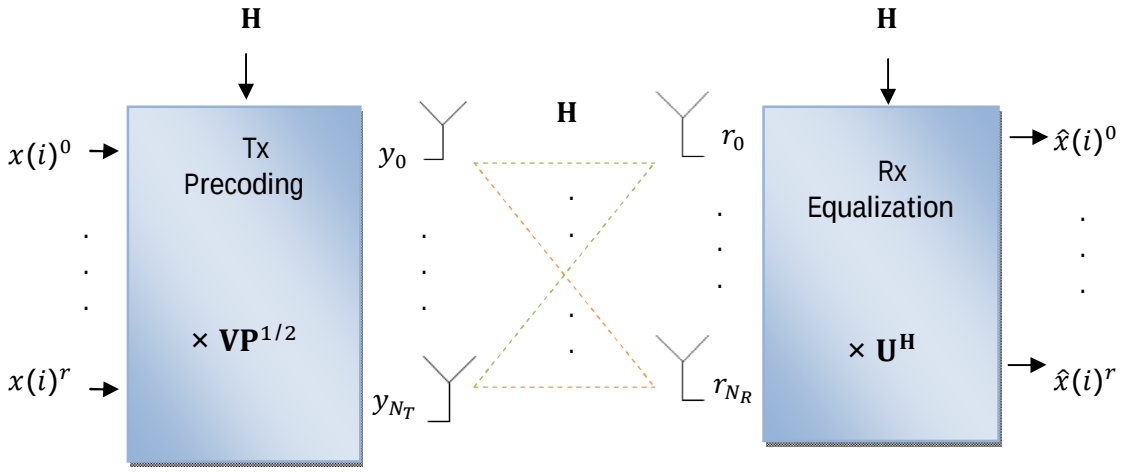

Figure 3. 15 - MIMO channel

Let's consider the following matrices and vectors,

$$\mathbf{x} = [x^0(i) \ldots x^r(i)]^T \qquad \hat{\mathbf{x}} = [\hat{x}^0(i) \ldots \hat{x}^r(i)]^T$$

$$\mathbf{y} = [y_0(i) \ldots y_{N_T}(i)]^T \qquad \mathbf{r} = [r_0(i) \ldots r_{N_R}(i)]^T$$

$$i - subcarrier\ index$$

The noise added in each receive antenna (not present in Figure 3.15) is the following,

$$\mathbf{n} = [n_0(i) \ldots n_{N_R}(i)]^T \tag{3. 32}$$

The MIMO channel matrix for a given subcarrier index is the following,

$$\mathbf{H} = \begin{bmatrix} h_{11} & \cdots & h_{1N_T} \\ \vdots & \ddots & \vdots \\ h_{N_R 1} & \cdots & h_{N_R N_T} \end{bmatrix} \tag{3. 33}$$

Like we seen before, the signal model is,

$$\mathbf{r} = \mathbf{Hy} + \mathbf{n} \tag{3. 34}$$

The SVD process starts after both the transmitter (BS) and receiver (UE) acquire the CSI **H**; then, using SVD they will decompose the channel in the following way,

$$\mathbf{H} = \mathbf{U}\mathbf{D}\mathbf{V}^{\mathrm{H}} \tag{3. 35}$$

The transmitter (BS) will use the diagonal $r \times r$ matrix **D** for select the correct power allocation, and also will use the $r \times N_T$ matrix $\mathbf{V}^{\mathrm{H}}$ to compute the precoding matrix **V**. The receiver (UE) will use the $N_R \times r$ matrix **U** to compute the equalization matrix $\mathbf{U}^{\mathrm{H}}$. It is important refer that matrices **U** and **V** are computed in order to be unitary matrices, i.e., the multiplication of these matrices by their respective conjugate transpose (Hermitian operation) results in an identity matrix.

Therefore the precoding at the transmitter will be the following,

$$\mathbf{W} = \mathbf{V}\mathbf{P}^{\frac{1}{2}} \tag{3. 36}$$

$$\mathbf{W} = \begin{bmatrix} v_{11} & \cdots & v_{1r} \\ \vdots & \ddots & \vdots \\ v_{N_T 1} & \cdots & v_{N_T r} \end{bmatrix} \begin{bmatrix} \sqrt{p_1} & 0 & 0 \\ 0 & \ddots & 0 \\ 0 & 0 & \sqrt{p_r} \end{bmatrix}$$

$$\mathbf{W}_{N_T \times r} = \begin{bmatrix} v_{11}\sqrt{p_1} & \cdots & v_{1r}\sqrt{p_r} \\ \vdots & \ddots & \vdots \\ v_{N_T 1}\sqrt{p_1} & \cdots & v_{N_T r}\sqrt{p_r} \end{bmatrix}$$

The $r \times r$ matrix $\mathbf{P}^{1/2}$ will be selected according the diagonal values λ (singular values of **H**) of matrix **D**. The singular values will tell us the channel/pipes of **H** which are in best condition, so that we are able to adapt the number of layers transmitted in the same frequency (rank value) performing a correct power allocation across each one of these r pipes.

The diagonal $r \times r$ matrix **D** is the following,

$$\mathbf{D} = \begin{bmatrix} \lambda_1 & 0 & 0 \\ 0 & \ddots & 0 \\ 0 & 0 & \lambda_r \end{bmatrix} \tag{3. 37}$$

Later we will talk about the algorithm used to allocate the power across the channels.

The transmitted signal **y** will be,

$$\mathbf{y} = \mathbf{V}\mathbf{P}^{\frac{1}{2}}\mathbf{x} \tag{3. 38}$$

The received signal is,

$$\mathbf{r} = \mathbf{Hy} + \mathbf{n} \tag{3. 39}$$

$$\mathbf{r} = \mathbf{UDV}^{\mathrm{H}}\mathbf{VP}^{\frac{1}{2}}\mathbf{x} + \mathbf{n}$$

The receiver will use $\mathbf{U}$ matrix to compute the equalization matrix $\mathbf{U}^{\mathrm{H}}$.

$$\mathbf{G} = \mathbf{U}^{\mathrm{H}} \tag{3. 40}$$

After equalization in the receiver the estimative $\hat{\boldsymbol{x}}$ will be,

$$\hat{\mathbf{x}} = \mathbf{Gr} \tag{3. 41}$$

$$\hat{\mathbf{x}} = \mathbf{U^H UDV}^{\mathrm{H}}\mathbf{VP}^{\frac{1}{2}}\mathbf{x} + \mathbf{U^H n}$$

With $\mathbf{U}$ and $\mathbf{V}$ being unitary matrices, the following result is obtained for $\hat{\mathbf{x}}$,

$$\hat{\mathbf{x}} = \mathbf{DP}^{\frac{1}{2}}\mathbf{x} + \mathbf{U^H n}$$

$$\begin{bmatrix} \hat{x}^0 \\ \vdots \\ \hat{x}^r \end{bmatrix} = \begin{bmatrix} \lambda_1 & 0 & 0 \\ 0 & \ddots & 0 \\ 0 & 0 & \lambda_r \end{bmatrix} \begin{bmatrix} \sqrt{p_1} & 0 & 0 \\ 0 & \ddots & 0 \\ 0 & 0 & \sqrt{p_r} \end{bmatrix} \begin{bmatrix} x^0 \\ \vdots \\ x^r \end{bmatrix} + \mathbf{U^H n}$$

$$\hat{x}^0 = \lambda_1\sqrt{p_1}x^0 + \bar{n}_0$$

$$\hat{x}^1 = \lambda_2\sqrt{p_2}x^1 + \bar{n}_1$$

$$\vdots$$

$$\hat{x}^r = \lambda_r\sqrt{p_r}x^r + \bar{n}_r$$

Looking to the above result we can see that using SVD based precoding/equalization we are able to eliminate interference between the r transmitted layers and also adapt the number of symbols transmitted in the same frequency computing a correct power allocation.

The channel capacity via SVD decomposition is the following,

$$C = \sum_{k=1}^{r} \log_2\left(1 + \frac{\lambda_k^2 p_k}{\sigma^2}\right) \quad bits/\,s\,/\,Hz \tag{3. 42}$$

The selection of power that we will allocate in each pipe is done in order maximize the system capacity. The amount of power put in each channel is done using 'water filling' power algorithm. This algorithm will see the SNR (λ_k^2/σ^2) in each pipe using the singular values, then according

the defined power constraint for this transmission, will select a limit (water level), used to decide the amount of power allocated in each channel. If the SNR of a pipe/channel is so low that results in water level override, the power allocated in this channel will be 0,transmitting least one symbol in the same frequency.

We can see a graphical representation of water filling algorithm in Figure 3.16.

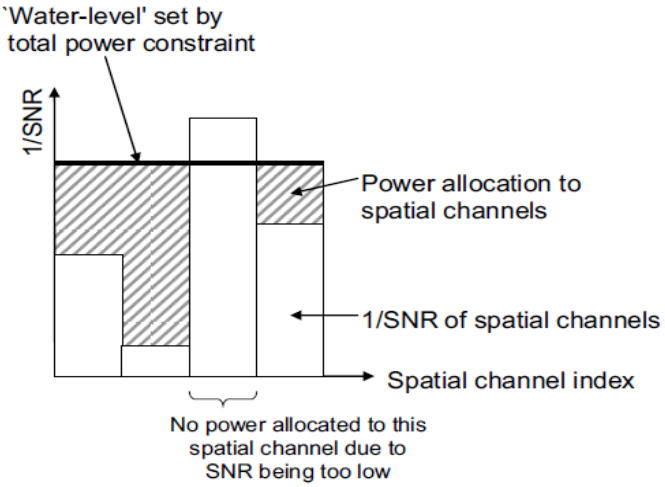

Figure 3. 16 - Water filling power scheme [2]

Using the mathematical Lagrangian method we will obtain the following expression that will tell us the best power allocation scheme to optimize system capacity.

$$p_i = \left(\beta - \frac{1}{SNR_k}\right)^+ \tag{3. 43}$$

$$p_i = \left(\beta - \frac{\sigma^2}{\lambda_k^2}\right)^+$$

Where k, β, σ^2 are the pipe index, the water level value and the noise power respectively.

$$a^+ = \max(a, 0) = \begin{cases} a^+ = a; & if\ a \geq 0 \\ a^+ = 0; & if\ a < 0 \end{cases} \tag{3. 44}$$

We can figure out that the "water-filling" algorithm principle is based in allocate more power in the better channels (high λ_k) and reduce the amount of power in the bad channels (low λ_k). Allocating more power in the better channels we are able to increase the data-rate in these channels, and at the same time reduce the rate in the bad ones; therefore the rank, the modulation size (QPSK, 16-QAM, 64-QAM) and the channel coding rate could be adapted according the 'singular-values' [2][8].

3.4.2. SU-MIMO with CSI known only at Rx

In the case of CSI only available at the receiver, we are not able to use the SVD channel decomposition, therefore no channel dependent precoding is done, and the separation of the r layers is achieved performing an equalization process at the receiver side. We can use linear equalizers, like Zero Forcing (ZF) and Minimum Mean Square Error (MMSE), or non-linear equalizers like Successive Interference Cancelation-ZF (SIC-ZF) or Successive Interference Cancelation-MMSE (SIC-MMSE).

In this part we will use the same signal model of the previous subchapter, with the only difference that now no CSI is available at the transmitter. Consider that we will perform a SM N_T rank transmission through an $N_R \times N_T$ MIMO channel $\mathbf{H}$ with $N_R \geq N_T$.

The precoding matrix $\mathbf{W}$ at the transmitter is only performed by an $N_T \times N_T$ identity matrix, and the transmitted signal $\mathbf{y}$ is the following,

$$\mathbf{y} = \mathbf{W}\mathbf{x} \tag{3. 45}$$

$$\mathbf{y} = \mathbf{I}_{\mathrm{N_T}}\mathbf{x}$$

$$\begin{bmatrix} y_0 \\ \vdots \\ y_{N_T} \end{bmatrix} = \begin{bmatrix} x^0 \\ \vdots \\ x^{N_T} \end{bmatrix}$$

The received signal will be,

$$\mathbf{r} = \mathbf{H}\mathbf{y} + \mathbf{n} \tag{3. 46}$$

At the receiver, if ZF (Zero-Forcing) equalizer is used, and $N_R \geq N_T$, we are able to full eliminate the inter-symbol interference.

$$\mathbf{G}_{\mathrm{ZF}} = \left(\mathbf{H}^{\mathrm{H}}\mathbf{H}\right)^{-1}\mathbf{H}^{\mathrm{H}} \tag{3. 47}$$

Using the ZF equalizer, the symbols are completely separated, and the output signal is only affected by the noise, like is shown below.

$$\hat{\mathbf{x}} = \mathbf{G}_{\mathrm{ZF}}\mathbf{r} \tag{3. 48}$$

$$\hat{\mathbf{x}} = \mathbf{G}_{\mathrm{ZF}}\mathbf{H}\mathbf{y} + \mathbf{G}_{\mathrm{ZF}}\mathbf{n}$$

$$\hat{\mathbf{x}} = \left(\mathbf{H}^{\mathrm{H}}\mathbf{H}\right)^{-1}\mathbf{H}^{\mathrm{H}}\mathbf{H}\mathbf{x} + \left(\mathbf{H}^{\mathrm{H}}\mathbf{H}\right)^{-1}\mathbf{H}^{\mathrm{H}}\mathbf{n}$$

$$\hat{\mathbf{x}} = \mathbf{I}_{\mathrm{N_T}}\mathbf{x} + \left(\mathbf{H}^{\mathrm{H}}\mathbf{H}\right)^{-1}\mathbf{H}^{\mathrm{H}}\mathbf{n}$$

$$\begin{bmatrix} \hat{x}^0 \\ \vdots \\ \hat{x}^{N_T} \end{bmatrix} = \begin{bmatrix} x^0 \\ \vdots \\ x^{N_T} \end{bmatrix} + \begin{bmatrix} \tilde{n}_0 \\ \vdots \\ \tilde{n}_{N_T} \end{bmatrix}$$

Despite we achieve full symbol separation; the received SNR can be low due noise increase $\mathbf{G}_{\mathrm{ZF}}\mathbf{n}$.

Instead of use ZF, we can improve the SNR using MMSE equalization. The MMSE equalizer makes a balance between channel orthogonality for symbol separation, and channel alignment, in order to increase the SNR for each symbol. The MMSE doesn't achieve full symbol separation, but we have the advantage of higher SNR for each symbol, resulting in BER overall results better than ZF equalizer, like we will see later.

$$\mathbf{G}_{\mathrm{MMSE}} = \left(\mathbf{H}^{\mathrm{H}}\mathbf{H} + \sigma^2\mathbf{I}_{\mathrm{N_T}}\right)^{-1}\mathbf{H}^{\mathrm{H}} \qquad (3.\ 49)$$

Another possibility to equalize the received signal, is the use of non-linear SIC-ZF or SIC-MMSE equalization, which we will present in more detail in chapter 6[2][8].

3.5. MU-MIMO Techniques

The basic principles used for layer separation and signal strength increase in MU-MIMO are the same used in SU-MIMO, but now we should note that the UE's only have CSI of their own receive spatial-signatures h_i, being totally blind about the overall CSI. Therefore, in MU-MIMO, the layers must be separated performing a beamforming/precoding at the transmitter where overall CSI is available, instead of separate them doing equalization at the receiver. We can see that all the signal processing work is done at the transmitter (BS), with the UE just waiting that their symbol arrives without interference. Another difference between SU-MIMO and MU-MIMO is the natural distance separation between the UE's, so natural low correlation conditions between the channels can be obtained doing a correct selection at the BS of the UE's that will share the same subcarriers.

As we said before, the principles used in SU-MIMO are the same used in MU-MIMO, therefore, like in SU-MIMO, where ZF and MMSE equalizers were used to separate the layers at the receiver, in MU-MIMO we also can use ZF and MMSE precoding to separate the layers, but now the separation is done at the transmitter (BS). In mathematical terms there are no difference between remove the interference at receiver or at the transmitter, the only difference is that in MU-MIMO we anticipate the channel effect in the signal, and according that, we adapt

the transmitted signal before the channel affect him; while in SU-MIMO (with CSI only at Rx) we perform the processing in the signal already affected by the channel and noise.

Let's assume $r = N_T = N_R$

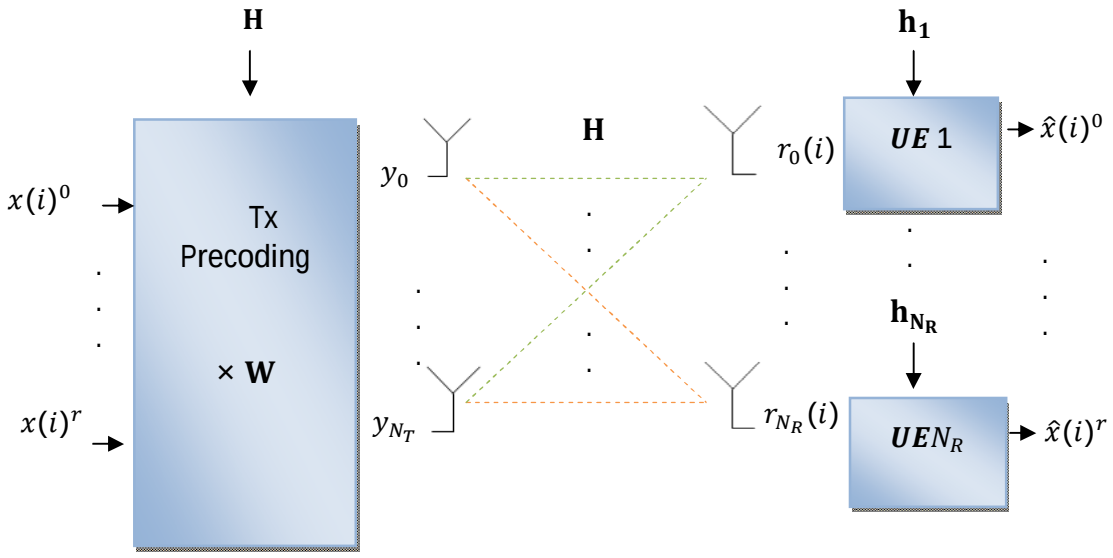

Figure 3. 17 - MU-MIMO model

Let's use as reference the MU-MIMO model presented in Figure 3.17, and also the signal vectors used in the previous subchapters.

Using the ZF precoding $\mathbf{W}_{ZF}$, the transmitted signal $\mathbf{y}$ is the following,

$$\mathbf{W}_{ZF} = \left(\mathbf{H}^{H}\mathbf{H}\right)^{-1}\mathbf{H}^{H} \tag{3. 50}$$

$$\mathbf{y} = \mathbf{W}_{ZF}\mathbf{x} \tag{3. 51}$$

$$\mathbf{y} = \left(\mathbf{H}^{H}\mathbf{H}\right)^{-1}\mathbf{H}^{H}\mathbf{x}$$

Looking to all UEs as a single UE with N_R antennas, the overall received signal will be,

$$\mathbf{r} = \mathbf{H}\mathbf{y} + \mathbf{n} \tag{3. 52}$$

$$\mathbf{r} = \left(\mathbf{H}^{H}\mathbf{H}\right)^{-1}\mathbf{H}^{H}\mathbf{H}\mathbf{x} + \mathbf{n}$$

$$\mathbf{r} = \mathbf{I}_{N_R}\mathbf{x} + \mathbf{n}$$

$$\begin{bmatrix} r_0 \\ \vdots \\ r_{N_R} \end{bmatrix} = \begin{bmatrix} x^0 + n_0 \\ \vdots \\ x^{N_T} + n_{N_R} \end{bmatrix}$$

Using the above result we should figure out that while in receive equalization the noise is affected by the equalization process, in this case the noise is not affected, so we are able to separate the layers without increase the noise. Note that the signal when arrives at each UE is already separated.

The processing methods referred above, are the optimal solution to recover data transmitted over a MIMO channel, but sometimes practical implementation of those methods is not possible to be done exactly like we describe above. We will see later that LTE spatial multiplexing transmission modes in FDD, uses a codebook limited set of matrices to perform precoding at transmission. The index of the matrix is feedback by the UE (CSI available only) to the BS in order to give some kind of CSI to the BS. In LTE, the missing of precise channel knowledge at transmitter for Spatial Multiplexing (SM) modes, makes precoding and equalization via SVD decomposition impossible, so the solution adopted in LTE was the use of a codebook index for transmission precoding, and some kind of equalizer (ZF, MMSE or SIC) at the receiver side [2][8].

4. LTE System Overview

4.1. Introduction to LTE

The LTE standard is a set of technological specifications used to define the interfaces of mobile wireless networks, covering not only the radio interface between BS and the UE, but also the interfaces between several network nodes.

The development of LTE was made by 3GPP specification group, and it was recognized by the ITU-R as a 3.9G technology. Due low performance results at the uplink direction, the International Telecommunications Union-Radio (ITU-R) didn't approved LTE as a 4G technology. The ITU-R is the international regulator for the radio communication sector, therefore every service that use the radio spectrum must be approved by ITU-R. Is the ITU-R that checks if radio technologies fulfill the requirements to be considered as a member of a technological family created by ITU-R. In the 4G family, ITU-R recognizes a radio technology as 4G if they fulfill the requirements specified in the International Mobile Telecommunications-Advanced (IMT-A) technological family. There are two technologies that fulfill the IMT-A requirements: LTE-Advanced from the 3GPP standardization group, and the IEEE 802.16 (WiMax) from the IEEE standardization group.

The 3GPP project towards 4G started with the creation of LTE and System Architecture Evolution (SAE) work items, with the aim of upgrade the RAN and the core parts of the system, respectively. These 2 work items led to the specification of Evolved-UTRA (E-UTRA) to define the radio interface, the Evolved-UTRAN (E-UTRAN) to define the physical infrastructure that supports the radio access network, and the Evolved Packet Core (EPC) for the core network. At the E-UTRA level, we can underline MIMO systems and OFDM radio access schemes as the main changes relatively to 3G UMTS/HSPA radio interface. For the E-UTRAN, the main

modifications are related with the new flat architecture, which led to the specification of x2 and s1 interfaces. At the core network, we can underline the full IP flat architecture and the possibility of interworking with other 3GPP and non-3GPP radio access technologies, as the main features. The massive upgrade of the entire system referred above, allowed a performance boost verified in main assessment metrics such as, spectral efficiency, peak transmission rate, UE latency and connection set-up. All these improvements are detailed in table 2 [2][3][15].

	Downlink Peak Transmission Rate (Mbps)	**Peak Spectral Efficiency(bps/Hz)**	**Latency(ms)**	**Mobility (Km/h)**
3G HSDPA R6	14.4	3	50	250
4G LTE	100 - 1x1 326 - 4x4 (FDD, 20 MHz, 64-QAM)	> 5	5	350

Table 2 - Performance target comparison between 4G LTE and 3G HSDPA

MIMO	**Modulation**	**Multiple Access**	**Duplexing**	**Channel Coding**	**Bandwidth (MHz)**
DW: 2x2, 4x2, 4x4 UP: 1x2, 1x4	QPSK, 16-QAM, 64-QAM	DW: OFDM UP: SC-FDMA	FDD TDD	Turbo Coding	1.25, 2.5, 5, 10, 15, 20

Table 3 - LTE main E-UTRA Specifications

4.2. LTE Network Architecture Overview

In this point is presented the network architecture in which the LTE radio interface is integrated. The LTE radio interface was developed in parallel with some design improvements at the Core Network (CN) level, which played an important role in the changing of the CN design paradigms. Therefore we will underline the functions of the main logical nodes at both CN and RAN parts of the network, then, we will compare with the 3G RAN architecture and finally we will overview the LTE protocol architecture.

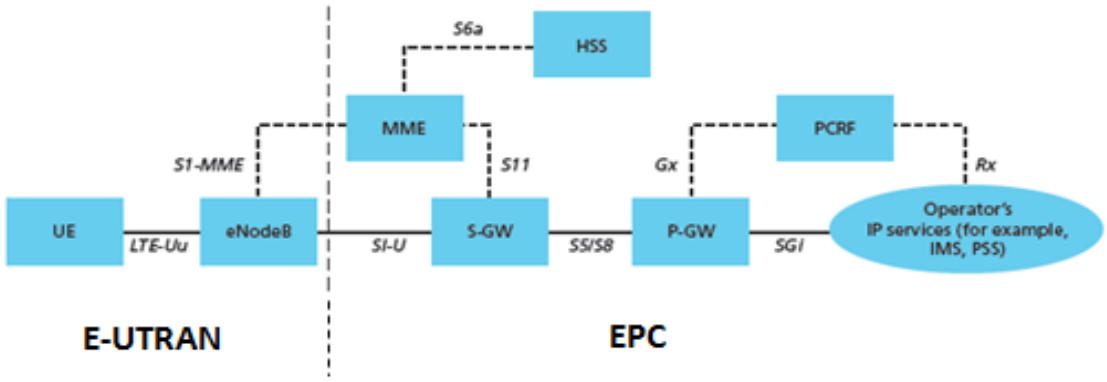

Figure 4. 1 - Logical Network Architecture for LTE [16]

The network in which LTE radio interface is implemented is composed by the E-UTRAN for RAN, and EPC for CN part, like is shown in the above figure. The E-UTRAN plus EPC results in the EPS, which is a fully IP packet switching system that uses standardized interfaces between the logical nodes to perform data and control communications throughout the network. In the above figure, the dashed lines are interfaces used for network control, while the non-dashed lines are data communication interfaces [1][2][16].

- **EPC Network Nodes**

Policy Control and Charging Rules (PCRF):

Controls the traffic flow charging aspects in the PDN-GW, and decides how the PDN-GW must treat in terms of Quality of Service(QoS) the data flow of a given subscription user profile.

Home Server Subscriber (HSS):

Storage of user subscription information like QoS profile, roaming access and PDNs which the UE can connect. It also holds dynamic information about the current MME in which the UE is linked. The HSS may also perform a security role generating authentication vectors and security keys for an Authentication Center (AUC).

Mobility Management Entity (MME):

The MME performs all the control signaling between the EPC and the E-UTRAN, using the Non Access Stratum (NAS) layer protocol between him and the UE. These signaling procedures are related with the creation, maintenance, release and reestablishment of packet data flows of a certain QoS, called bearers. Being more precise, the MME performs the following procedures: informs eNodeB for page a given UE in the radio interface for connection establishment; tracks

the UE location in case of UE change to other MME area; put UE in idle mode when it doesn't have data to transmit or receive, and back to put him in active mode when data is available; informs the E-UTRAN and the S-GW about QoS requirements for a given data flow. The MME also creates and assures the connection security.

PDN - Gateway (P - GW):

The Packet Data Network (PDN) -Gateway performs UE IP address allocation; assures the realization of the charging rules defined by the PCRF node, and filter the downlink UE IP packets in the correct QoS bearers. The PDN-GW is also a link point with other non-3GPP radio access technologies like CDMA-2000 and WiMax.

Serving - Gateway (S - GW):

The S-GW transfers all the IP packets to/from the UE. Thus, when a handover is done by the UE, is the S-GW that buffers the downlink bearer context (data and QoS class) during the paging procedure performed by the eNodeB. Is also in the S-GW that legal communication interceptions are done. The S-GW is a link point for interworking with other 3GPP radio technologies like UMTS.

- **E-UTRAN for LTE Radio Access Network**

The E-UTRAN is the radio access network that supports radio communication through the LTE radio interface specification. The main functions of the E-UTRAN are related with radio resource management, IP packet compression, data encryption and signaling with the EPC using the MME and S-GW nodes. All these tasks are performed by the eNodeB and are organized in the "AS" protocol stack, which describe the communication between eNodeB and the UE.

In the right side of Figure 4.2 is presented the E-UTRAN network architecture, which is composed by a mesh of eNodeB linked via the x2 interface. The paradigm underlying the design of the E-UTRAN was the changing of a complex hierarchical structure (3G UTRAN) to a flat one structure, where all the radio network intelligence is concentrate at the edges nodes (eNodeB). Note that E-UTRAN strategy of put the UTRAN Radio Network Control (RNC) functions in each eNodeB, will allow reduce the delays imposed by the necessity of exchanging information with a central RNC node, like it happens in 3G UTRAN.

Another important difference relative to 3G UTRAN architecture is the possibility that each eNodeB connects to the CN (MME/S-GW) using more than one link point, which allow to share the network load and increase redundancy against node failures [1][2].

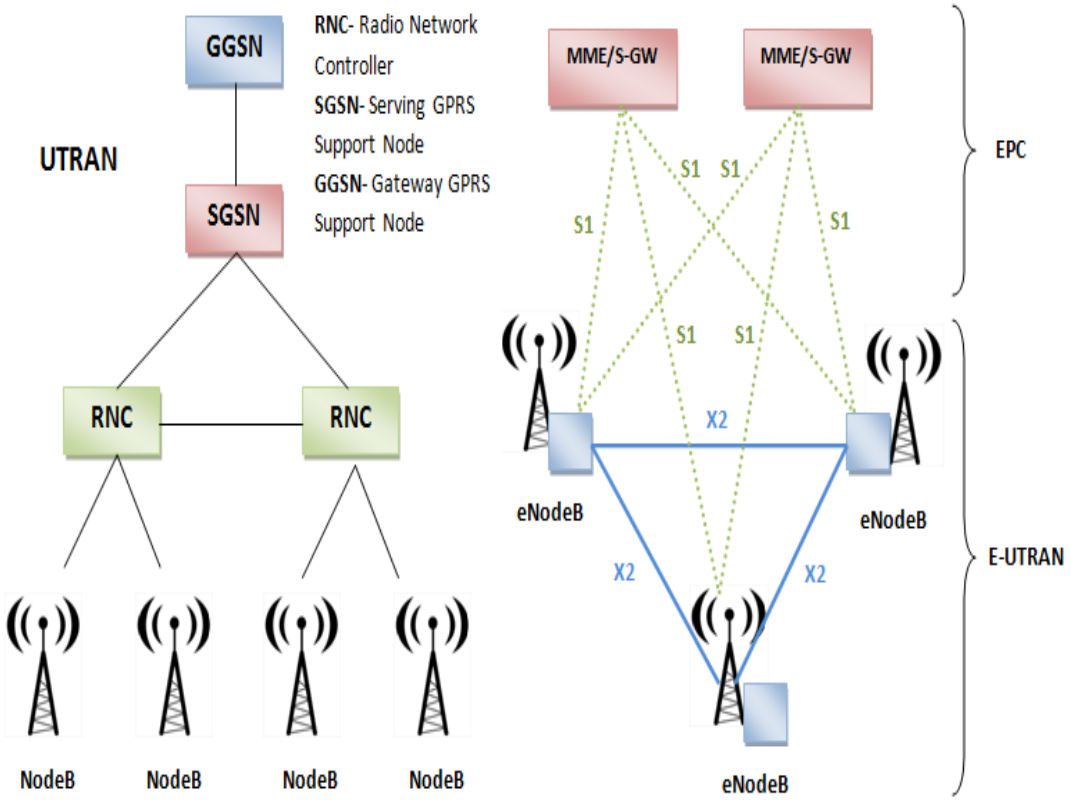

Figure 4. 2 - 3G UTRAN (left) and 4G E-UTRAN (right) Architecture

- **LTE Protocol Architecture**

The LTE protocol architecture is split in control plane protocols, and UE data plane protocols, being the lower layers like Packet Data Convergence Protocol (PDCP), Radio Link Controller (RLC), Medium Access Control (MAC) and L1 (Physical layer) common to both. Next we will present control plane and UE plane protocol structure, but we will just explain the layers related to the LTE radio interface, which are in this thesis work context. More precisely is in the L1 Physical layer of LTE radio interface, that all the MIMO signal processing is performed. Therefore, the final signal processing related to the MIMO LTE Transmission Modes (presented next) is performed in this part of the network.

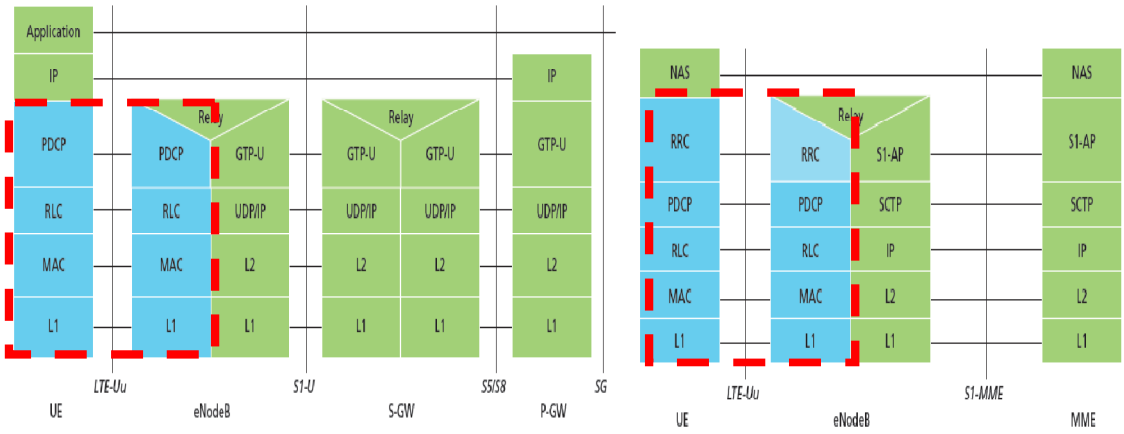

Figure 4. 3 - UE plane protocols (left) and Control plane protocols (right) [16]

The aim of the Figure 4.3 is provide an overview about the entire protocol stack (control plane and UE plane) within the EPS system. The E-UTRAN protocol stack for control and UE plane is the left side blue stack.

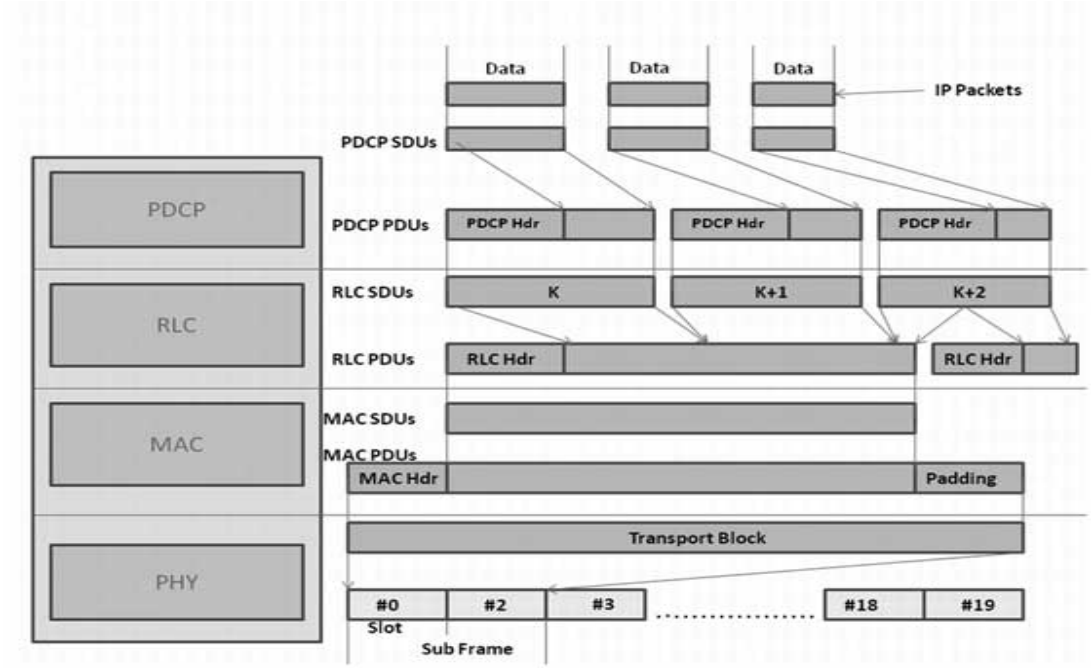

Figure 4. 4 - E-UTRAN protocol stack [17]

In Figure 4.4 is presented how the IP packets are treated when across a given layer. Before proceed, we should refer that a packet received by a layer is called Service Data Unit (SDU), and the output packet of a layer is called Packet Data Unit (PDU).So, looking to the above figure we can see that in each layer the SDU packet is encapsulated using a header, which will provide a given service to the above layers. These headers will be used in the correspondent receiver side layers to execute the service provide by that layers [2][16][17].

PDCP (Packet Data Convergence Protocol):

The PDCP performs IP header compression (decompression in the receiver side) reducing the 20 bytes (minimum) IP header to 1-4 bytes. So, the amount of bits that are transmitted over the radio interface will be strongly reduced. Another important task performed by PDCP is encryption/decryption using a ciphering algorithm.

RLC (Radio Link Control):

The RLC layer performs RLC SDU segmentation and distribution of those segments among the RLC PDUs, like is shown in Figure 4.4. Note that just one RLC PDU is mapped in one transport block, thus we can increase the transmission rate for a set of IP packets mapping more than one non-segmented RLC SDU in the same RLC PDU (high QoS class); in the case of lower QoS class we can split the RLC SDU segments across several RLC PDUs, transmitting the same IP packet using more than one transport block. Another important task done by RLC layer is the handling of Automatic Repeat Request (ARQ) retransmissions when an error is detected.

MAC (Medium Access Control):

The MAC layer is responsible over the radio resources scheduling information for downlink/uplink transmissions. Is the MAC layer that tells the physical layer in which frequency resources that a given MAC PDU must be mapped. It also handles with the Hybrid-ARQ (HARQ) retransmissions.

L1 Physical Layer:

The physical layer is responsible by the last level of processing used to adapt the signal to the radio channel response. Hence, tasks like channel coding/decoding (FEC), modulation/demodulation, mapping in time/frequency-space resources are performed at this level.

4.3. OFDM for LTE Downlink

One of the most important points in the physical layer of a wireless communication system is the technique used to perform data allocation along the radio frequency resources. In LTE downlink, the technology used to modulate the radio frequency resources with input data is called OFDM. What OFDM does is distribute the complex symbols by several orthogonal subcarriers, which are transmitted in parallel. While in a single carrier modulation system a high bit rate sequence is used to modulate just one carrier, in OFDM we split the high bit rate sequence in several lower bit rate sequences, then, each one of these lower rate sequences is

used to modulate a particular subcarrier.

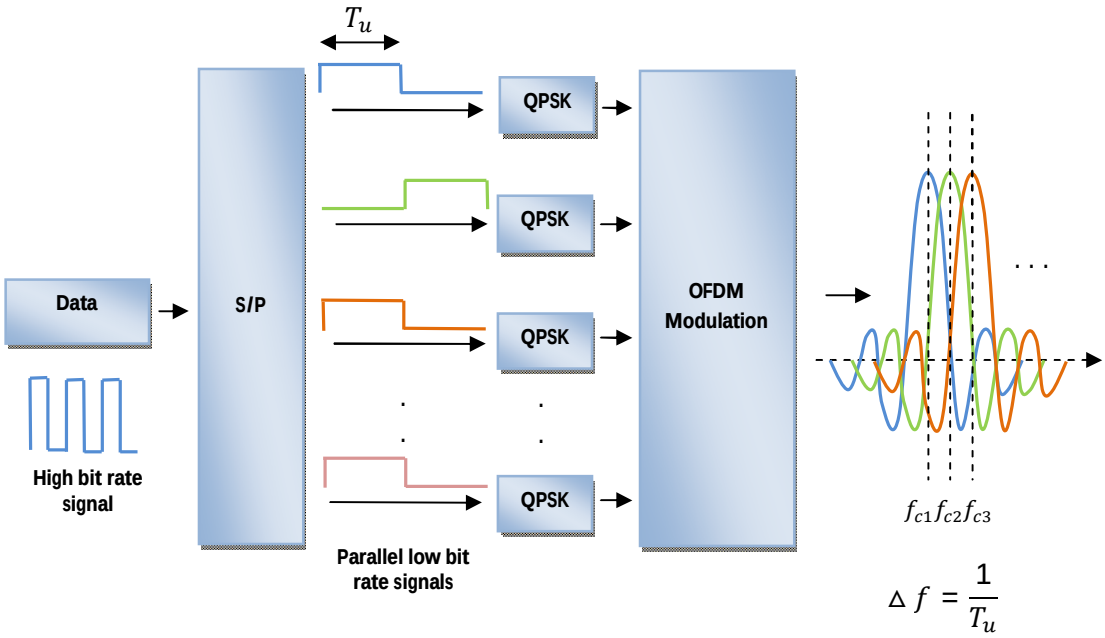

Figure 4. 5 - OFDM principle

The use of OFDM is suited to transmit a signal across a multipath propagation scenario where frequency selective fading is verified at the channel response. Note that instead of use a low time period signal to modulate a single carrier, which results in a high bandwidth occupation, with OFDM we use pulses with wider time period to modulate each one of the subcarriers, therefore each subcarrier will occupy a narrow bandwidth. Using these parallel narrowband signals, we can fit each one in the coherence bandwidth of the channel, which will allow experiment flat fading frequency response in each of the parallel subcarriers. At the time domain we can see that using a time period larger than the time delay spread of the channel, we are able to increase protection against signal distortion caused by multipath characteristic, like is presented in Figure 4.6 [3][8][9].

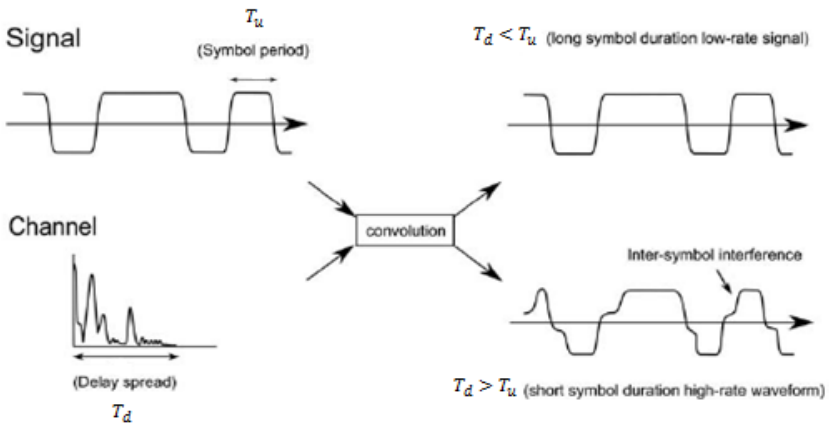

Figure 4. 6 - Signal distortion caused by a multipath fading channel [2]

- **OFDM modulation**

In OFDM modulation what we do is multiply each one of the complex symbols by a set of orthogonal subcarriers. Then, after adding all of those terms, an OFDM symbol is generated as can be seen in the Figure 4.7. The latter is performed by the Inverse Fast Fourier Transform (IFFT) operation. The use of orthogonal subcarriers ($f_k = k\Delta f$) is necessary to separate the symbols at the receiver. Note that the cross-correlation between subcarrier f_k and all the other subcarriers different from f_k results in 0 (considering the received signals aligned and orthogonal), and the auto-correlation of f_k with f_k results in value greater than 0, so we are able to separate the symbol transported by f_k subcarrier from the other symbols transported by each orthogonal subcarrier. Hence, doing correlation at the receiver using the carrier frequency from where we want take the symbol, we can separate the symbols in the frequency.

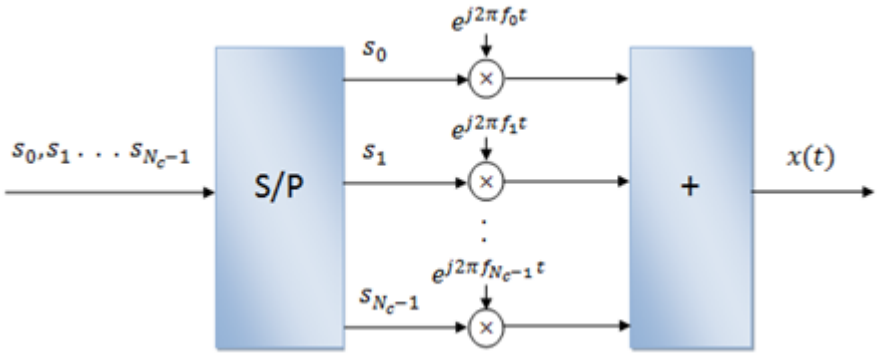

Figure 4. 7 - OFDM modulation with IFFT

The mathematical expression that generates one OFDM symbol $x(t)$ using N_c subcarriers with a separation of Δf is the following,

$$x(t) = \sum_{k=0}^{N_c-1} s_k e^{j2\pi k\Delta f t} \quad (4.1)$$

At the above expression s_k is a complex symbol, which in MIMO systems is a precoded complex symbol.

In practice OFDM subcarrier modulation is done in a digital form using the Inverse Discrete Fourier Transform (IDFT) operation. What IDFT operation does is sample the OFDM symbol shown in IFFT expression, therefore x_0 is the sample of OFDM symbol at instant T_s, x_1 is the sample of the same OFDM symbol at $2T_s$, and so on. The sample frequency must be $f_s = N\Delta f$,

with $N > N_{carriers}$ in order to sample at sufficient rate to rebuild the signal which has a bandwidth of $N_{carriers}\Delta f$ (N is the IFFT size). After the IDFT operation, the samples are changed from parallel to series and is added a cyclic prefix (not shown below).

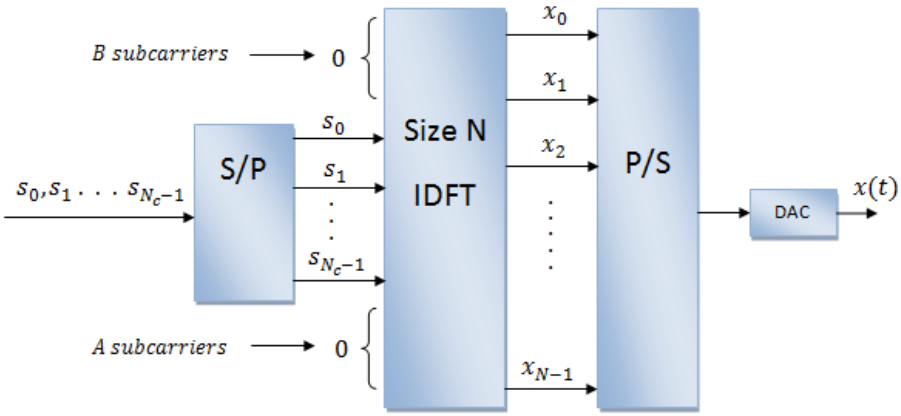

Figure 4. 8 - OFDM practical modulation with IDFT

In each band, a set of side subcarriers is modulated with 0 in order to insert guard band intervals to separate bands. In Figure 4.8 these guard bands are represented by A and B.
The expression for a size *N* IDFT operation is the following,

$$x_n = x(nT_s) = \sum_{k=0}^{N-1} b_k e^{j2\pi k\Delta f n T_s} = \sum_{k=0}^{N-1} b_k e^{j2\pi k\frac{n}{N}} \quad (4.\ 2)$$

$$b_k = \begin{cases} 0, & (N-1)-A \le k \le N-1 \\ s_i, & B \le k < N-1-A \ \ and \ \ i = 0 \ldots N_c - 1 \\ 0, & 0 \le k < B \end{cases}$$

$$T_s = \frac{1}{N\Delta f} \quad (4.\ 3)$$

In figure 4.9 at the left side we can see a time domain OFDM symbol modulated with 5 orthogonal subcarriers, each one with a T_u time duration. At the right side is presented one OFDM signal at the frequency domain using several subcarriers with a frequency separation of $\Delta f = 1/T_u$. Note that using the frequency structure of a sinc we can select $\Delta f = 1/T_u$ in order to align the main lob of each sinc with the null points of the other sincs, which will result in a set of non-interfering orthogonal sincs [9][19].

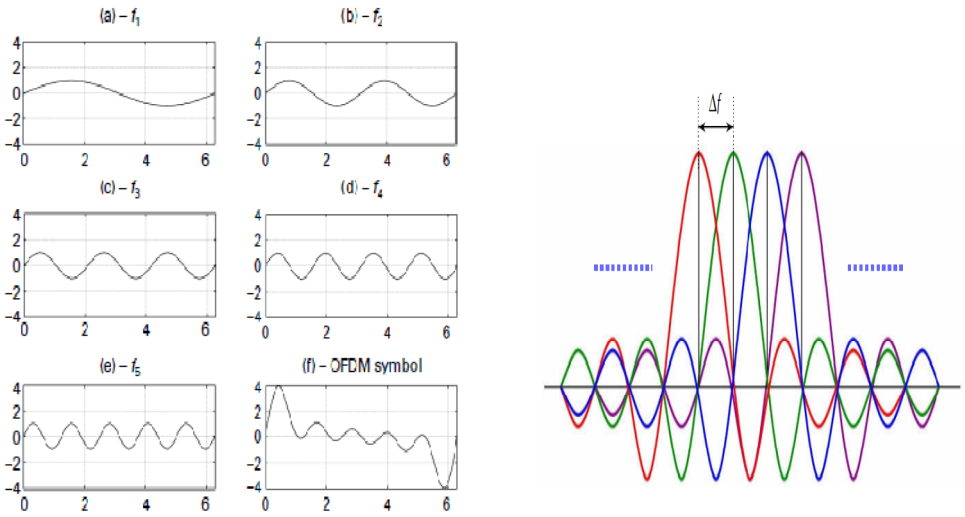

Figure 4. 9 - Time (left) [9] and frequency (right) [19] representations of an OFDM signal

- **OFDM demodulation**

The OFDM signal that arrives at receiver (during one OFDM period) is a sum of several sinusoids of orthogonal frequencies, each one modulated by a complex information symbol. Thus, when we compute the correlation in each branch of the receiver, using the subcarrier where is the symbol k that we want get in that branch, the correlation result with the terms of the somatory that have orthogonal frequencies to f_k is 0, and with f_k term a high value of correlation is obtained. Therefore, is possible separate s_k symbol from the other symbols in that branch. The same process is used in the other branches for the other subcarriers [2][3].

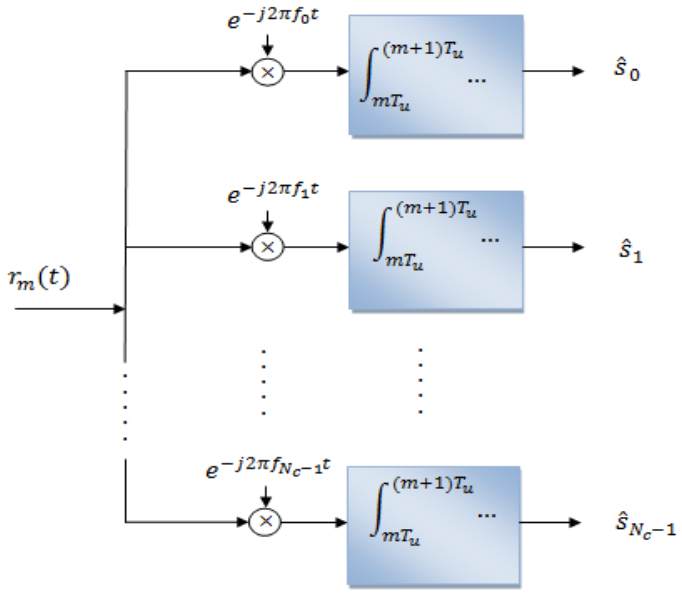

Figure 4. 10 - OFDM demodulation principle

In the bellow expression is shown the correlation result between 2 orthogonal signals. As said before, the result is 0 for perfect orthogonal feature.

$$r_m(t) = s_0 e^{j2\pi f_0 t} + s_1 e^{j2\pi f_1 t} + \cdots + s_{N_c-1} e^{j2\pi f_{N_c-1} t} \quad (4.4)$$

$$\int_{mT_u}^{(m+1)T_u} s_{k_0} e^{j2\pi f_{k_0} t} e^{-j2\pi f_{k_1} t} dt = 0, \quad for \quad k_0 \neq k_1 \quad (4.5)$$

In practice, the demodulation is done using Discrete Fourier Transform (DFT) operation like is shown in Figure 4.11.

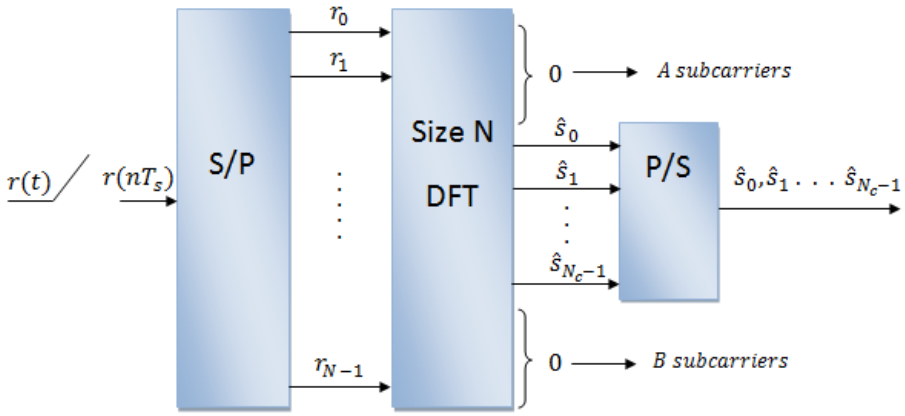

Figure 4. 11 - OFDM practical demodulation

The DFT expression is the following,

$$\hat{S}_k = \sum_{n=0}^{N-1} r_n e^{-j2\pi k \Delta f n T_s} = \sum_{k=0}^{N-1} r_n e^{-j2\pi k \frac{n}{N}} \quad (4.6)$$

- **OFDM in LTE**

While 3G UMTS only consider a 5 MHz bandwidth, LTE specifies several bandwidths which range from 1.25 MHz to 20 MHz, therefore the parameters used to generate the OFDM signal depends of the bandwidth selected. In Table 4 is presented the main parameters related with the OFDM generation for each specified bandwidth case. Look that for all the bandwidths, around 10% of the available band is not used to transmit information. We also should refer that the

subcarriers used to transmit information are selected performing the correct mapping of the symbols at the input of the IFFT block. In the case of the guard subcarriers we fill the IFFT input with zeros in the correct locations [19].

Bandwidth (MHz)	**1.25**	**2.5**	**5**	**10**	**15**	**20**
Subcarrier Spacing (Δf)	15 KHz					
IFFT size (N)	128	256	512	1024	1536	2048
Sampling Frequency (MHz) **($f_s = N \times \Delta f$)**	1.92	3.84	7.68	15.36	23.04	30.72
Guard Subcarriers	52	105	211	423	635	847
Occupied Subcarriers	76	151	301	601	901	1201
Occupied Band (MHz)	1.14	2.265	4.515	9.015	13.515	18.015
DW Band Efficiency	90%	90%	90%	90%	90%	90%

Table 4 - OFDM parameters in LTE [19]

In a multipath channel, the multiple delayed OFDM signal copies that arrive to the receiver could cause interference between consecutive OFDM signals, which will result in partial lost of orthogonality feature creating an inter-symbol interference problem. In order to resolve this interference issue, the Cyclic Prefix (CP) concept is used in LTE. What CP does is replicate the samples of the last part of each OFDM signal at the beginning, like is presented in figure 4.12. Note that to avoid interference between consecutive OFDM signals we need to use a T_{CP} duration at least equal the time delay spread of the channel, otherwise we will continue to experiment interference.

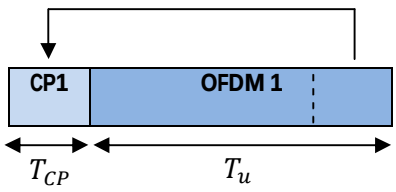

Figure 4. 12 - CP insertion

At figure 4.13 we can see 2 paths which arrive added with the presented alignment at the receiver. The receiver will only use in demodulation the samples where interference between consecutive OFDM signals is not verified [3][8].

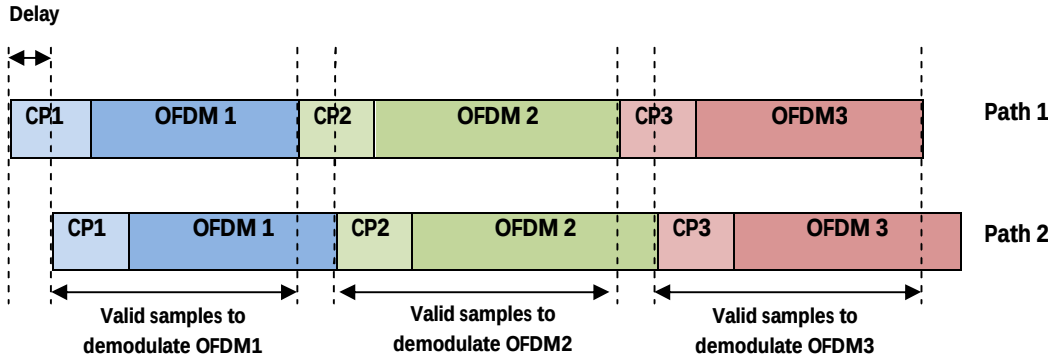

Figure 4. 13 - CP effect in a multipath channel

- **OFDMA for user multiplexing**

The OFDM modulation is used to share the spectrum medium between UEs inside the same cell. This subcarrier allocation between UEs can be continuous or distributed.

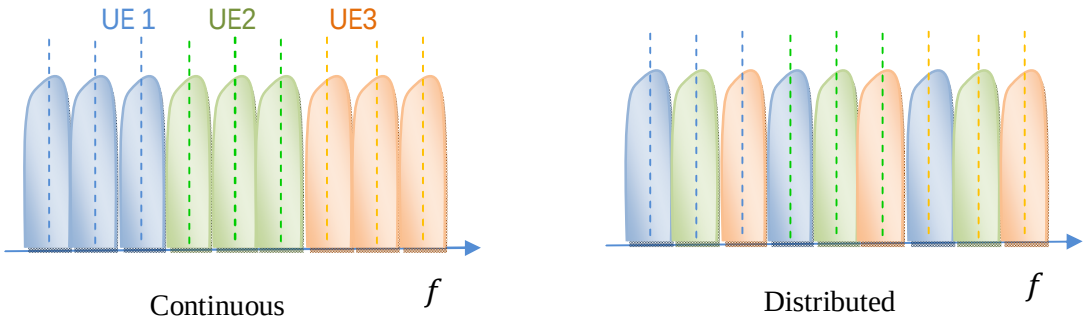

Figure 4. 14 - Continuous and Distributed UE allocation in OFDM

This share is done giving at each UE different sets of orthogonal subcarriers, making that each UE receives in the downlink just the information that was modulated with their set of subcarriers. In order to avoid put all the data information of a given UE in a contiguous part of the band where high fading is verified, we can distribute the information of a given UE along non-contiguous subcarriers [3].

4.4. Structure of Time-Frequency Resources in LTE Downlink

The LTE FDD time domain structure is divided in several time intervals, where each interval is a multiple of a basic time unity $Ts = 32\,ns$. The great time interval resource is a 10 ms frame, which enclose 10 sub-frames of 1ms, with each sub-frame divided in 2 slots of 0.5 ms each. According the type of Cyclic Prefix (CP) used in each OFDM symbol, each slot can be composed by 6 or 7 useful OFDM symbols of 66.7 µs each. In 20 MHz bandwidth case, $Ts = 32\,ns$ is the time used to sample one OFDM symbol computed with an IFFT size of 2048 subcarriers, using subcarrier spacing Δf = 15 KHz, which results in a $Ts = 1/(2048 \times 15KHz)$. We should note that despite different IFFT sizes are used in the other LTE bands, resulting in different time samples within each OFDM symbol, the OFDM period remains the same (66.7µs) in all bands, because only depends of the subcarrier spacing that is equal to 15 KHz for all bands.

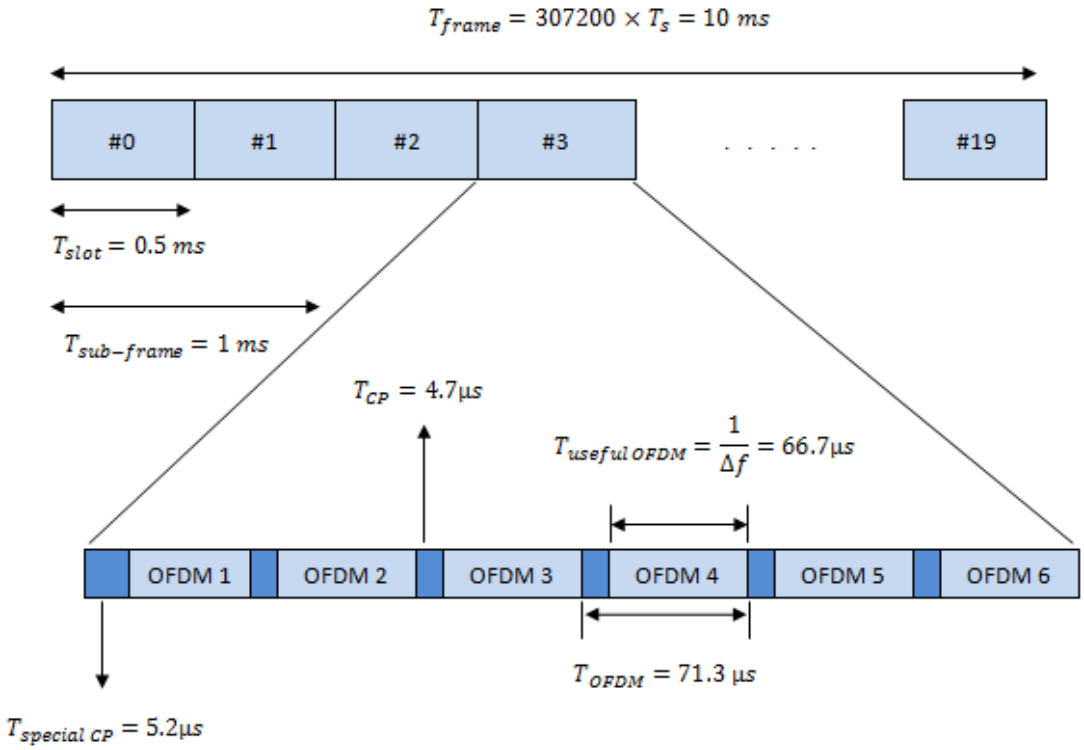

Figure 4. 15 - LTE Type 1 resource time structure for FDD

The transmission scheduling is done in a Resource Block (RB) basis, with each RB being a time-frequency grid formed by 12 OFDM subcarriers during 1 slot time of $0.5\,ms$. So, the minimal bandwidth that is possible allocate to a transmission is $12 \times 15KHz = 180\,KHz$, which is used during $0.5\,ms$. The smallest time-frequency resource inside a RB is the Resource

Element (RE), which is composed by one OFDM subcarrier in the frequency axis, and one OFDM time period in the time axis.

Looking to the below time-frequency grid we can see 2 RB, formed each one by 84 RE's. Each RB has time duration of 7 OFDM periods, during which a band of 180 KHz is allocated for a given UE.

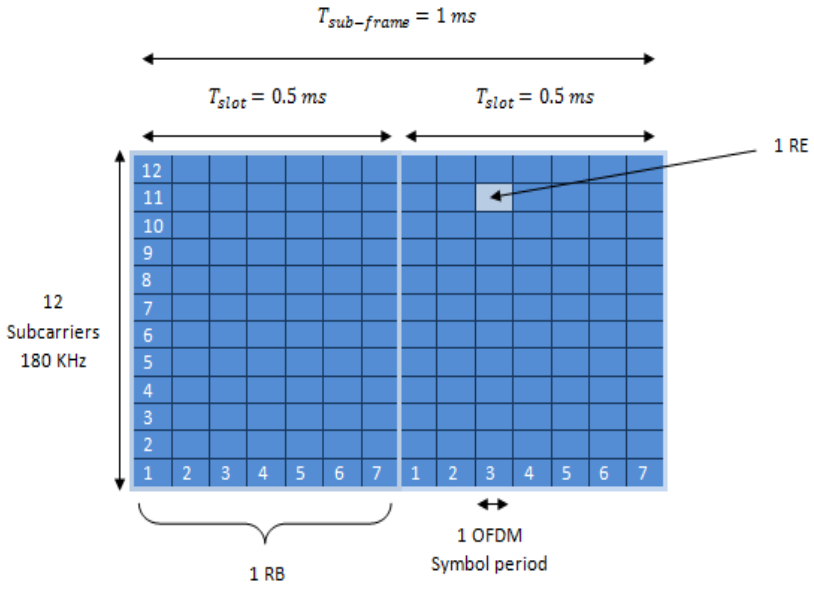

Figure 4. 16 - LTE time-frequency RB grid

In the case of LTE TDD variant, the time domain structure is composed by 7 frames with different Downlink (DW) and Uplink (UP) load configurations. So if in a given moment we need to schedule more or less UP/DW sub-frames, we can switch the frame structure [12][19].

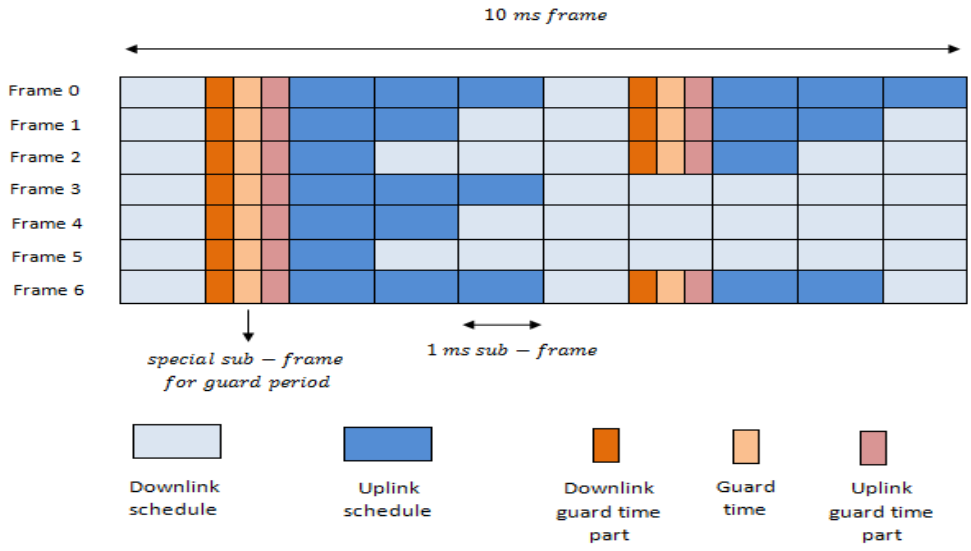

Figure 4. 17 - LTE resource time structure for TDD

4.5. Reference signals in LTE Downlink

Reference signals (RS) are pre-known complex symbols which are mapped within data RBs in order to perform channel estimation for data coherent demodulation purposes. These RS are generated using pseudo-random sequences, therefore with the pre-knowledge of these sequences at both transmitter and receiver, is possible to the UE analyze the phase and amplitude shift that the channel will cause on RS, hence using that information, channel estimation can be computed in order to allow channel dependent precoding and equalization. The mapping of RS will increase the system overhead, therefore the level of density with which these RS are mapped within data RB is a trade-off between channel estimation accuracy and spectral efficiency. Another important considerations used to define the time/frequency granularity of RS mapping, is the expected time and band coherence conditions related with channel, therefore in the frequency domain, channel estimation should be done with an interval equals the coherence band, while in the time domain, the estimation must take in account the time coherence of the channel in order to optimize channel tracking. Note that the channel is only estimated on the RE where the RS are mapped, therefore an interpolation process must be computed in order to apply those estimations for coherent demodulation in the other REs where data is really transmitted.

The LTE standard defines RS for downlink and uplink directions, which are organized in virtual antenna ports on a sub-frame basis. The RS in each antenna port could be mapped by one physical antenna (CRS), or else by multiple antennas (UE-RS). The 3 types of RS specified for LTE downlink are: Cell-specific Reference Signals (CRS); Multimedia Broadcast Single Frequency Network (MBSFN) reference signals and UE-specific Reference Signals (UE-RS)[2][20]. In this section just CRS and UE-RS are presented.

In all the 3 types of RS defined in LTE downlink, the RS value is computed using the following expression [20],

$$r_{l,n_s}(m) = \frac{1}{\sqrt{2}}[1 - 2c(2m)] + j\frac{1}{\sqrt{2}}[1 - 2c(2m+1)] \quad (4.7)$$

Where m is the RS index, l is the OFDM symbol number, n_s is the slot number and c is a pseudo random Gold bit sequence.

- **Cell-specific RS**

The cell specific RS are transmitted across the entire system bandwidth in all the sub-frames; therefore they are available for all the UEs inside a cell. According the number of antennas used for transmission, 1, 2 or 4 antenna ports are used, like is presented in figures 4.18, 4.19 and 4.20. In this case each physical antenna will map one antenna port.

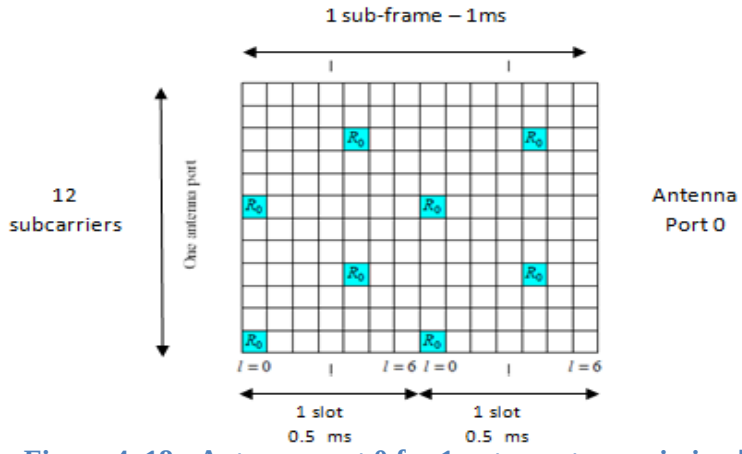

Figure 4. 18 - Antenna port 0 for 1 antenna transmission [20]

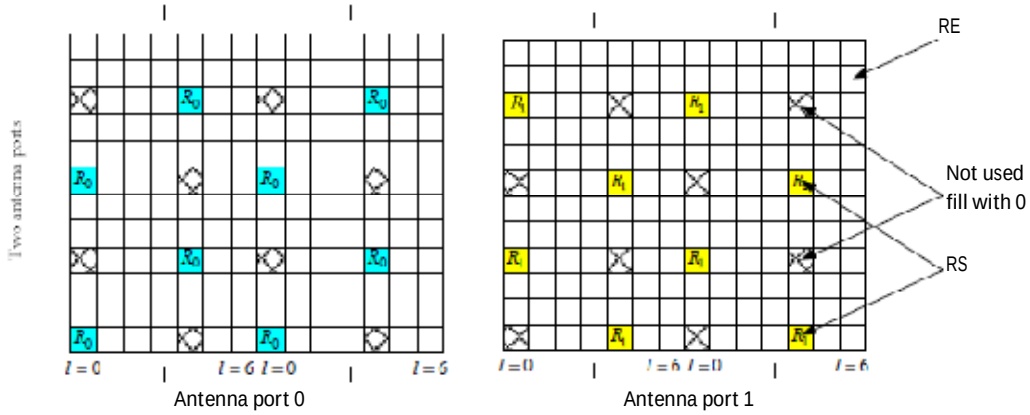

Figure 4. 19 - Antenna port 0 and 1 for 2 antenna transmission [20]

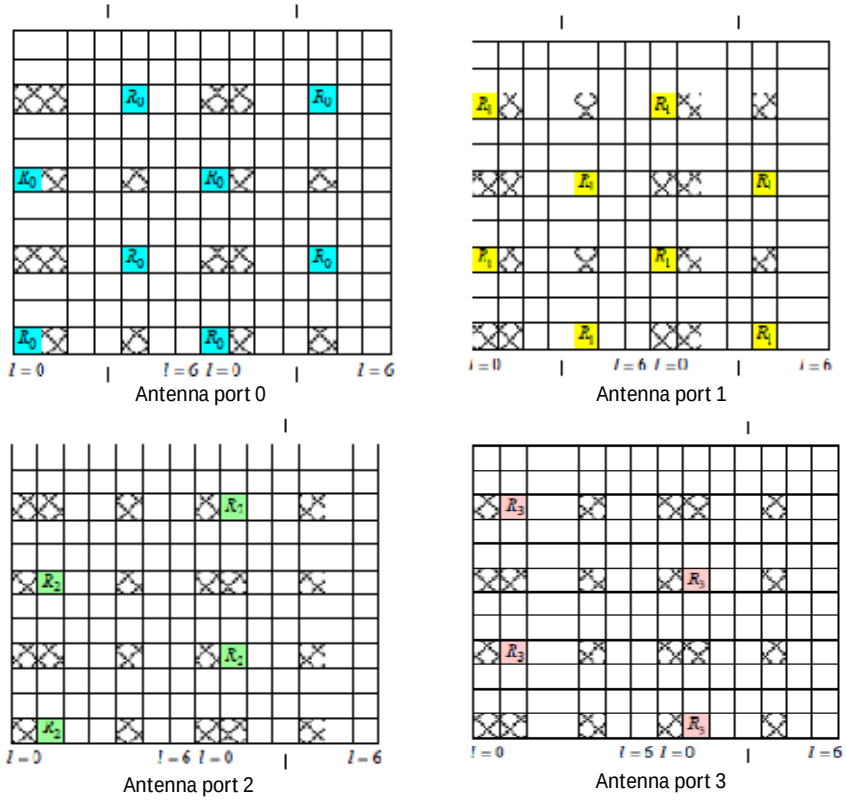

Figure 4. 20 - Antenna port 0, 1, 2, 3 for 4 antenna transmission [20]

We should refer that the RS mapped in one antenna port never overlap with data or RS from another antenna port, therefore 0 are used to fill those RE, like is presented in figure 4.19.

- **UE specific RS**

The UE-RS are used when a transmission beamforming mode is configured, thus using this type of RS, the BS will precode UE-RS with the same weights selected for beamforming data transmission, which will allow the UE acquire the necessary information for demodulation. In this case the RS are only mapped on the RB allocated for a specific UE. While in CRS each antenna port is mapped in a different physical antenna, in this case one antenna port is associated to a set of antennas, only the correct beamforming weight is adapted in each antenna [20][21].

In single layer beamforming, antenna port 5 is used.

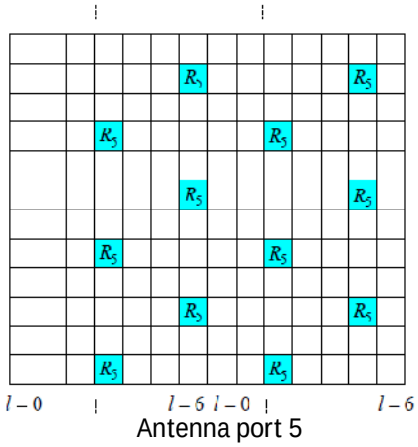

Figure 4. 21 - Antenna port 5 [20]

In dual layer beamforming, the following antenna ports are used,

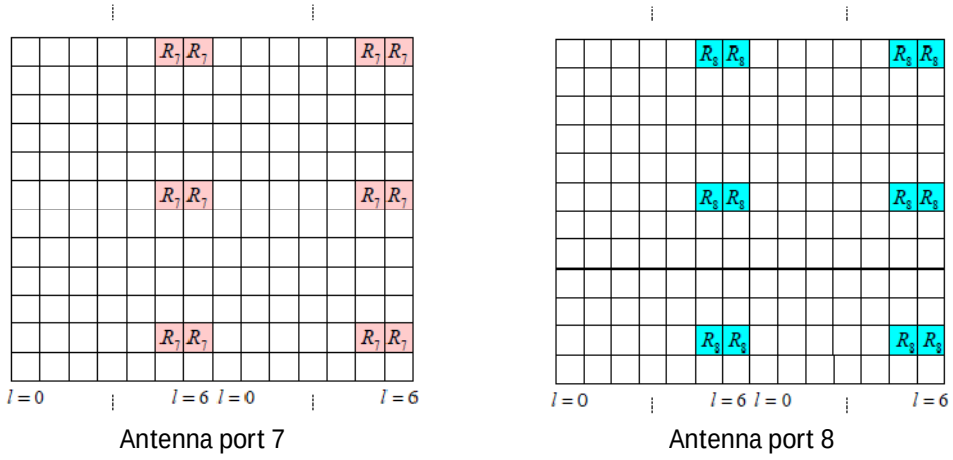

Figure 4. 22 - Antenna port 7 and 8 [20]

4.6. Chain Structure for LTE Downlink Physical Layer

In this point we will see the main blocks within LTE Physical layer that are responsible for all signal processing applied in LTE MIMO Transmission Modes. We will see how the downlink chain computes the signals for both Diversity and SM modes, giving special emphasis to the last 4 blocks of the chain (layer mapping, precoding, RE mapping, OFDM modulation), which are the blocks that adapts the signal for MIMO transmission.

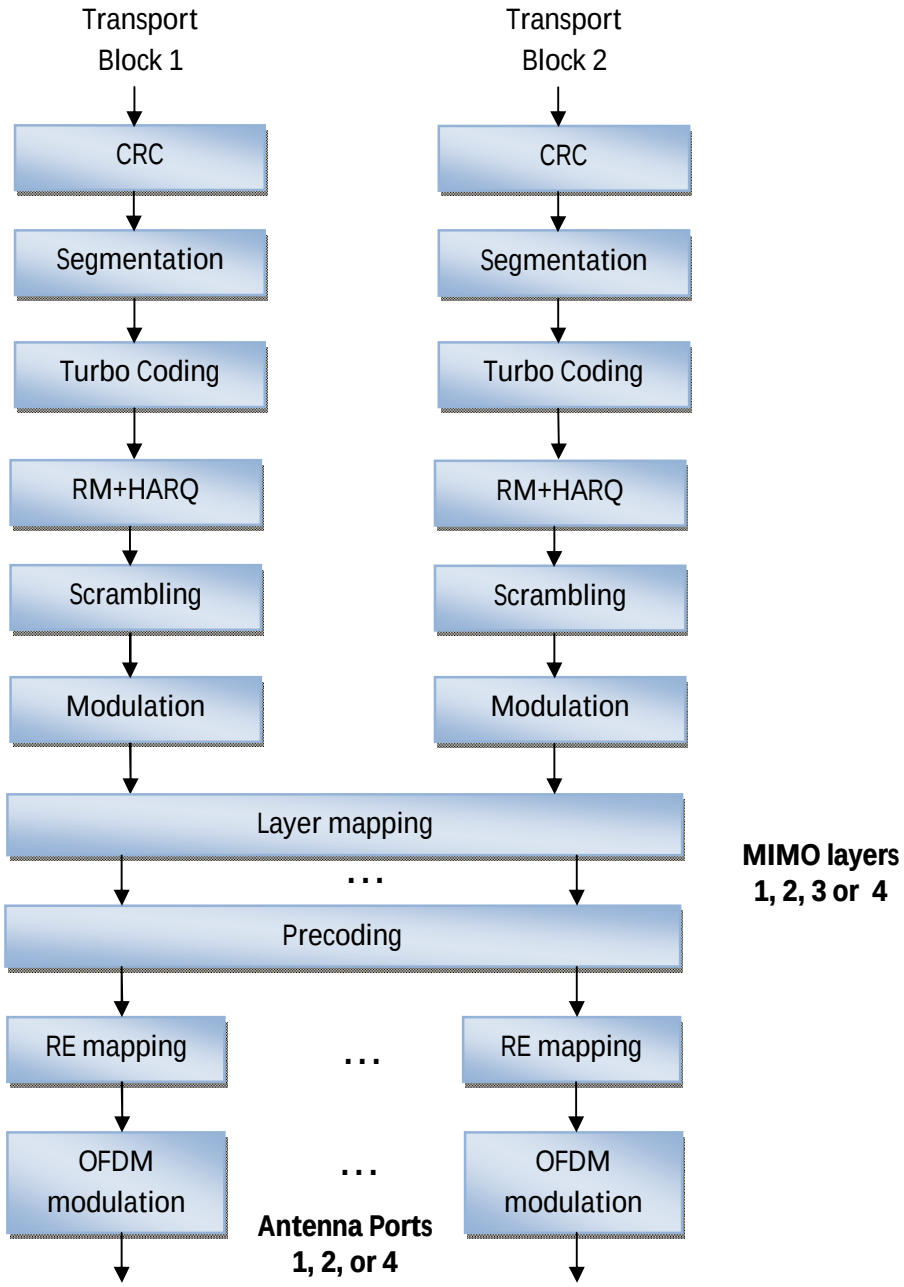

Figure 4. 23 - LTE Downlink Physical Chain [3]

In Figure 4.23 is presented the structure of LTE physical chain used in the downlink direction. According the type of MIMO transmission mode selected, one or two transport blocks can be coded by the physical chain. Therefore, if a diversity mode is used, only one transport block is coded, while in a spatial multiplexing mode, 2 transport blocks are coded in parallel for rank transmissions greater than one [2][3][20][22].

4.6.1. Coding Layers

Now we will overview the first 6 layers used in LTE downlink chain, which are used to code and modulate the data transport block.

- **Cyclic Redundancy Check (CRC) layer**

The CRC layer receives a transport block from the MAC layer, and computes over that block a 24 bit CRC sequence, which is added to that block in order to check at the receiver the occurrence of errors. The computed CRC is the remainder bit result of a binary division, using the transport block as dividend and a cyclic polynomial generator as divisor.

The receiver performs the same binary division over the entire received block (data+CRC), and checks if the remainder is 0. If remainder result is 0, means that no error occurrence, otherwise error is detected and receiver asks for retransmission using H-ARQ.

LTE specifies 4 cyclic polynomial generators, being two of them for 24 bits CRC, and the others for 16 and 8 bits CRC [3][20].

CRC Length/Type	CRC Generator
24/A	$g_{CRC24A} = x^{24} + x^{23} + x^{18} + x^{17} + x^{14} + x^{11} + x^{10} + x^{7} + x^{6} + x^{5} + x^{4} + x^{3} + x + 1$
24/B	$g_{CRC24B} = x^{24} + x^{23} + x^{6} + x^{5} + x + 1$
16	$g_{CRC16} = x^{16} + x^{12} + x^{5} + 1$
8	$g_{CRC8} = x^{8} + x^{7} + x^{4} + x^{3} + x + 1$

Table 5 - CRC polynomial generators for LTE [22]

- **Segmentation layer**

The internal interleaver inside the Turbo Coding is only prepared to work with a set of defined code block sizes, so the segmentation layer assures that the sizes of blocks at the input of the Turbo Coding are in accordance with that set. The maximum block size defined for Turbo Coding interleaver is 6144 bits, so in case the transport block exceeds that value, segmentation is performed and filler bits might be used in some segments when the transport block size is not a perfect multiple of the block size selected for Turbo Coding input. In case of the transport block doesn't exceed the 6144 bits and also doesn't match with any block size defined for the interleaver, filler bits are used to match the size [3].

We should refer that in case of segmentation a new 24 bits CRC is added at each segment, like is shown in Figure 4.24.

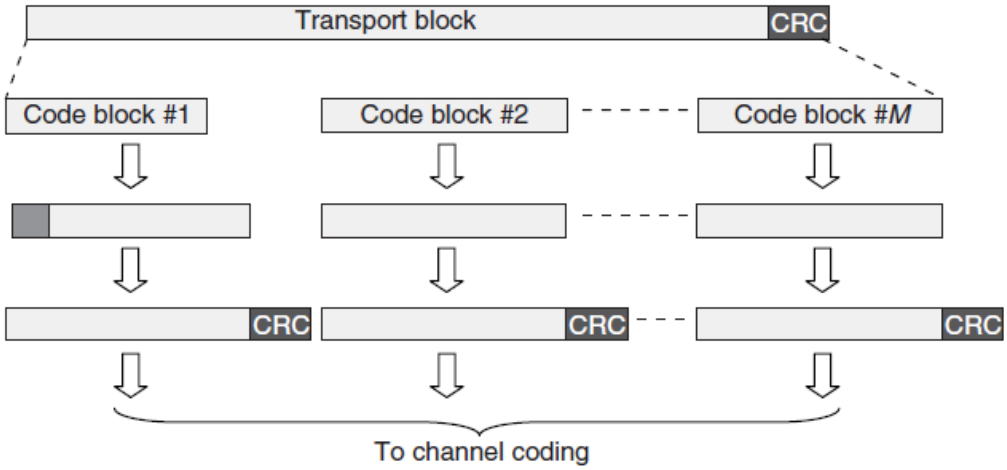

Figure 4. 24 - Segmentation process [3]

- **Turbo Coding**

One of the main and complex components of a digital wireless communication system is the channel coding layer. The aim of channel coding is provide Forward Error Correction (FEC) capacity at the receiver, using coding schemes which add redundant bits to the transmitted block. Therefore we can improve FEC capacity at the receiver reducing the FEC code rate, but with the cost of also reduce the spectral efficiency.

The FEC encoder selected for LTE data channels was a code rate 1/3 Turbo Coding. The scheme selected for Turbo encoder is called Parallel Concatenated Convolutional Code (PCCC) which is composed by 3 main blocks, that are: a Quadratic Permutation Polynomial (QPP)

based-interleaver and 2 eight-state Recursive Systematic Convolutional (RSC) encoders, each one with a code rate of 1/2, like is shown in Figure 4.25.

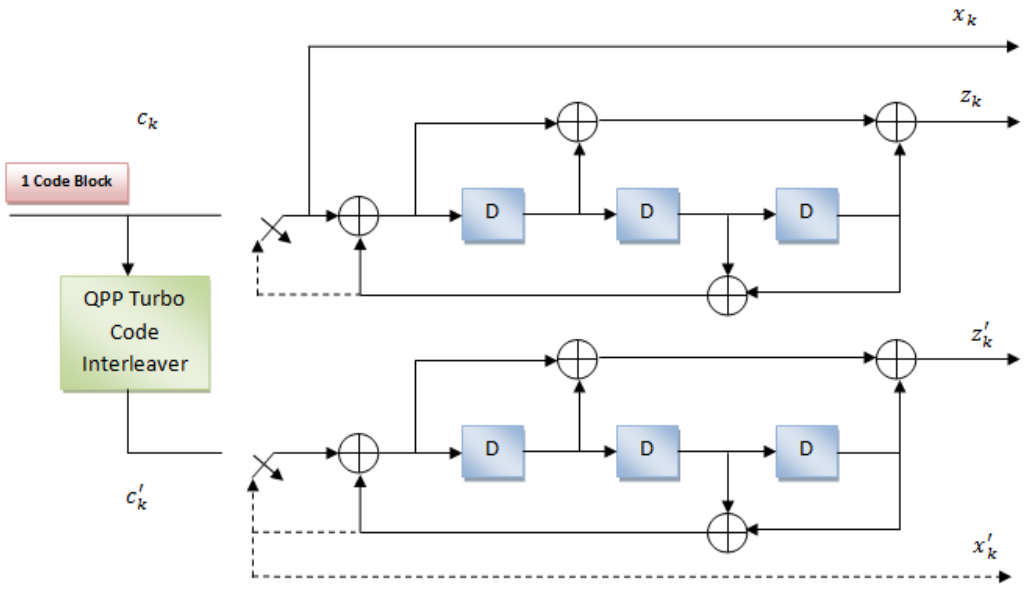

Figure 4. 25 - PCCC Code rate 1/3 Turbo Encoder [22]

The feedback and feed forward transfer function for the constituent encoders are $g_0(D)$ and $g_1(D)$ respectively.

$$g_0(D) = 1 + D^2 + D^3 \quad (4.8)$$

$$g_1(D) = 1 + D + D^3 \quad (4.9)$$

The overall transfer function of each RSC encoder is the following,

$$G(D) = [1, \frac{g_1(D)}{g_0(D)}] \quad (4.10)$$

The 2 switches in the above PCCC encoder are used to reset the shift registers to a zero state after encode the input sequence. The normal encoding of the input block is done with the 2 switches in high position at the same time, and the outputs of the Turbo encoder are x_k, z_k and $z_k^{'}$.

Note that to reset the shift registers after normal encoding, we must treat the 2 constituent encoders separately. So, the reset of constituent encoder 1 is done using a specific set of 3 bits at the input, with encoder 1 switch at high position, and the encoder 2 switch at low position. The reset of encoder 2 is done using another specific set of 3 bits, but now the constituent encoder 2 switch is in high position while encoder 1 is in low position (reset state) [2][3][22].

The input of the second RSC encoder is an interleaved version of the code block at the input of PCCC. Therefore a QPP (Quadrature Permutation Polynomial) interleaver is used to perform the correct bit permutation.

The permutation pattern expression $\prod(i)$ is defined by parameters f_1 and f_2, which are selected according the size K of the input code block.

$$\prod(i) = (f_1 \times i + f_2 \times i^2) mod K \quad (4.\ 11)$$

$$i = 1, 2, \ldots . K - 1$$

The value of the output block in index$i$, is the value of the input block in index$\prod(i)$.

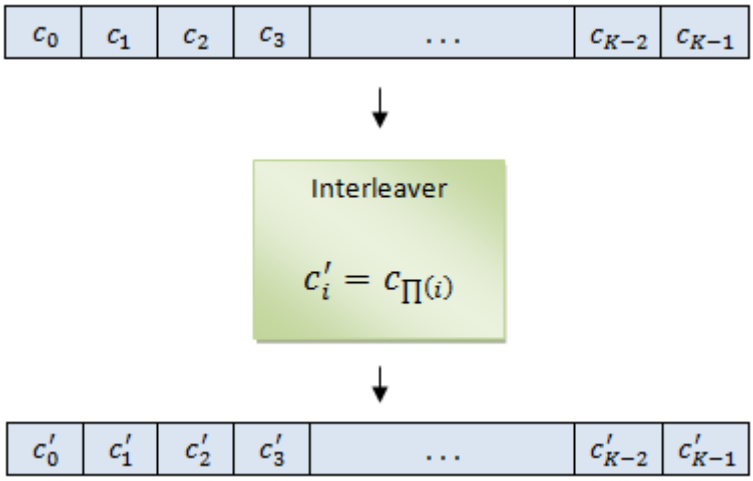

Figure 4. 26 - Interleaver pattern

In the case of control channels, LTE uses a Tail Biting Convolutional encoder with a rate of 1/3, like is presented in Figure 4.27.

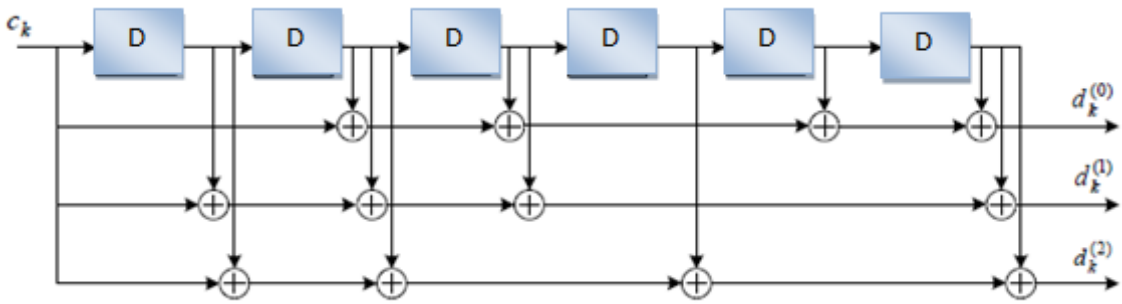

Figure 4. 27 - Rate 1/3 Tail Biting Convolutional Encoder [22]

The generator polynomials for each output d_k are the following,

$$G_0 = 1 + D^2 + D^3 + D^5 + D^6 \rightarrow (133)_8 \quad (4.12)$$

$$G_1 = 1 + D + D^2 + D^3 + D^6 \rightarrow (171)_8 \quad (4.13)$$

$$G_2 = 1 + D + D^2 + D^4 + D^6 \rightarrow (165)_8 \quad (4.14)$$

- **Rate Matching (RM)**

The main task of RM+HARQ layer is to perform code rate adaptation in order to match the transmission parameters with the channel conditions. Hence, performing puncturing operation over some redundant bits, we can change the code rate of Turbo coding which allows reduce the amount of overhead mapped in the radio resources. Individual code rate adaptation is done for HARQ retransmissions [2][3][22].

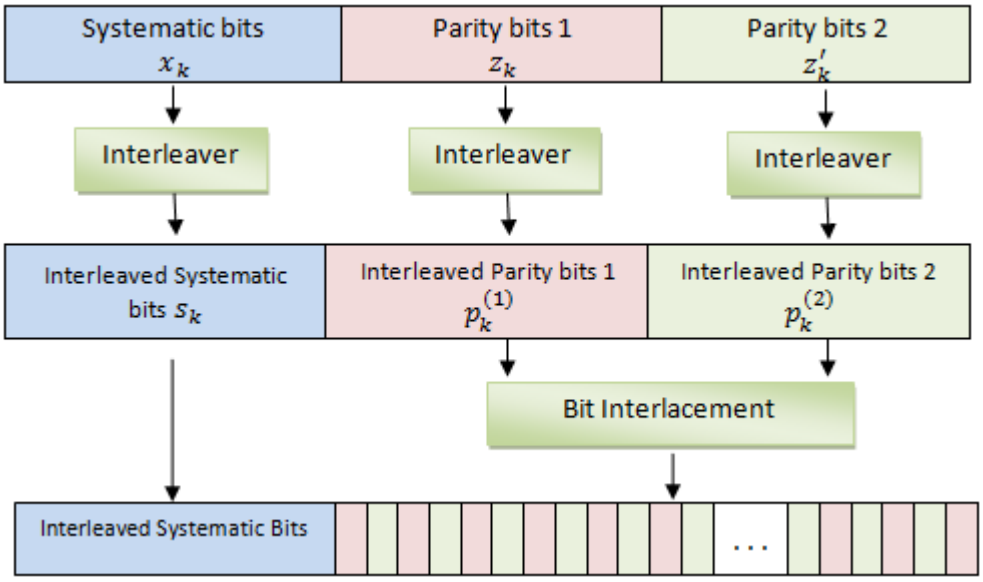

Figure 4. 28 - RM sub-block interleaving

The RM block starts to perform a new interleaving operation in each one of the 3 coded streams at the output of the Turbo Coding, then the resulting interleaved sub-blocks of the non-systematic streams (z_k andz'_k) are interlaced, like is shown in Figure 4.28.

After the above operations, the interleaved systematic bits and interleaved/interlaced parity bits are put sequentially in a circular buffer, then, the bits are selected for transmission also in a sequential way. In order to perform rate adaptation, puncturing and/or repetition of some bits is

done selecting the correct bits in the circular buffer. The start point of the sequential selection is defined by a Redundancy Version (RV) parameter, like is shown in Figure 4.29.

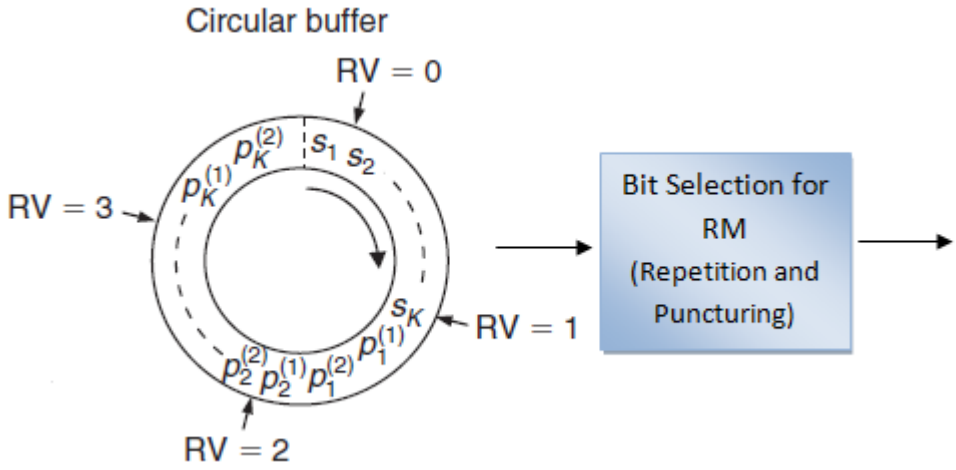

Figure 4. 29 - Circular buffer used in RM layer [3]

- **Scrambling**

The scrambling layer uses pseudo-random Gold sequences of length 31 to code the input codeword. Gold codes are bit sequences with low cross-correlation properties between them, or in another words, we can say that are almost fully orthogonal sequences. So, the aim of scrambling the input codeword with Gold sequences is to assure that interference between adjacent cells operating in the same band is reduced. The principle used here is the same applied in 3G CDMA for radio access sharing, where the users within a cell are separated using codes with good orthogonal properties. Note that when we perform correlation between 2 orthogonal codes for a specific alignment, the result is 0.

The scrambling of input codeword q is done performing an EXOR operation between input bit sequence b^q and Gold sequence c^q, resulting in the output scrambled signal $\tilde{b}^q$ which is transmitted in one sub-frame. In the below expression is presented the EXOR scrambling operation for downlink physical channels.

$$\tilde{b}^q(i) = \left(b^q(i) + c^q(i)\right) mod\ 2 \quad (4.\ 15)$$

The generation of Gold codes is done performing the EXOR operation between 2 initial x_1 and x_2 Gold sequences, where each generated Gold code is the result of EXOR operation between different shifted versions of these 2 initial sequences x_1 and x_2.

In LTE the Gold codes are computed based on the following EXOR expressions with x_1 and x_2 being the 2 initial sequences.

$$c(n) = \left(x_1(n + N_C) + x_2(n + N_C)\right) mod\ 2 \quad (4.\ 16)$$

$$n = 0, 1, 2 \ldots, M_{NP}$$

$$N_C = 1600$$

The generation sequences x_1 and x_2 are computed based on the following EXOR operations,

$$x_1(n + 31) = \left(x_1(n + 3) + x_1(n)\right) mod\ 2 \quad (4.\ 17)$$

$$x_2(n + 31) = \left(x_2(n + 3) + x_2(n + 2) + x_2(n + 1) + x_2(n)\right) mod\ 2 \quad (4.\ 18)$$

The first 31 bits of x_1 are $x_1(0) = 1$ and $x_1(n) = 0$ for $n = 1, 2 \ldots 30$, while in the case of x_2 the value is not fixed [20].

- **Modulation**

After bit scrambling, a modulation scheme is applied over the output codeword of scrambler layer. The LTE specification allows QPSK, 16-QAM and 64-QAM modulation schemes, with each one corresponding to 2, 4 and 6 bits respectively.

Due the channel adaptative principle embedded in LTE, modulation scheme is adapted according the channel fading conditions, therefore a CQI index is reported to the BS in order to select the best modulation scheme. The frequency granularity of CQI reports is flexible, ranging from wideband to lower sub-band basis reports [20][23].

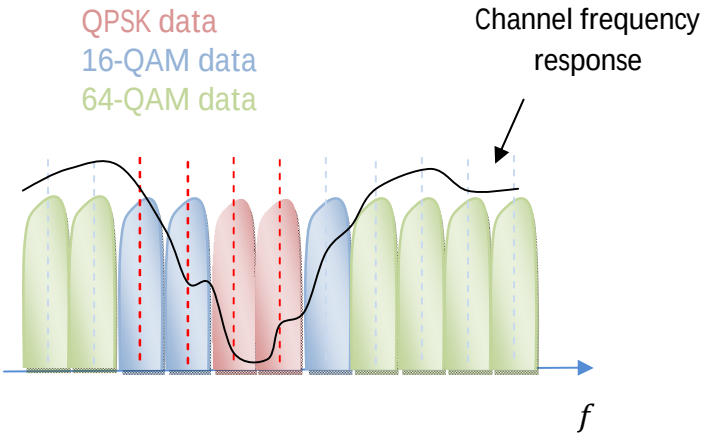

Figure 4. 30 - Modulation scheme adaptation

4.6.2. MIMO Processing Layers

In this section we present the last 4 layers of LTE physical chain, which are the layer mapping, precoding, RE mapping and OFDM modulation. Before we start to see each layer individually, there are some important concepts related with MIMO spatial multiplexing modes that we consider important the understanding of their meaning in this context. As discussed before, in a spatial multiplexing (SM) mode several data streams or layers can be transmitted in parallel on the same frequency subcarrier. The number of parallel layers that can be transmitted reliably across the channel is assessed computing the rank value of the channel, therefore in a $N_R \times N_T$ MIMO channel, the number of parallel layers supported is always $\leq min(N_R, N_T)$ which is also the range of the rank variation. So, when the channel rank is equals to $min(N_R, N_T)$, a full rank channel matrix is obtained and maximum throughput can be achieved, otherwise, if the rank $< min(N_R, N_T)$ a defficient rank matrix is verified and lower SM gains must be used. Note that computing the rank we adapt the transmission according the channel correlation conditions.
In a mathematical point of view the rank of a matrix is equal the numbers rows/columns which are independent. Being more precise, the rank is computed over the rows and columns, but due the fact that the row rank is always equals the column rank we just say matrix rank. In the following sections is considered that the number of parallel transmitted layers is equal the rank transmission in a SM context [2][20].
The MIMO processing layers (layer mapping, precoding, RE mapping, OFDM) referred in this section are used to process the signal in order to adapt the transmission to the MIMO channel. Although LTE specifies several MIMO transmission modes, the same layer structure is used to perform the MIMO processing operations; therefore an internal adaptation of the MIMO layers is done to compute a specific MIMO transmission mode. In order to present the set of operations performed by each one of these layers, we will use LTE TM2, which defines a MIMO diversity mechanism. Therefore SFBC and SFBC-FSTD diversity schemes are used to perform the next demonstrations.

- **Layer Mapping**

The layer mapping performs a type of demux operation over the codeword symbols, so if a 2 antennas transmission diversity scheme is selected, the layer mapping execute a demux of 2 symbols, and in the case of a 4 antennas diversity scheme, a demux of 4 symbols is done. So, in diversity schemes only one codeword is used and the number of layers for mapping is equal the number of antennas used for transmission [2][20].

Layer mapping for 2 antennas Diversity mode – SFBC in LTE:

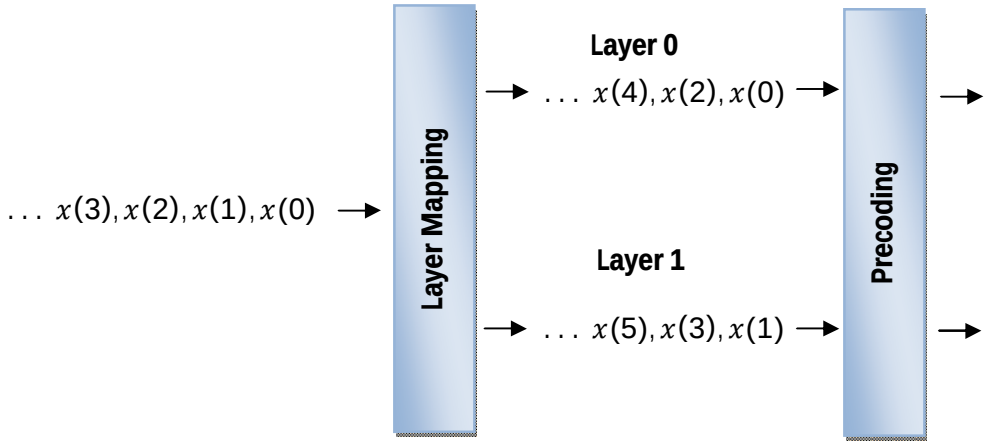

Figure 4. 31 - Layer mapping for 2 Tx antennas SFBC

Layer mapping for 4 antennas Diversity mode – SFBC-FSTD in LTE:

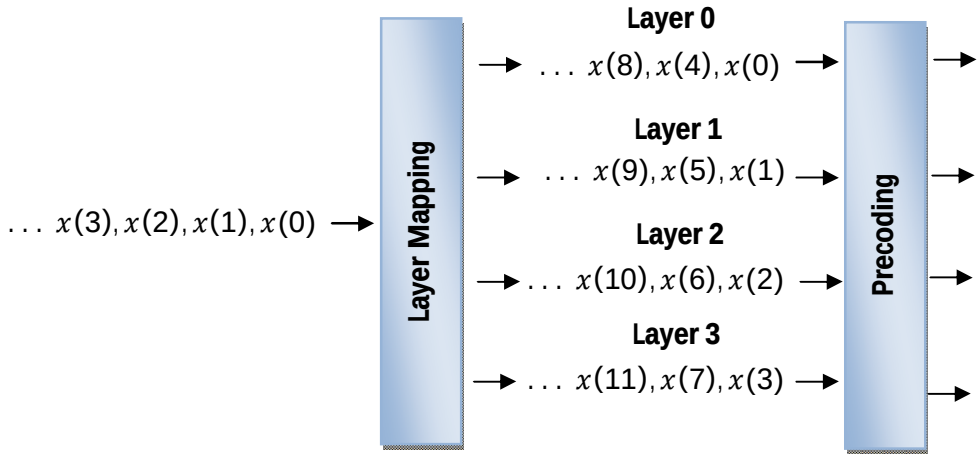

Figure 4. 32 - Layer mapping for 4 Tx antennas

As we said before, the layer mapping is adapted according the LTE transmission mode choice, therefore in case of switch to a spatial multiplexing mode, LTE layer mapping is done in the following form for each rank selected.

Rank 1 layer mapping for SM mode:

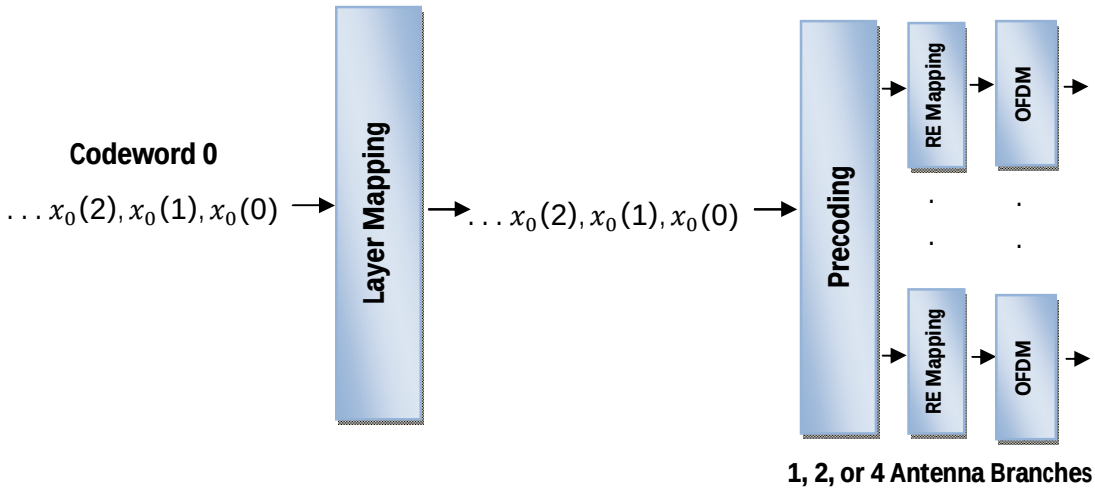

Figure 4. 33 - Rank 1 layer mapping

The rank 1 transmission is used when the UE experiments high correlation channel conditions. The codeword to layer mapping is straightforward in this case, therefore just one symbol is transmitted in one subcarrier using 1, 2 or 4 antennas (BS depending). Latter we will see in more detail the precoding operation.

Rank 2 layer mapping for SM mode:

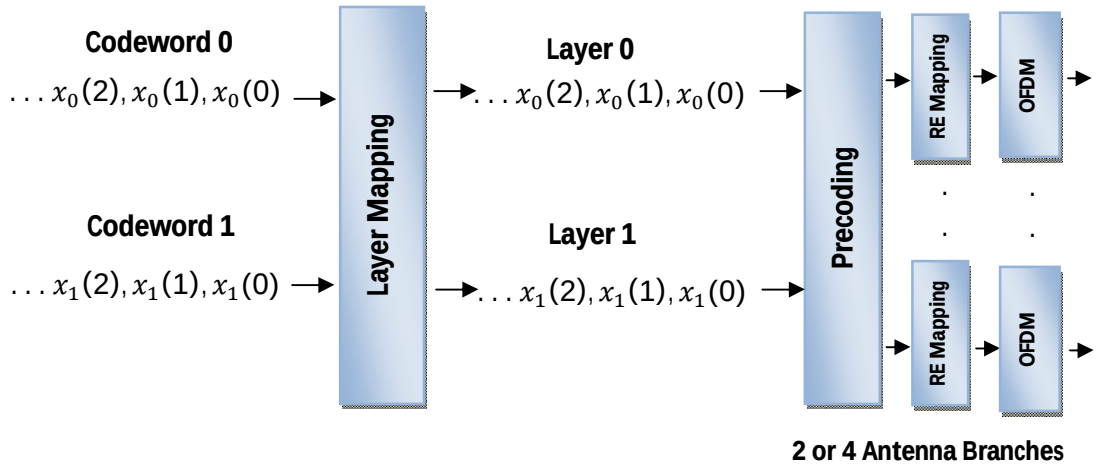

Figure 4. 34 - Rank 2 layer mapping

In rank 2 transmission at least 2 antennas must be available at BS to transmit 2 codeword's, which are coded and modulated in independent way. Each one of the codeword's can use different modulation schemes and different FEC code-rate, therefore a Channel Quality Indicator (CQI) - says the best modulation scheme and code-rate for FEC according channel

measures at UE - is feedback for each one of the codeword's, increasing the overhead. Looking to the above figure we can see that 2 layers are used, with each codeword directly mapped in one layer. Note that 2 different information symbols are transmitted in the same subcarrier across 2 or 4 antennas.

Rank 3 layer mapping for SM mode:

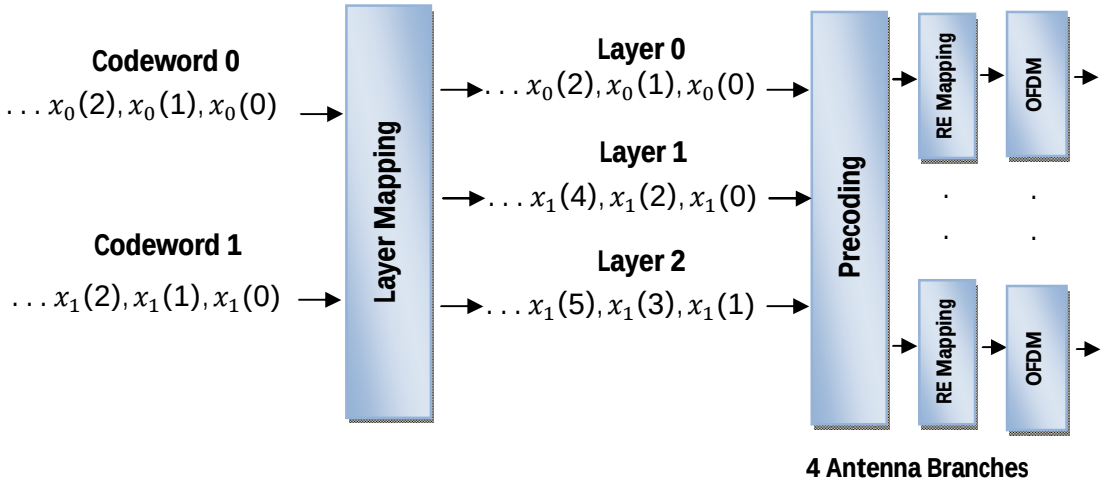

Figure 4. 35 - Rank 3 layer mapping

In a rank 3 transmission we are able to transmit 3 different information symbols in the same frequency subcarrier at the same time using 4 antennas (4 parallel OFDM symbols). A rank 3 transmission maps the entire codeword 0 at layer 0, and codeword 1 is split between layer 1 and 2, hence the number of symbols at layer 1 and 2 is half of layer 0 (padding needed).

Rank 4 layer mapping for SM mode:

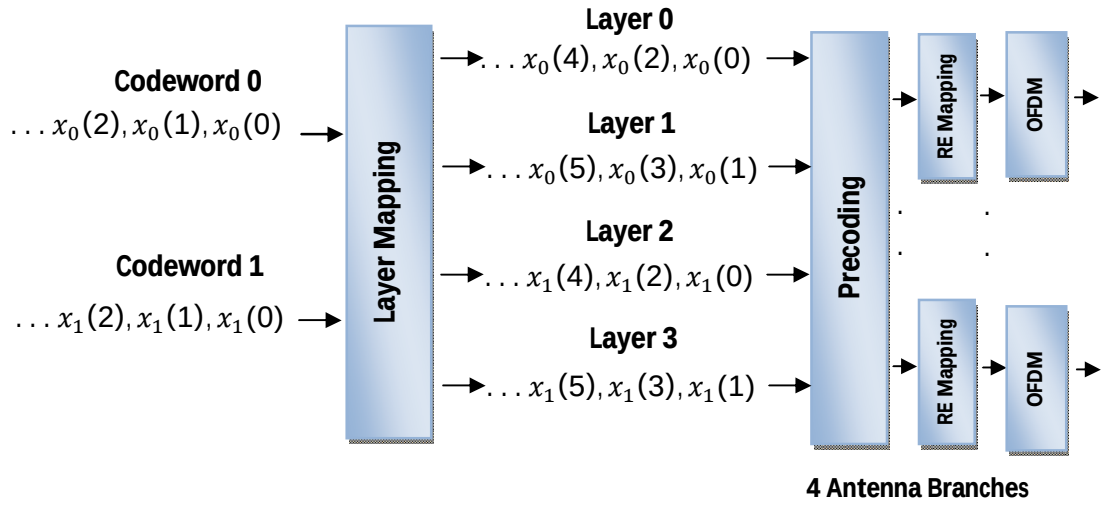

Figure 4. 36 - Rank 4 layer mapping

A rank 4 transmission mode allow high data throughput at the UE (MIMO-SU) sending 4 parallel data streams. This transmission mode is used for UEs which are under uncorrelated and high rank channel conditions. When a UE is in the edge of the cell, normally is used a rank 1 beamforming transmission mode, that shapes the antenna beam in the UE direction. In a rank 4 transmission, codeword 0 is split between layers 0 and 1, and codeword 1 by layer 2 and 3, therefore each codeword experiment 2 layers of diversity.

- **Precoding operation**

Like the SFBC scheme was the choice for LTE 2 antennas transmission diversity mode, and SFBC-FSTD was the choice for 4 antennas we will use these schemes to exemplify the precoding operation and also the RE mapping. In the next explanation we will split the complex symbols in their real and imaginary parts, and also we will index them to the layer l from where they provide. Consider the mapping of M_{Layer} complex symbols in each layer l [2][20].

$$x^l(i) = x_R^l(i) + jx_I^l(i) \tag{4. 19}$$

Using as reference the layer mapping of Figure 4.31, we will define the following layer mapping,

$$x^0(i) = x(2i) \tag{4. 20}$$

$$x^1(i) = x(2i+1) \tag{4. 21}$$

$$i = 0, 1, 2, 3, \dots, M_{Layer}$$

The precoding operation for SFBC is done applying the follow matrix operation.

$$\begin{bmatrix} y_0(2i) \\ y_1(2i) \\ y_0(2i+1) \\ y_1(2i+1) \end{bmatrix} = \frac{1}{\sqrt{2}} \begin{bmatrix} 1 & j & 0 & 0 \\ 0 & 0 & -1 & j \\ 0 & 0 & 1 & j \\ 1 & -j & 0 & 0 \end{bmatrix} \begin{bmatrix} x_R^0(i) \\ x_I^0(i) \\ x_R^1(i) \\ x_I^1(i) \end{bmatrix} \tag{4. 22}$$

$$\begin{bmatrix} y_0(2i) \\ y_1(2i) \\ y_0(2i+1) \\ y_1(2i+1) \end{bmatrix} = \frac{1}{\sqrt{2}} \begin{bmatrix} x^0(i) \\ -x^1(i)^* \\ x^1(i) \\ x^0(i)^* \end{bmatrix}$$

Then, according the frequency-space grid of SFBC, we will map the precoded signals in the correct frequency-space positions.

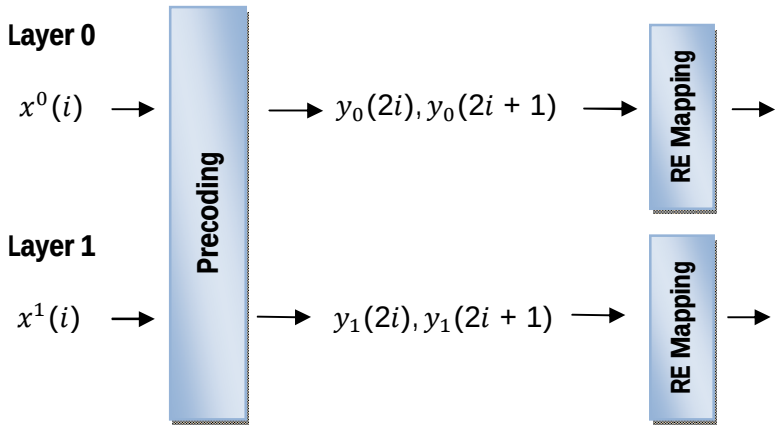

Figure 4. 37 - Precoding for 2 Tx antennas SFBC in LTE

In the case of 4 transmit antennas diversity, the LTE choice was SFBC-FSTD that is precoded in the following way,

$$\begin{bmatrix} y_0(4i) \\ y_1(4i) \\ y_2(4i) \\ y_3(4i) \\ y_0(4i+1) \\ y_1(4i+1) \\ y_2(4i+1) \\ y_3(4i+1) \\ y_0(4i+2) \\ y_1(4i+2) \\ y_2(4i+2) \\ y_3(4i+2) \\ y_0(4i+3) \\ y_1(4i+3) \\ y_2(4i+3) \\ y_3(4i+3) \end{bmatrix} = \frac{1}{\sqrt{2}} \begin{bmatrix} 1 & j & 0 & 0 & 0 & 0 & 0 & 0 \\ 0 & 0 & 0 & 0 & 0 & 0 & 0 & 0 \\ 0 & 0 & -1 & j & 0 & 0 & 0 & 0 \\ 0 & 0 & 0 & 0 & 0 & 0 & 0 & 0 \\ 0 & 0 & 1 & j & 0 & 0 & 0 & 0 \\ 0 & 0 & 0 & 0 & 0 & 0 & 0 & 0 \\ 1 & -1 & 0 & 0 & 0 & 0 & 0 & 0 \\ 0 & 0 & 0 & 0 & 0 & 0 & 0 & 0 \\ 0 & 0 & 0 & 0 & 0 & 0 & 0 & 0 \\ 0 & 0 & 0 & 0 & 1 & j & 0 & 0 \\ 0 & 0 & 0 & 0 & 0 & 0 & 0 & 0 \\ 0 & 0 & 0 & 0 & 0 & 0 & -1 & j \\ 0 & 0 & 0 & 0 & 0 & 0 & 0 & 0 \\ 0 & 0 & 0 & 0 & 0 & 0 & 1 & j \\ 0 & 0 & 0 & 0 & 0 & 0 & 0 & 0 \\ 0 & 0 & 0 & 0 & 1 & -j & 0 & 0 \end{bmatrix} \begin{bmatrix} x_R^0(i) \\ x_I^0(i) \\ x_R^1(i) \\ x_I^1(i) \\ x_R^2(i) \\ x_I^2(i) \\ x_R^3(i) \\ x_I^3(i) \end{bmatrix} = \frac{1}{\sqrt{2}} \begin{bmatrix} x^0(i) \\ 0 \\ -x^1(i)^* \\ 0 \\ x^1(i) \\ 0 \\ x^0(i)^* \\ 0 \\ 0 \\ x^2(i) \\ 0 \\ -x^3(i)^* \\ 0 \\ x^3(i) \\ 0 \\ x^2(i)^* \end{bmatrix} \quad (4.\ 23)$$

After the precoding operation we have now all the symbols needed for mapping in the resource blocks in order to perform OFDM modulation. The RE mapping just put the symbols at the input of OFDM (IFFT operation) block in the correct sequence, according to the code frequency-space grid specifications, so that the symbols will be distributed in the correct subcarriers.

The LTE MIMO layers configuration for SFBC-FSTD precoding is the follow,

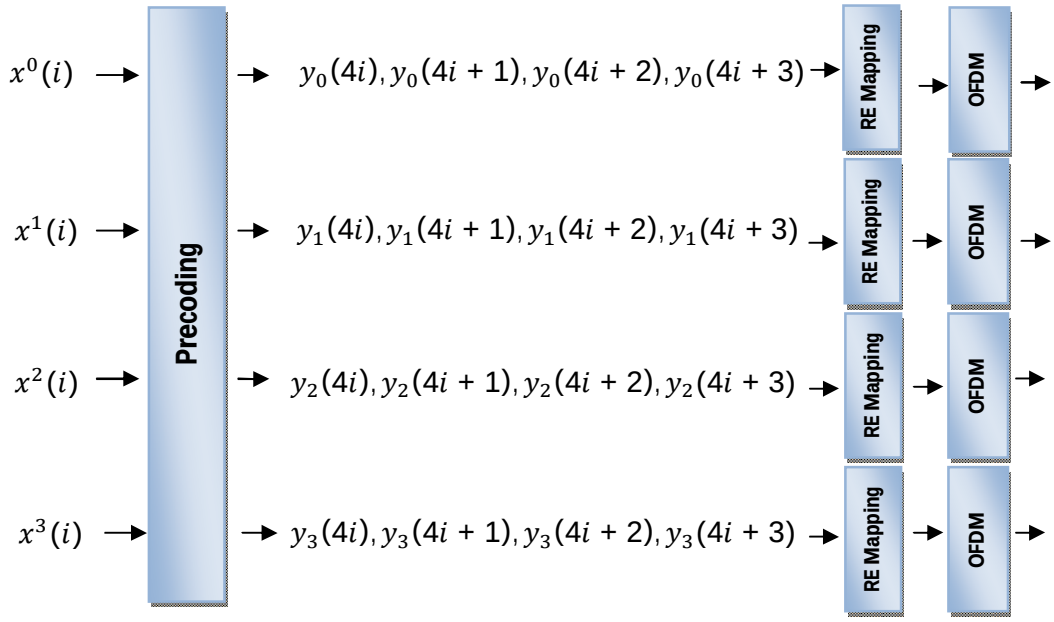

Figure 4. 38 - Precoding for 2 Tx antennas SFBC-FSTD in LTE

In the case of MIMO spatial multiplexing just different precoding matrices are used.

- **Resource Mapping and OFDM modulation**

In the SFBC and SFBC-FSTD case, the symbols of one codeword are distributed in the frequency domain. Thus, in SFBC one codeword is transmitted in one OFDM period, sending 2 OFDM symbols in parallel [2][20].

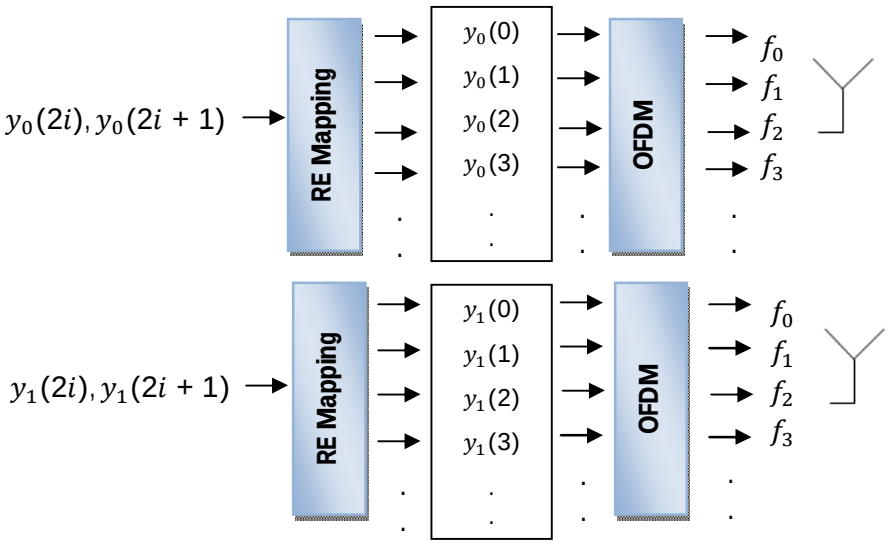

Figure 4. 39 - RE mapping and OFDM modulation for 2 Tx antennas SFBC

For the case of SFBC-FSTD the mapping and OFDM modulation is done in the same way, but now using 4 antenna branches.

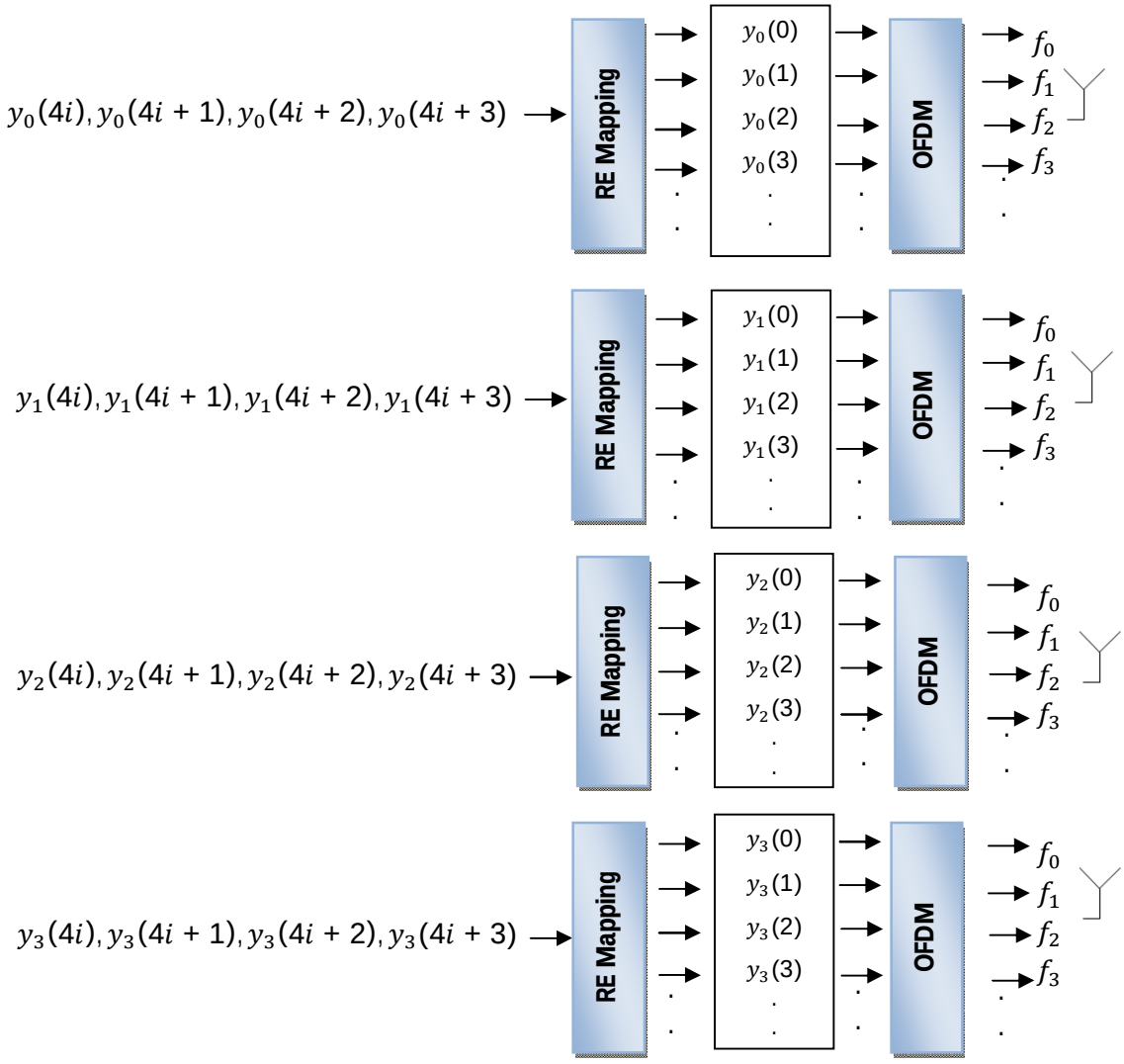

Figure 4. 40 - RE mapping and OFDM modulation for 4 Tx antennas SFBC-FSTD

5. MIMO Transmission Modes in LTE

In this chapter we discuss how the MIMO mechanisms are implemented in practical LTE cellular standard. The LTE physical layer adapts the type of MIMO mechanism used for downlink, selecting a specific MIMO Transmission Mode (TM), which could be a SM mode, a diversity mode or a beamforming mode.

We will see that the selection of the TM used for a given UE is based on the channel conditions, which varies according the scenario context where the UE is operating. Due system practical constraints, sometimes is difficult to obtain in both sides of the link the precise channel conditions, therefore we will show how LTE adapts the several MIMO mechanisms in a real implementation scenario.

5.1. TM1 - Single Antenna port 0

The LTE Transmission Mode 1 (TM1) only allows the configuration of one antenna for transmission, even that the BS is equipped with multiple antennas. The used antenna is characterized by the structure of the transmitted reference signals seen by UE, and in this case the cell-specific reference signal port 0 is used for channel estimation. Using just one antenna at

the BS doesn't allow spatial multiplexing techniques, neither spatial transmit diversity or beamforming, and because of that, throughput rates and cell coverage is reduced. Due the limited throughput and coverage, TM1 is used in small cell sites for services where high speed connections are not required by the UEs.

The only diversity that is possible with this antenna configuration is done repeating the symbols across different time-slots and frequency subcarriers, therefore just time and frequency diversity is possible.

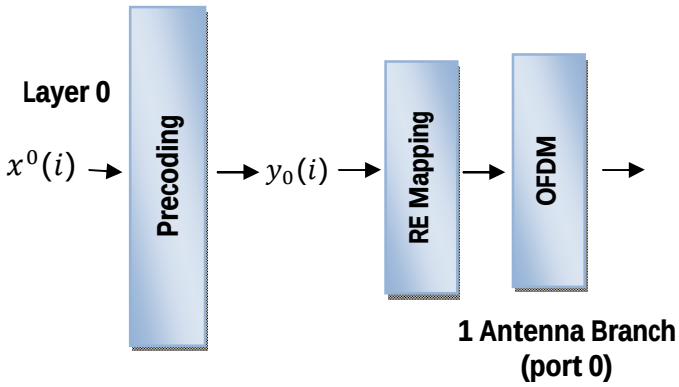

Figure 5. 1 - Layer mapping and precoding for TM1

$$y_0(i) = x^0(i) \tag{5. 1}$$

Looking to Figure 5.1 is possible see part of the transmission chain structure adapted to this mode. In TM1, one codeword is directly mapped in just one layer, which is subsequently mapped to the REs without any kind of precoding [20][21][25][27].

5.2. TM2 - Transmit Diversity Mode

As discussed before, the aim of MIMO diversity mechanism is to improve transmission reliability, thus LTE specifies SFBC and SFBC-FSTD diversity schemes in TM2. This diversity mode is also used as fallback mode by LTE, therefore if at a certain moment, the correct working of a initial selected TM is strongly affected by the changing of channel conditions, LTE by default switch's to TM2.

LTE specifies for 2 antennas transmission an SFBC diversity mode, and in the case of 4 antennas, SFBC-FSTD is the selected one. In order to be used as default transmission mode, the

diversity TM2 is the only MIMO mode that is available for all downlink physical channels, while the other MIMO modes are used just in data channel Physical Downlink Shared Channel (PDSCH).

- **SFBC**

The Space Frequency Block Coding (SFBC) was the choice in LTE for 2 antennas transmission diversity mode. SFBC decoding is done in the exact same way of STBC, but now the coding is over the frequency [2][20][30].

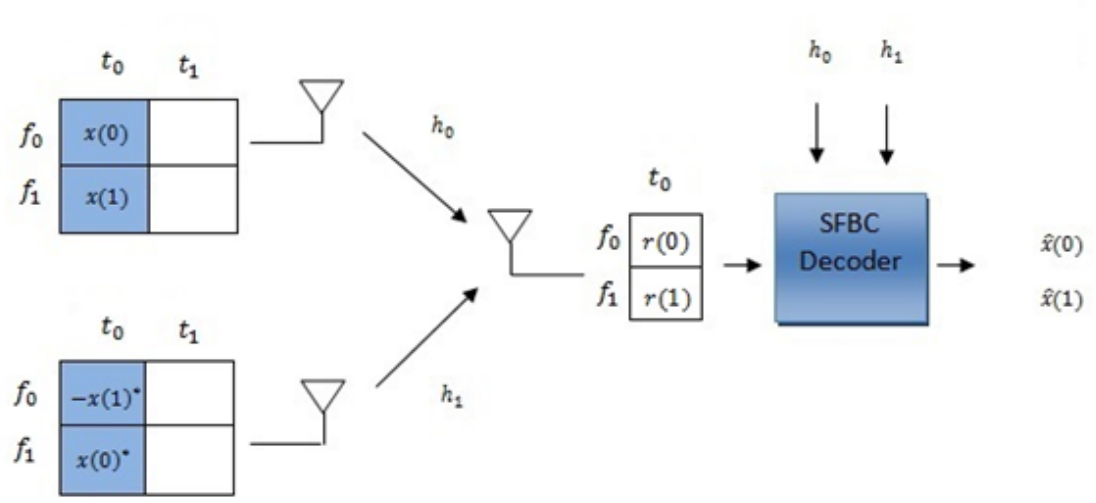

Figure 5. 2 - SFBC Alamouti Tx-Rx

After coding, the received signal is,

$$r(f_0) = h_0 x(0) - h_1 x(1)^* + n(f_0) \quad (5.\ 2)$$

$$r(f_1) = h_0 x(1) + h_1 x(0)^* + n(f_1) \quad (5.\ 3)$$

Then, the receiver computes the complex conjugate version of the received $r(f_1)$ signal. Note that with $r(f_1)^*$ we can see the rearranged received signal in the following form,

$$r(f_0) = h_0 x(0) - h_1 x(1)^* + n(f_0) \quad (5.\ 4)$$

$$r(f_1)^* = h_0^* x(1)^* + h_1^* x(0) + n(f_1)^* \quad (5.\ 5)$$

$$\tilde{\mathbf{r}} = \mathbf{H_{eq}}\mathbf{x} + \tilde{\mathbf{n}} \quad (5.\ 6)$$

$$\begin{bmatrix} r(f_0) \\ r(f_1)^* \end{bmatrix} = \begin{bmatrix} h_0 & -h_1 \\ h_1^* & h_0^* \end{bmatrix} \begin{bmatrix} x(0) \\ x(1)^* \end{bmatrix} + \begin{bmatrix} n(f_0) \\ n(f_1)^* \end{bmatrix}$$

With channel knowledge available at the receiver, we will decode the symbols $\hat{\mathbf{x}}$, using $\tilde{\mathbf{r}}$ and the matched filter version of $\mathbf{H_{eq}}$.

$$\mathbf{H_{eq}^{H}} = \begin{bmatrix} h_0^* & h_1 \\ -h_1^* & h_0 \end{bmatrix} \tag{5. 7}$$

The estimated symbols will be,

$$\hat{\mathbf{x}} = \mathbf{H_{eq}^{H}}\tilde{\mathbf{r}} \tag{5. 8}$$

$$\hat{\mathbf{x}} = \mathbf{H_{eq}^{H}}\mathbf{H_{eq}}\mathbf{x} + \mathbf{H_{eq}^{H}}\tilde{\mathbf{n}}$$

$$\begin{bmatrix} \hat{x}(0) \\ \hat{x}(1) \end{bmatrix} = \begin{bmatrix} h_0^* & h_1 \\ -h_1^* & h_0 \end{bmatrix}\begin{bmatrix} h_0 & -h_1 \\ h_1^* & h_0^* \end{bmatrix}\begin{bmatrix} x(0) \\ x(1)^* \end{bmatrix} + \begin{bmatrix} h_0^* & h_1 \\ -h_1^* & h_0 \end{bmatrix}\begin{bmatrix} n(f_0) \\ n(f_1)^* \end{bmatrix}$$

$$\begin{bmatrix} \hat{x}(0) \\ \hat{x}(1) \end{bmatrix} = \begin{bmatrix} h_0h_0^* + h_1h_1^* & 0 \\ 0 & h_1^*h_1 + h_0^*h_0 \end{bmatrix}\begin{bmatrix} x(0) \\ x(1)^* \end{bmatrix} + \begin{bmatrix} h_0^* & h_1 \\ -h_1^* & h_0 \end{bmatrix}\begin{bmatrix} n(f_0) \\ n(f_1)^* \end{bmatrix}$$

The expressions to obtain the output symbols on SFBC receiver are the same of STBC, but now instead of slot-times we use frequency subcarriers.

$$\hat{x}(0) = (|h_0|^2 + |h_1|^2)x(0) + h_0^*n(f_0) + h_1n(f_1)^* \tag{5. 9}$$

$$\hat{x}(1) = (|h_0|^2 + |h_1|^2)x(1)^* - h_1^*n(f_0) + h_0n(f_1)^* \tag{5. 10}$$

Finally we compute the complex conjugate of $\hat{x}(1)$ in order to take $x(1)$.

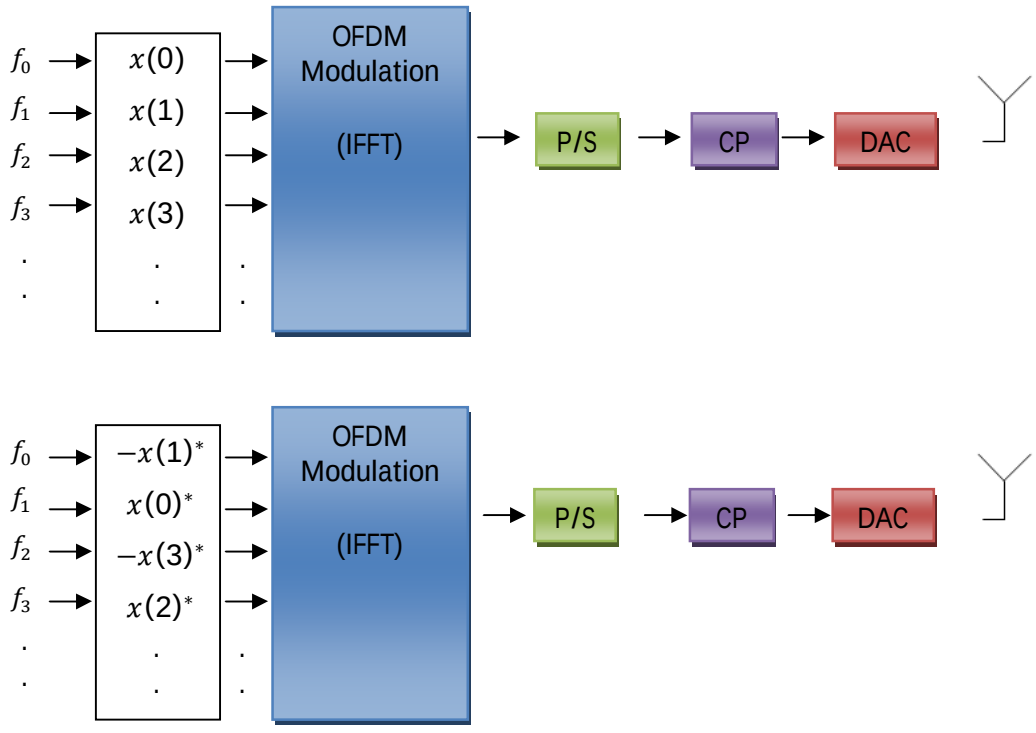

Figure 5. 3 - SFBC OFDM modulation Tx

The above figure shows an SFBC implementation using OFDM modulation. Looking the figure we can see that the first thing to do is mapping the precoded (Alamouti) symbols on the subcarriers, next is generated the OFDM symbols using IFFT, and is added CP to the samples of the OFDM signal. Due to the fact that Alamouti coding only maintain full orthogonality in the case of 2 antennas transmitter, the SFBC and STBC seen before just can be applied for the case of 2 transmit antennas.

- **SFBC-FSTD**

SFBC-FSTD was the LTE choice for transmit diversity mode in the case of 4 antennas at the transmitter. The SFBC-FSTD is used in 2 antenna pairs, where Alamouti SFBC is applied within each one of the antenna pairs, and the FSTD scheme is used in the 2 pairs. Therefore FSTD shifts the frequency between the antenna pair [2][20][30].

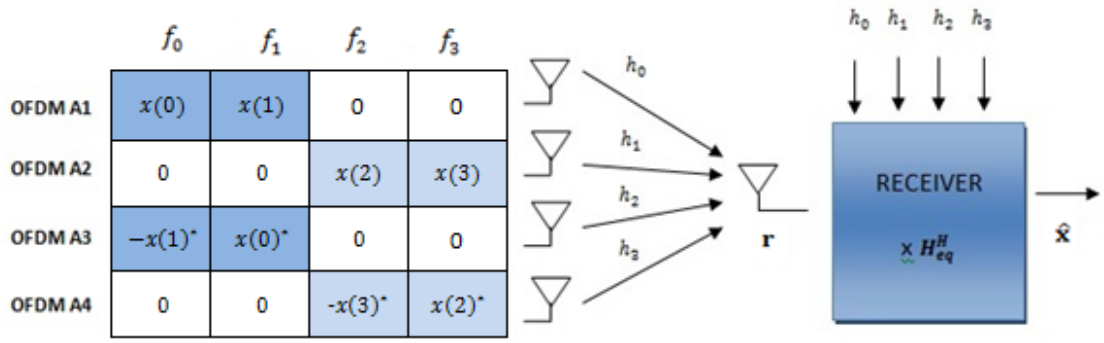

Figure 5. 4 - SFBC-FSTD mapping in LTE in 4 transmit antennas

Looking to the mapping of the above figure we can see that SFBC-FSTD is the same of 2 antennas SFBC, with the difference that now we have the liberty of choose the pair of antennas that we will use within each SFBC Alamouti block.

Using the SFBC-FSTD mapping specified in LTE, which is presented in Figure 5.4, the received signal **r** is the following,

$$\begin{bmatrix} r(f_0) \\ r(f_1) \\ r(f_2) \\ r(f_3) \end{bmatrix} = \frac{1}{\sqrt{2}} \begin{bmatrix} x(0) & 0 & -x(1)^* & 0 \\ x(1) & 0 & x(0)^* & 0 \\ 0 & x(2) & 0 & -x(3)^* \\ 0 & x(3) & 0 & x(2)^* \end{bmatrix} \begin{bmatrix} h_0 \\ h_1 \\ h_2 \\ h_3 \end{bmatrix} + \begin{bmatrix} n(f_0) \\ n(f_1) \\ n(f_2) \\ n(f_3) \end{bmatrix} \quad (5.\ 11)$$

$$r(f_0) = \frac{1}{\sqrt{2}}[x(0)h_0 + 0 - x(1)^* h_2 + 0] + n(f_0)$$

$$r(f_1) = \frac{1}{\sqrt{2}}[x(1)h_0 + 0 + x(0)^* h_2 + 0] + n(f_1)$$

$$r(f_2) = \frac{1}{\sqrt{2}}[0 + x(2)h_1 + 0 - x(3)^* h_3] + n(f_2)$$

$$r(f_3) = \frac{1}{\sqrt{2}}[0 + x(3)h_1 + 0 + x(2)^* h_3] + n(f_3)$$

Then, the receiver will compute the complex conjugate of received signals $r(f_0)$ and $r(f_2)$, which after rearranged we can see in the following form,

$$r(f_0)^* = \frac{1}{\sqrt{2}}[x(0)^* h_0^* - x(1)h_2^*] + n(f_0)^* \quad (5.\ 12)$$

$$r(f_1) = \frac{1}{\sqrt{2}}[x(1)h_0 + x(0)^* h_2] + n(f_1) \quad (5.\ 13)$$

$$r(f_2)^* = \frac{1}{\sqrt{2}}[x(2)^* h_1^* - x(3)h_3^*] + n(f_2)^* \quad (5.\ 14)$$

$$r(f_3) = \frac{1}{\sqrt{2}}[x(3)h_1 + x(2)^* h_3] + n(f_3) \quad (5.\ 15)$$

Using matrix notation we can compute the equivalent channel matrix $\mathbf{H}_{\mathbf{eq}_{\mathbf{SFBC-FSTD}}}$ and see the following rearrangement,

$$\tilde{\mathbf{r}} = \mathbf{H}_{\mathbf{eq}_{\mathbf{SFBC-FSTD}}}\mathbf{x} + \tilde{\mathbf{n}} \quad (5.\ 16)$$

$$\begin{bmatrix} r(f_0)^* \\ r(f_1) \\ r(f_2)^* \\ r(f_3) \end{bmatrix} = \frac{1}{\sqrt{2}} \begin{bmatrix} h_0^* & -h_2^* & 0 & 0 \\ h_2 & h_0 & 0 & 0 \\ 0 & 0 & h_1^* & -h_3^* \\ 0 & 0 & h_3 & h_1 \end{bmatrix} \begin{bmatrix} x(0)^* \\ x(1) \\ x(2)^* \\ x(3) \end{bmatrix} + \begin{bmatrix} n(f_0) \\ n(f_1)^* \\ n(f_2) \\ n(f_3)^* \end{bmatrix}$$

Based on the above matrix treatment and with channel knowledge available, the receiver can compute the matched filter version of $\mathbf{H}_{\mathbf{eq}_{\mathbf{SFBC-FSTD}}}$ using the Hermitian operator.

$$\mathbf{H}_{\mathbf{eq}_{\mathbf{SFBC-FSTD}}}^{\mathrm{H}} = \begin{bmatrix} h_0 & h_2^* & 0 & 0 \\ -h_2 & h_0^* & 0 & 0 \\ 0 & 0 & h_1 & h_3^* \\ 0 & 0 & -h_3 & h_1^* \end{bmatrix} \quad (5.\ 17)$$

Then, the receiver will use $\tilde{\mathbf{r}}$ and $\mathbf{H_{eq}}^{\mathrm{H}}_{\mathbf{SFBC-FSTD}}$ to decode the transmitted symbols $\hat{\mathbf{x}}$.

$$\hat{\mathbf{x}} = \mathbf{H_{eq}}^{\mathrm{H}}_{\mathbf{SFBC-FSTD}}\tilde{\mathbf{r}} \tag{5. 18}$$

$$\hat{\mathbf{x}} = \mathbf{H_{eq}}^{\mathrm{H}}_{\mathbf{SFBC-FSTD}}\mathbf{H_{eq}}_{\mathbf{SFBC-FSTD}}\mathbf{x} + \mathbf{H_{eq}}^{\mathrm{H}}_{\mathbf{SFBC-FSTD}}\tilde{\mathbf{n}}$$

We can expand the above expressions in the following matrix notation,

$$\begin{bmatrix}\hat{x}(0)^*\\ \hat{x}(1)\\ \hat{x}(2)^*\\ \hat{x}(3)\end{bmatrix} = \frac{1}{\sqrt{2}}\begin{bmatrix}h_0 & h_2^* & 0 & 0\\ -h_2 & h_0^* & 0 & 0\\ 0 & 0 & h_1 & h_3^*\\ 0 & 0 & -h_3 & h_1^*\end{bmatrix}\begin{bmatrix}h_0^* & -h_2^* & 0 & 0\\ h_2 & h_0 & 0 & 0\\ 0 & 0 & h_1^* & -h_3^*\\ 0 & 0 & h_3 & h_1\end{bmatrix}\begin{bmatrix}x(0)^*\\ x(1)\\ x(2)^*\\ x(3)\end{bmatrix} + \mathbf{H_{eq}}^{\mathrm{H}}_{\mathbf{SFBC-FSTD}}\tilde{\mathbf{n}}$$

$$\begin{bmatrix}\hat{x}(0)^*\\ \hat{x}(1)\\ \hat{x}(2)^*\\ \hat{x}(3)\end{bmatrix} = \frac{1}{\sqrt{2}}\begin{bmatrix}A & 0 & 0 & 0\\ 0 & A & 0 & 0\\ 0 & 0 & B & 0\\ 0 & 0 & 0 & B\end{bmatrix}\begin{bmatrix}x(0)^*\\ x(1)\\ x(2)^*\\ x(3)\end{bmatrix} + \mathbf{H_{eq}}^{\mathrm{H}}_{\mathbf{SFBC-FSTD}}\tilde{\mathbf{n}}$$

$$A = |h_0|^2 + |h_2|^2 \tag{5. 19}$$

$$B = |h_1|^2 + |h_3|^2 \tag{5. 20}$$

Finally the receiver compute the complex conjugate of $\hat{x}(0)^*$ and $\hat{x}(2)^*$ in order to obtain the transmitted symbols.

We can see that with SFBC-FSTD the receiver is able to recover the symbols without interference between them. Also figure that we continue with the same diversity order of SFBC, which is 2.

Note that with SFBC-FSTD we reduce the channel correlation effect at transmission, mapping each Alamouti block in non consecutive antennas. Thus, with a relative large distance between the antennas used within each block set, we increase the channel frequency diversity, which is the ideal scenario to perform this transmission mode.

The OFDM mapping for SFBC-FSTD is performed in the following way.

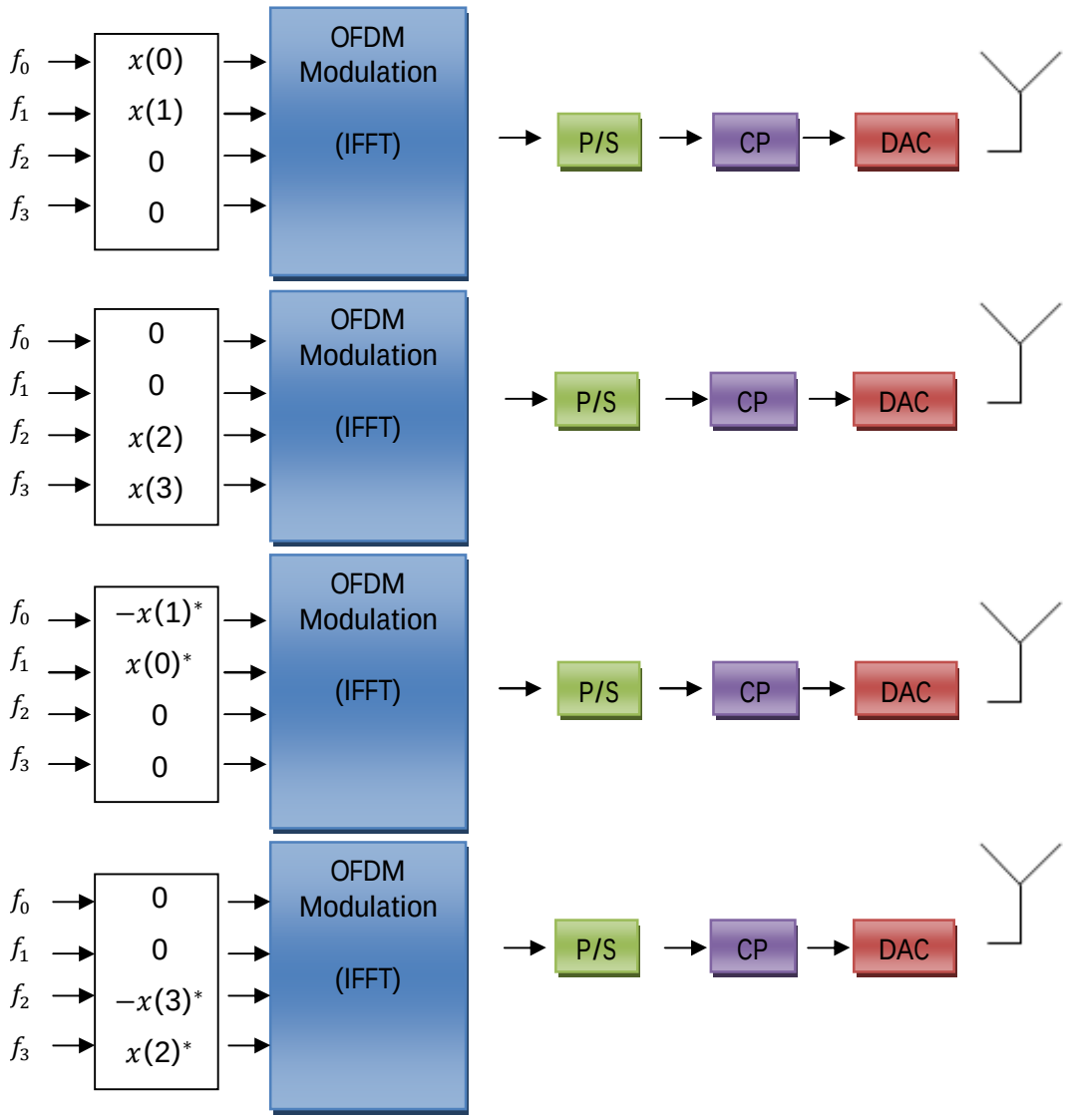

Figure 5. 5 - SFBC-FSTD OFDM modulation

5.3. TM3 - Open-Loop MIMO Mode

The Open-Loop MIMO transmission mode is a spatial multiplexing mode used when is not possible for the BS tracking the channel using feedback signals transmitted from the UE. An example of this kind of situation is when the UE moves at high speed, making feedback delays to high compared to channel variation speed.

This LTE mode uses 3 precoding matrices that are cyclically shifted according to the subcarrier index used.

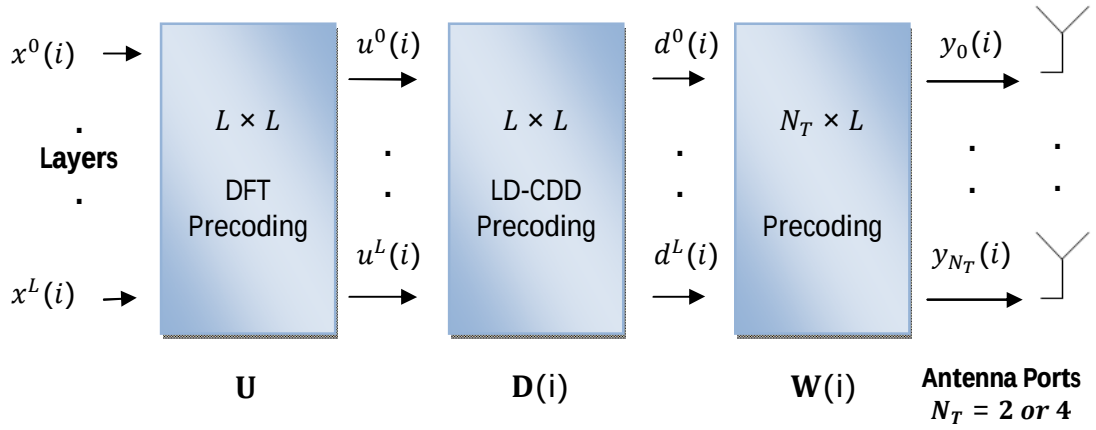

Figure 5. 6 - TM3 precoding structure

Consider L the number of layers, N_T the number of transmit antennas and i the subcarrier index.

$$\begin{bmatrix} y_0(i) \\ \cdot \\ \cdot \\ y_{N_T}(i) \end{bmatrix} = \mathbf{W}(i)\mathbf{D}(i)\mathbf{U} \begin{bmatrix} x^0(i) \\ \cdot \\ \cdot \\ x^L(i) \end{bmatrix} \quad (5.\ 21)$$

The second matrix $\mathbf{D}(i)$ is a Large-Delay Cyclic Delay Diversity (LD-CDD) identity matrix that cyclically shifts the columns position of the fixed DFT $\mathbf{U}$ matrix according the subcarriers index$i$. The last $\mathbf{W}(i)$ matrix is selected from a codebook set of matrices used also in the closed loop mode (TM4), being switched at each L subcarrier blocks. In open loop mode, a transmit diversity mode is used for rank 1 transmission for the cases of 2 and 4 antennas, therefore large-delay CDD with precoding is only applied for ranks greater than 1.

- **Precoding for 2 antennas**

In the case of 2 antennas, a rank 2 transmission is done using a 2x2 large delay CDD matrix $\mathbf{D}(i)$. The $\mathbf{D}(i)$ matrix shifts the columns of a 2x2 fixed DFT matrix. The third used matrix $\mathbf{W}(i)$ is a 2x2 identity matrix from the codebook used in closed loop mode.
The large-delay CDD matrix is given by,

$$\mathbf{D}_{2\times2}(i) = \begin{bmatrix} 1 & 0 \\ 0 & e^{-j\pi i} \end{bmatrix} \quad (5.\ 22)$$

We can see that $\mathbf{D}_{2\times2}(i)$ performs a phase shift in the second antenna of 0° for even subcarriers, and 180° for odd subcarriers.

The fixed DFT matrix is given by,

$$\mathbf{U_{2\times 2}} = \frac{1}{\sqrt{2}}\begin{bmatrix}1 & 1\\ 1 & e^{-j\pi}\end{bmatrix} = \frac{1}{\sqrt{2}}\begin{bmatrix}1 & 1\\ 1 & -1\end{bmatrix} \quad (5.\ 23)$$

The cyclic column shift is performed in the following way in the case of i subcarrier index being an even value,

$$\mathbf{D_{2\times 2}}(i)\mathbf{U_{2\times 2}} = \begin{bmatrix}1 & 0\\ 0 & 1\end{bmatrix}\frac{1}{\sqrt{2}}\begin{bmatrix}1 & 1\\ 1 & -1\end{bmatrix} = \frac{1}{\sqrt{2}}\begin{bmatrix}1 & 1\\ 1 & -1\end{bmatrix} \quad (5.\ 24)$$

In the case of odd subcarriers,

$$\mathbf{D_{2\times 2}}(i)\mathbf{U_{2\times 2}} = \begin{bmatrix}1 & 0\\ 0 & -1\end{bmatrix}\frac{1}{\sqrt{2}}\begin{bmatrix}1 & 1\\ 1 & -1\end{bmatrix} = \frac{1}{\sqrt{2}}\begin{bmatrix}1 & 1\\ -1 & 1\end{bmatrix}, \quad (5.\ 25)$$

Looking to the above calculations is possible to see the columns shift.

In 2 antennas case, $\mathbf{W}(i)$ is a fixed matrix from the codebook set (index 0) used in closed loop mode for 2 transmit antennas.

$$\mathbf{W_{2\times 2}}(i) = \frac{1}{\sqrt{2}}\begin{bmatrix}1 & 0\\ 0 & 1\end{bmatrix} \quad (5.\ 26)$$

The precoded signals for odd and even subcarriers are the following,

$$\begin{bmatrix}y_0(i)\\ y_1(i)\end{bmatrix} = \mathbf{W}(i)\mathbf{D}(i)\mathbf{U}\begin{bmatrix}x^0(i)\\ x^1(i)\end{bmatrix} \quad (5.\ 27)$$

For even subcarriers,

$$\begin{bmatrix}y_0(i)\\ y_1(i)\end{bmatrix} = \frac{1}{\sqrt{2}}\begin{bmatrix}1 & 0\\ 0 & 1\end{bmatrix}\begin{bmatrix}1 & 0\\ 0 & 1\end{bmatrix}\begin{bmatrix}1 & 1\\ 1 & -1\end{bmatrix}\begin{bmatrix}x^0(i)\\ x^1(i)\end{bmatrix} \quad (5.\ 28)$$

$$y_0(i) = \frac{1}{\sqrt{2}}(x^0(i) + x^1(i))$$

$$y_1(i) = \frac{1}{\sqrt{2}}(x^0(i) - x^1(i))$$

For odd subcarriers,

$$\begin{bmatrix}y_0(i)\\ y_1(i)\end{bmatrix} = \frac{1}{\sqrt{2}}\begin{bmatrix}1 & 0\\ 0 & 1\end{bmatrix}\begin{bmatrix}1 & 0\\ 0 & -1\end{bmatrix}\begin{bmatrix}1 & 1\\ 1 & -1\end{bmatrix}\begin{bmatrix}x^0(i)\\ x^1(i)\end{bmatrix} \quad (5.\ 29)$$

$$y_0(i) = \frac{1}{\sqrt{2}}(x^0(i) + x^1(i))$$

$$y_1(i) = \frac{1}{\sqrt{2}}(-x^0(i) + x^1(i))$$

From 5.28 and 5.29 we can see that only the signals transmitted from the second antenna changes according the subcarrier index [9][20][21][30].

- **Precoding for 4 antennas**

In the case of 4 antennas, the precoding structure is the same of 2 antennas. In this case a large delay CDD+precoding matrices are used to perform rank 2, 3 and 4 transmissions, while in rank 1 case a transmission diversity mode is used. The matrices **U** and $\mathbf{D}(i)$ used for precoding in rank 2, 3 and 4 are in Tables 6 and 7 respectively.

Layers/rank	$L \times L$ *DFT matrix* **U**
2	$\mathbf{U}_{2\times 2} = \frac{1}{\sqrt{2}}\begin{bmatrix} 1 & 1 \\ 1 & e^{-j\pi} \end{bmatrix}$
3	$\mathbf{U}_{3\times 3} = \frac{1}{\sqrt{3}}\begin{bmatrix} 1 & 1 & 1 \\ 1 & e^{-j2\pi/3} & e^{-j4\pi/3} \\ 1 & e^{-j4\pi/3} & e^{-j8\pi/3} \end{bmatrix}$
4	$\mathbf{U}_{4\times 4} = \frac{1}{\sqrt{4}}\begin{bmatrix} 1 & 1 & 1 & 1 \\ 1 & e^{-j2\pi/4} & e^{-j4\pi/4} & e^{-j6\pi/4} \\ 1 & e^{-j4\pi/4} & e^{-j8\pi/4} & e^{-j12\pi/4} \\ 1 & e^{-j6\pi/4} & e^{-j12\pi/4} & e^{-j18\pi/4} \end{bmatrix}$

Table 6 - Set of DFT U matrices used for rank 2, 3 and 4 [21]

Layers/rank	$L \times L$ *matrix* $\mathbf{D}(i)$
2	$\mathbf{D}(i)_{2\times 2} = \begin{bmatrix} 1 & 0 \\ 0 & e^{-j\pi i} \end{bmatrix}$
3	$\mathbf{D}(i)_{3\times 3} = \begin{bmatrix} 1 & 0 & 0 \\ 0 & e^{-j2\pi i/3} & 0 \\ 0 & 0 & e^{-j4\pi i/3} \end{bmatrix}$
4	$\mathbf{D}(i)_{4\times 4} = \begin{bmatrix} 1 & 0 & 0 & 0 \\ 0 & e^{-j2\pi i/4} & 0 & 0 \\ 0 & 0 & e^{-j4\pi i/4} & 0 \\ 0 & 0 & 0 & e^{-j6\pi i/4} \end{bmatrix}$

Table 7 - Set of Large Delay-CDD matrices used for rank 2, 3 and 4 [21]

The column cyclic shift performed over the U matrix in a rank 3 transmission is shown below.

$$i = 0, 3, 6, 9 \ldots$$

$$\mathbf{D}(0)_{3\times 3}\mathbf{U}_{3\times 3} = \begin{bmatrix} 1 & 0 & 0 \\ 0 & e^{0} & 0 \\ 0 & 0 & e^{0} \end{bmatrix} \frac{1}{\sqrt{3}} \begin{bmatrix} 1 & 1 & 1 \\ 1 & e^{-j2\pi/3} & e^{-j4\pi/3} \\ 1 & e^{-j4\pi/3} & e^{-j8\pi/3} \end{bmatrix} \tag{5. 30}$$

$$\mathbf{D}(0)_{3\times 3}\mathbf{U}_{3\times 3} = \frac{1}{\sqrt{3}} \begin{bmatrix} 1 & 1 & 1 \\ 1 & e^{-j2\pi/3} & e^{-j4\pi/3} \\ 1 & e^{-j4\pi/3} & e^{-j8\pi/3} \end{bmatrix}$$

In the case of subcarriers

$$i = 1, 4, 7, 10 \ldots$$

$$\mathbf{D}(1)_{3\times 3}\mathbf{U}_{3\times 3} = \begin{bmatrix} 1 & 0 & 0 \\ 0 & e^{-j2\pi/3} & 0 \\ 0 & 0 & e^{-j4\pi/3} \end{bmatrix} \frac{1}{\sqrt{3}} \begin{bmatrix} 1 & 1 & 1 \\ 1 & e^{-j2\pi/3} & e^{-j4\pi/3} \\ 1 & e^{-j4\pi/3} & e^{-j8\pi/3} \end{bmatrix} \tag{5. 31}$$

$$\mathbf{D}(1)_{3\times 3}\mathbf{U}_{3\times 3} = \frac{1}{\sqrt{3}} \begin{bmatrix} 1 & 1 & 1 \\ e^{-j2\pi/3} & e^{-j4\pi/3} & 1 \\ e^{-j4\pi/3} & e^{-j8\pi/3} & 1 \end{bmatrix}$$

For subcarriers,

$$i = 2, 5, 8, 11 \ldots$$

$$\mathbf{D}(2)_{3\times 3}\mathbf{U}_{3\times 3} = \begin{bmatrix} 1 & 0 & 0 \\ 0 & e^{-j4\pi/3} & 0 \\ 0 & 0 & e^{-j8\pi/3} \end{bmatrix} \frac{1}{\sqrt{3}} \begin{bmatrix} 1 & 1 & 1 \\ 1 & e^{-j2\pi/3} & e^{-j4\pi/3} \\ 1 & e^{-j4\pi/3} & e^{-j8\pi/3} \end{bmatrix} \tag{5. 32}$$

$$\mathbf{D}(2)_{3\times 3}\mathbf{U}_{3\times 3} = \frac{1}{\sqrt{3}} \begin{bmatrix} 1 & 1 & 1 \\ e^{-j4\pi/3} & 1 & e^{-j2\pi/3} \\ e^{-j8\pi/3} & 1 & e^{-j4\pi/3} \end{bmatrix}$$

For rank 2 and 4 the cyclic principle is the same of rank 3.

The precoding matrix $\mathbf{W}(i)$ in this case changes at each L subcarrier block. The used matrices are selected from a set of matrices defined in a codebook. Each matrix in this codebook is computed using a Householder transformation applied over a $\mathbf{u_n}$ vector. The Householder transformation is done using the following expression.

$$\mathbf{W_n} = \mathbf{I}_{4\times 4} - 2\mathbf{u_n}\mathbf{u_n^H}/\mathbf{u_n^H}\mathbf{u_n} \tag{5. 33}$$

The used matrices $\mathbf{W}(i)$for each rank are shown in Table 7.

C_k	u_n	Layer 2	Layer 3	Layer 4
C_1	$u_{12} = [1 \ -1 \ -1 \ 1]^T$	$\mathbf{W}_{12}^{\{12\}}/\sqrt{2}$	$\mathbf{W}_{12}^{\{123\}}/\sqrt{3}$	$\mathbf{W}_{12}^{\{1234\}}/\sqrt{4}$
C_2	$u_{13} = [1 \ -1 \ 1 \ -1]^T$	$\mathbf{W}_{13}^{\{13\}}/\sqrt{2}$	$\mathbf{W}_{13}^{\{123\}}/\sqrt{3}$	$\mathbf{W}_{13}^{\{1324\}}/\sqrt{4}$
C_3	$u_{14} = [1 \ 1 \ -1 \ -1]^T$	$\mathbf{W}_{14}^{\{13\}}/\sqrt{2}$	$\mathbf{W}_{14}^{\{123\}}/\sqrt{3}$	$\mathbf{W}_{14}^{\{3214\}}/\sqrt{4}$
C_4	$u_{15} = [1 \ 1 \ 1 \ 1]^T$	$\mathbf{W}_{15}^{\{12\}}/\sqrt{2}$	$\mathbf{W}_{15}^{\{123\}}/\sqrt{3}$	$\mathbf{W}_{15}^{\{1234\}}/\sqrt{4}$

Table 8 - Precoding set of matrices for LTE Open-Loop mode [9]

The form used to obtain the precoding matrices $\mathbf{W}(i)$ is based in the concatenation of rank columns from the $\mathbf{W_n}$ 4x4 matrix. Therefore in layer 2, $\mathbf{W_n^{\{xy\}}}$ matrices only uses the columns $x$and y of $\mathbf{W_n}$, for the layer 3 case the matrices $\mathbf{W_n^{\{xyz\}}}$ uses columns x, y and z of the 4x4 $\mathbf{W_n}$ matrix, and finally $\mathbf{W_n^{\{xyzw\}}}$ uses the columns x, y, z and w by the present order.

Like we said before, the $\mathbf{W}(i)$ matrix is not fixed, changing at each L subcarriers according the following expression.

$$\mathbf{W}(i) = C_k \tag{5. 34}$$

$$k = mod\left(\frac{i}{L}, 4\right) + 1 \tag{5. 35}$$

The switching pattern of matrix $\mathbf{W}(i)$ for each rank/layer mode is presented in Table 8.

i	0	1	2	3	4	5	6	7	8	9	10	11	12	....
Layer 2	C_1	C_1	C_2	C_2	C_3	C_3	C_4	C_4	C_1	C_1	C_2	C_2	C_3	....
Layer 3	C_1	C_1	C_1	C_2	C_2	C_2	C_3	C_3	C_3	C_4	C_4	C_4	C_1	....
Layer 4	C_1	C_1	C_1	C_1	C_2	C_2	C_2	C_2	C_3	C_3	C_3	C_3	C_4	....

Table 9 - Switching matrix pattern for LTE Open Loop mode [9]

While the large delay CDD distributes each codeword across the different layers, the $\mathbf{W}(i)$ precoding matrix allows the transmission of each layer over all the 4 antennas. We should refer that despite this is an open-loop mode, the feedback signals Rank Indicator (RI) and CQI are transmitted from the UE to the BS. The difference between the closed loop and open loop mode

is that in the closed loop the UE recommends a specific precoding matrix, while in the open loop mode the used precoding matrices changes periodically along the subcarriers without Precoding Matrix Index (PMI) feedback [9][20][21][30].

5.4. TM4 - Closed Loop MIMO Mode

While the open loop transmission mode is used when we pretend increase the data throughput of UEs in high mobility conditions, the closed loop mode is also a spatial multiplexing mode, but optimized to increase the data throughput for UEs in low mobility conditions, where the channel variation is slow and the tracking of those conditions is possible. Note that the tracking of channel conditions will delay the transmission, so if these delays were bigger than the coherence time of the channel, when the BS performs the transmission, the feedback signals will no longer represent the real channel conditions when the transmission starts to be done, therefore this transmission mode should be used in low mobility environments. The tracking of channel conditions is performed by the UE using reference signals sent by the BS in the downlink direction. Then, based on channel estimation performed with these reference signals, UE will compute a set of indexes (CQI, RI and PMI), which will be sent to the BS in order to advice for the best transmission adaptation. After the BS gets the feedback signals, it can decide if follow the UE recommendation or selects another matrix from the codebook, therefore BS must always inform the UE of that decision.

Note that in an FDD scheme, due the existence of separate frequency bands for the downlink and uplink, the only way for the BS track the channel conditions is receiving the information from the UE. In order not increase overhead in the uplink with the precise real channel coefficients, a set of 3 indexes is used jointly with a set of matrices organized in a codebook, which is known at both the UE and BS. The 3 indexes are: CQI, used to advice for the best modulation scheme (QPSK, 16-QAM, 64-QAM) and code rate for each transport block; the PMI index, which selects the best precoding matrix from the codebook set; and RI to adapts the number of layers for transmission (multiplexing gain), which is performed selecting a set of columns from the PMI selected matrix. While the PMI computation in the UE is done selecting the codebook matrix that minimizes the correlation level between the channels coefficients, the RI is selected computing the rank of the channel, which can be done performing the SVD channel decomposition, and with that, look the number of singular-values which are above a minimum limit. The number of singular values above that limit is selected as the value of the RI. See that in a ideal scenario, the BS would be able to acquire the precise channel coefficients, and with that, perform the optimal precoding, but due FDD constraints that is impossible,

therefore we can look to the selection of the precoding matrix within the codebook set as an approximation of the matrix that would be used in case of optimal precoding performed with real channel coefficients. We will present latter in more detail that the aim of precoding operation is decrease channel correlation, which is done performing a phase rotation on channel coefficients. Therefore we can reduce the inter-symbol interference and optimize the individual separation of each transmitted symbol at the receiver [2][8][20][26][27][30].

The LTE standard specifies the following codebook sets for 2 and 4 antennas transmission.

Codebook index	Number of layers υ	
	1	2
0	$\frac{1}{\sqrt{2}}\begin{bmatrix}1\\1\end{bmatrix}$	$\frac{1}{\sqrt{2}}\begin{bmatrix}1 & 0\\0 & 1\end{bmatrix}$
1	$\frac{1}{\sqrt{2}}\begin{bmatrix}1\\-1\end{bmatrix}$	$\frac{1}{2}\begin{bmatrix}1 & 1\\1 & -1\end{bmatrix}$
2	$\frac{1}{\sqrt{2}}\begin{bmatrix}1\\j\end{bmatrix}$	$\frac{1}{2}\begin{bmatrix}1 & 1\\j & -j\end{bmatrix}$
3	$\frac{1}{\sqrt{2}}\begin{bmatrix}1\\-j\end{bmatrix}$	-

Table 10 - Codebook for 2 antennas transmission [2]

Codebook index	u_n	Number of layers υ			
		1	2	3	4
0	$u_0 = [1 \quad -1 \quad -1 \quad -1]^T$	$W_0^{\{1\}}$	$W_0^{\{14\}}/\sqrt{2}$	$W_0^{\{124\}}/\sqrt{3}$	$W_0^{\{1234\}}/2$
1	$u_1 = [1 \quad -j \quad 1 \quad j]^T$	$W_1^{\{1\}}$	$W_1^{\{12\}}/\sqrt{2}$	$W_1^{\{123\}}/\sqrt{3}$	$W_1^{\{1234\}}/2$
2	$u_2 = [1 \quad 1 \quad -1 \quad 1]^T$	$W_2^{\{1\}}$	$W_2^{\{12\}}/\sqrt{2}$	$W_2^{\{123\}}/\sqrt{3}$	$W_2^{\{3214\}}/2$
3	$u_3 = [1 \quad j \quad 1 \quad -j]^T$	$W_3^{\{1\}}$	$W_3^{\{12\}}/\sqrt{2}$	$W_3^{\{123\}}/\sqrt{3}$	$W_3^{\{3214\}}/2$
4	$u_4 = [1 \quad (-1-j)/\sqrt{2} \quad -j \quad (1-j)/\sqrt{2}]^T$	$W_4^{\{1\}}$	$W_4^{\{14\}}/\sqrt{2}$	$W_4^{\{124\}}/\sqrt{3}$	$W_4^{\{1234\}}/2$
5	$u_5 = [1 \quad (1-j)/\sqrt{2} \quad j \quad (-1-j)/\sqrt{2}]^T$	$W_5^{\{1\}}$	$W_5^{\{14\}}/\sqrt{2}$	$W_5^{\{124\}}/\sqrt{3}$	$W_5^{\{1234\}}/2$
6	$u_6 = [1 \quad (1+j)/\sqrt{2} \quad -j \quad (-1+j)/\sqrt{2}]^T$	$W_6^{\{1\}}$	$W_6^{\{13\}}/\sqrt{2}$	$W_6^{\{134\}}/\sqrt{3}$	$W_6^{\{1324\}}/2$
7	$u_7 = [1 \quad (-1+j)/\sqrt{2} \quad j \quad (1+j)/\sqrt{2}]^T$	$W_7^{\{1\}}$	$W_7^{\{13\}}/\sqrt{2}$	$W_7^{\{134\}}/\sqrt{3}$	$W_7^{\{1324\}}/2$
8	$u_8 = [1 \quad -1 \quad 1 \quad 1]^T$	$W_8^{\{1\}}$	$W_8^{\{12\}}/\sqrt{2}$	$W_8^{\{124\}}/\sqrt{3}$	$W_8^{\{1234\}}/2$
9	$u_9 = [1 \quad -j \quad -1 \quad -j]^T$	$W_9^{\{1\}}$	$W_9^{\{14\}}/\sqrt{2}$	$W_9^{\{134\}}/\sqrt{3}$	$W_9^{\{1234\}}/2$
10	$u_{10} = [1 \quad 1 \quad 1 \quad -1]^T$	$W_{10}^{\{1\}}$	$W_{10}^{\{13\}}/\sqrt{2}$	$W_{10}^{\{123\}}/\sqrt{3}$	$W_{10}^{\{1324\}}/2$
11	$u_{11} = [1 \quad j \quad -1 \quad j]^T$	$W_{11}^{\{1\}}$	$W_{11}^{\{13\}}/\sqrt{2}$	$W_{11}^{\{134\}}/\sqrt{3}$	$W_{11}^{\{1324\}}/2$
12	$u_{12} = [1 \quad -1 \quad -1 \quad 1]^T$	$W_{12}^{\{1\}}$	$W_{12}^{\{12\}}/\sqrt{2}$	$W_{12}^{\{123\}}/\sqrt{3}$	$W_{12}^{\{1234\}}/2$
13	$u_{13} = [1 \quad -1 \quad 1 \quad -1]^T$	$W_{13}^{\{1\}}$	$W_{13}^{\{13\}}/\sqrt{2}$	$W_{13}^{\{123\}}/\sqrt{3}$	$W_{13}^{\{1324\}}/2$
14	$u_{14} = [1 \quad 1 \quad -1 \quad -1]^T$	$W_{14}^{\{1\}}$	$W_{14}^{\{13\}}/\sqrt{2}$	$W_{14}^{\{123\}}/\sqrt{3}$	$W_{14}^{\{3214\}}/2$
15	$u_{15} = [1 \quad 1 \quad 1 \quad 1]^T$	$W_{15}^{\{1\}}$	$W_{15}^{\{12\}}/\sqrt{2}$	$W_{15}^{\{123\}}/\sqrt{3}$	$W_{15}^{\{1234\}}/2$

Table 11 - Codebook for 4 antennas transmission [2]

The codebook used to perform precoding with 4 antennas is computed based on a Householder transformation using the below expression.

$$\mathbf{W_n} = \mathbf{I_{4\times 4}} - 2\mathbf{u_n}\mathbf{u_n^H}/\mathbf{u_n^H}\mathbf{u_n} \quad (5.\ 36)$$

Like it was explained in the open-loop mode, the 4x4 precoding matrix is selected based on a vector $\mathbf{u_n}$, which is used by the Householder expression to compute a 4x4 matrix. Then, based on rank computation applied over each channel matrix estimation, concatenation of rank columns of the Householder matrix is done.

In the next chapter we will present the implemented simulation platform of this transmission mode, therefore we will not detail the signal processing in here.

5.5. TM5 -MU-MIMO Mode

The Closed Loop and the Open Loop SU-MIMO modes seen before are used to perform a link communication between a BS and a single UE with multiple antennas, allowing the transmission of parallel data streams between both in the same RE. In the case of MU-MIMO, the spatial multiplexing is used to serve several UEs at the same RE. Comparing SU-MIMO with MU-MIMO, we can quickly figure out the following advantages of MU-MIMO systems: a SU-MIMO system needs complex multi-antenna UE to provide full multiplexing gain, while a MU-MIMO system only needs low cost single-antenna UEs to achieve full multiplexing gain; another advantage over the SU-MIMO is the distance between the UE, which makes channel decorrelation between UEs greater than in SU-MIMO case. As discussed before, using multiple antennas and doing a correct precoding transmission is possible to the UEs recover their data stream with low interference levels from the data streams transmitted to the other users. In real scenarios the number of UEs waiting to be served by the BS is greater than the number of users that a MU-MIMO system can attend simultaneously (4 antenna BS - 4 UE), thus a selection process must be performed by the BS.

Before we proceed, we should refer that LTE standard only specifies interoperability procedures between the BS and UE, therefore some algorithms used for instance to perform precoding matrix selection from the specified codebook set, doesn't make part of LTE technical specifications.

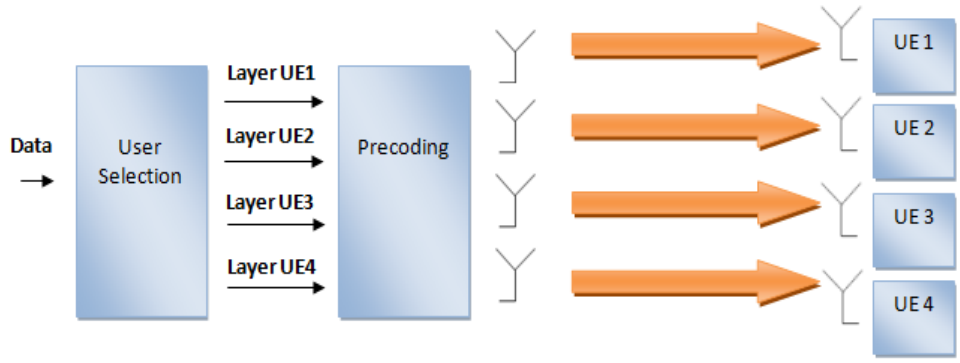

Figure 5. 7 - MU-MIMO system

In the remain part of this section, we present one possible algorithm [28] - which don't make part LTE specifications - that can be used to select the best UE set using the LTE codebook specified matrices. Using the referred algorithm, the precoding matrix can be selected based on the same feedback signals used in closed loop mode, but now each UE will feedback a PMI and RI values according the number of layers (1 in LTE) received from the BS. The selection of the UEs that will share the same RE, is based on the PMI index transmitted by each one of them, thus BS just selects the UEs which the feedback vectors form an orthogonal set. Then, is selected a precoding matrix closest the matrix formed by the concatenation of those orthogonal vectors. Note that the selection of the correct UEs is crucial to reduce the interference between them, therefore complex and efficient algorithms must be used in this stage [2][21][25][27][28]. In order to detail the algorithm pointed above, as well to show how the correct UEs selection is crucial to reduce interference between UEs, consider the scenario presented on Figure 5.8, where a 2x2 MU-MIMO system is used to serve two UEs in the same subcarrier i.

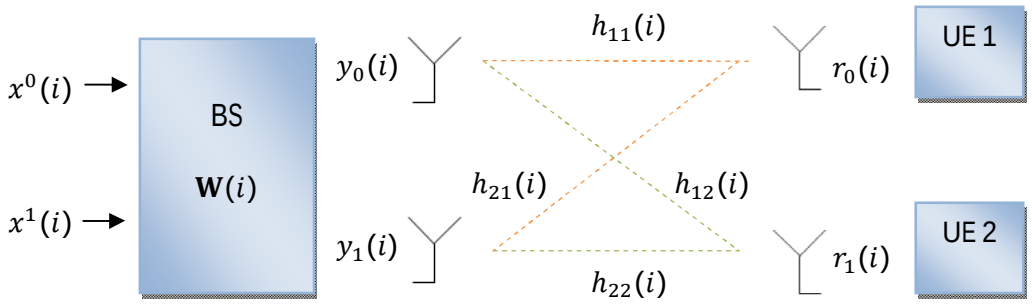

Figure 5. 8 - MU-MIMO 2x2 system

Let's start to define the following rank 2 precoding matrix (i omitted in the following calculus),

$$\mathbf{W} = \begin{bmatrix} w_{11} & w_{12} \\ w_{21} & w_{22} \end{bmatrix} \qquad \begin{aligned} \mathbf{w_1} &= [w_{11} w_{21}]^T \\ \mathbf{w_2} &= [w_{12} w_{22}]^T \end{aligned} \tag{5. 37}$$

The channels seen by UE1 and UE2 are $\mathbf{h_1}$ and $\mathbf{h_2}$ respectively,

$$\mathbf{H} = \begin{bmatrix} h_{11} & h_{21} \\ h_{12} & h_{22} \end{bmatrix} \qquad \begin{aligned} \mathbf{h_1} &= [h_{11} h_{21}] \\ \mathbf{h_2} &= [h_{12} h_{22}] \end{aligned} \tag{5. 38}$$

The precoded transmitted signals at each antenna are,

$$\begin{bmatrix} y_0 \\ y_1 \end{bmatrix} = \mathbf{W} \begin{bmatrix} x^0 \\ x^1 \end{bmatrix} \tag{5. 39}$$

$$y_0 = [w_{11} w_{12}] \begin{bmatrix} x^0 \\ x^1 \end{bmatrix} = w_{11} x^0 + w_{12} x^1$$

$$y_1 = [w_{21} w_{22}] \begin{bmatrix} x^0 \\ x^1 \end{bmatrix} = w_{21} x^0 + w_{22} x^1$$

The received signals at each UE are the following,

$$\begin{bmatrix} r_0 \\ r_1 \end{bmatrix} = \mathbf{H} \begin{bmatrix} y_0 \\ y_1 \end{bmatrix} + \begin{bmatrix} n_0 \\ n_1 \end{bmatrix} \tag{5. 40}$$

$$r_0 = \mathbf{h_1} \begin{bmatrix} y_0 \\ y_1 \end{bmatrix} + n_0 = h_{11} y_0 + h_{21} y_1 + n_0$$

$$r_1 = \mathbf{h_2} \begin{bmatrix} y_0 \\ y_1 \end{bmatrix} + n_1 = h_{12} y_0 + h_{22} y_1 + n_1$$

To see how the selected precoding matrix reduces the interference and increase the received power, let's treat the received signals in the following way,

$$r_0 = h_{11}(w_{11} x^0 + w_{12} x^1) + h_{21}(w_{21} x^0 + w_{22} x^1) + n_0 \tag{5. 41}$$

$$r_0 = (h_{11} w_{11} + h_{21} w_{21}) x^0 + (h_{11} w_{12} + h_{21} w_{22}) x^1 + n_0$$

$$r_1 = h_{12}(w_{11} x^0 + w_{12} x^1) + h_{22}(w_{21} x^0 + w_{22} x^1) + n_1 \tag{5. 42}$$

$$r_1 = (h_{12} w_{11} + h_{22} w_{21}) x^0 + (h_{12} w_{12} + h_{22} w_{22}) x^1 + n_1$$

Looking to the above expressions we should figure out that UE1 selects a precoding vector $\mathbf{w_1}$ that maximizes the signal strength $|h_{11} w_{11} + h_{21} w_{21}|^2$of x_0, while UE2 selects the precoding vector $\mathbf{w_2}$ that maximizes the signal strength $|h_{12} w_{12} + h_{22} w_{22}|^2$ of x_1. The precoding matrices used, only perform phase rotations of 0°, +90°, -90° or 180°, thus $\mathbf{w_1}$has the aim of try to align h_{11} withh_{21}, while $\mathbf{w_2}$ aligns h_{12} with h_{22}. Note that each UE only have the knowledge of their respective channels $\mathbf{h_1}$ (UE1) and $\mathbf{h_2}$ (UE2).

The vector selected by each UE can be the quantification of the matched filter version (MRC) of their respective channels $\mathbf{h_1}$and $\mathbf{h_2}$. In the case of UE1, the selected precoder will be the one closest the following channel vector $\mathbf{w_{1M}}$, and in UE2 is selected the vector closest $\mathbf{w_{2M}}$.

$$\mathbf{w_{1M}} = \mathbf{h_1^H} = \begin{bmatrix} h_{11}^* \\ h_{21}^* \end{bmatrix} \qquad \mathbf{w_{2M}} = \mathbf{h_2^H} = \begin{bmatrix} h_{12}^* \\ h_{22}^* \end{bmatrix} \tag{5. 43}$$

Note that replacing $\mathbf{w_{1M}}$ and $\mathbf{w_{2M}}$ in r_0 and r_1, we maximize the signal strength for x^0 in UE1, and x^1 in UE2.

$$r_0 = (|h_{11}|^2 + |h_{21}|^2)x^0 + (h_{11}h_{12}^* + h_{21}h_{22}^*)x^1 + n_0 \tag{5. 44}$$

$$r_1 = (h_{12}h_{11}^* + h_{22}h_{21}^*)x^0 + (|h_{12}|^2 + |h_{22}|^2)x^1 + n_1 \tag{5. 45}$$

Due the first element of the 2 antennas codebook precoder matrices being 1, UEs will normalize the first element of $\mathbf{w_{1M}}$ and $\mathbf{w_{2M}}$.

$$\mathbf{w_{1M}} = \frac{h_{11}}{|h_{11}|^2}\begin{bmatrix} h_{11}^* \\ h_{21}^* \end{bmatrix} = \begin{bmatrix} 1 \\ \frac{h_{21}^* h_{11}}{|h_{11}|^2} \end{bmatrix} \qquad \mathbf{w_{2M}} = \frac{h_{12}}{|h_{12}|^2}\begin{bmatrix} h_{12}^* \\ h_{22}^* \end{bmatrix} = \begin{bmatrix} 1 \\ \frac{h_{22}^* h_{12}}{|h_{12}|^2} \end{bmatrix} \tag{5. 46}$$

Let's assume that in the codebook set for 2 antennas transmission, the closest vector of $\mathbf{w_{1M}}$ is $[1\ j]^T$ and the closest of $\mathbf{w_{2M}}$ is $[1\ -j]^T$, therefore UE1 and UE2 will feedback respectively the following $\mathbf{w_1}$and $\mathbf{w_2}$ vectors,

$$\mathbf{w_1} = \frac{1}{\sqrt{2}}\begin{bmatrix} 1 \\ j \end{bmatrix} \qquad \mathbf{w_2} = \frac{1}{\sqrt{2}}\begin{bmatrix} 1 \\ -j \end{bmatrix} \tag{5. 47}$$

Then, BS looks to the PMI reported by each UE, and sees that the precoding vectors form an orthogonal set. Therefore, UE1 and UE2 are selected by BS to receive in the same time-frequencies resources. The precoding matrix $\mathbf{W}$ used by BS will be the concatenation of $\mathbf{w_1}$ and $\mathbf{w_2}$ vectors.

$$\mathbf{W} = \frac{1}{2}\begin{bmatrix} 1 & 1 \\ j & -j \end{bmatrix} \tag{5. 48}$$

Doing the precoding operation, the received signals will be the following,

$$r_0 = \mathbf{h_1 w_1} x^0 + \mathbf{h_1 w_2} x^1 + n_0 \quad (5.49)$$

$$r_0 = \frac{1}{2}(h_{11} + jh_{21})x^0 + \frac{1}{2}(h_{11} - jh_{21})x^1 + n_0$$

$$r_1 = \mathbf{h_2 w_1} x^0 + \mathbf{h_2 w_2} x^1 + n_1 \quad (5.50)$$

$$r_1 = \frac{1}{2}(h_{12} + jh_{22})x^0 + \frac{1}{2}(h_{12} - jh_{22})x^1 + n_1$$

Note that in r_0, the precoding vector $\mathbf{w_1}$ try to put in the same quadrant the channel complex values h_{11} and h_{21}, while $\mathbf{w_2}$ should reduce x^1 interference putting out of phase h_{11} with h_{21}. In r_1 expression, $\mathbf{w_2}$ put in the same quadrant h_{12} and h_{22}, while $\mathbf{w_1}$ reduce the interference of x^0 in x^1, putting h_{12} out of phase with h_{22}.

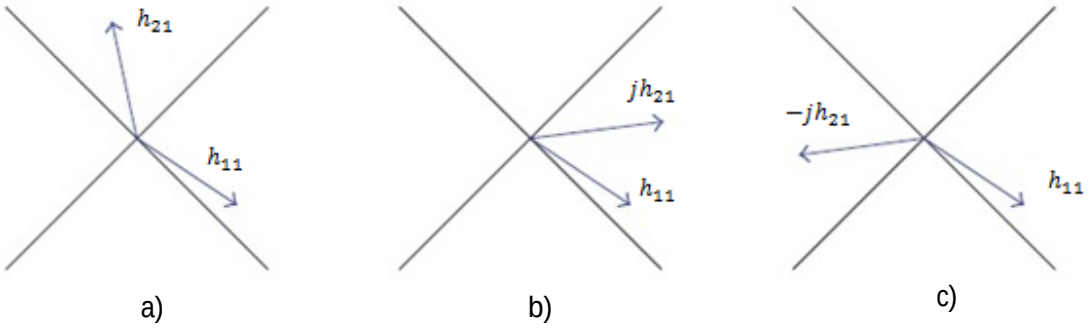

Figure 5. 9 - Phase rotation of channel response performed by precoding operation in UE1 [28]

In the above figure is illustrated the phase rotation performed by the precoding operation over the channel seen by UE1. In image a) the original channel response is presented, while in images b) and c) we can see the phase rotation performed by $\mathbf{w_1}$ and $\mathbf{w_2}$ respectively.

5.6. TM6 -Closed Loop rank 1 precoding

The following TM is a particular case of TM4 Closed Loop mode. The TM6 uses the same feedback signals and codebook set of TM4, but now only rank 1 matrices can be selected by the BS for precoding, therefore only 4 precoding matrices are available for 2 antennas transmission, and 16 matrices to 4 antennas case. Note that this TM is a kind of beamforming mode performed by a codebook set of matrices which are used for precoding; therefore we can see this TM as a beamforming mode adapted to be used in LTE-FDD system.

Codebook index	0	1	2	3
Matrix	$\frac{1}{\sqrt{2}}\begin{bmatrix}1\\1\end{bmatrix}$	$\frac{1}{\sqrt{2}}\begin{bmatrix}1\\-1\end{bmatrix}$	$\frac{1}{\sqrt{2}}\begin{bmatrix}1\\j\end{bmatrix}$	$\frac{1}{\sqrt{2}}\begin{bmatrix}1\\-j\end{bmatrix}$

Table 12 - 2 antennas codebook rank 1 matrices [27]

In figure 5.10 is presented the beam directions performed by each one of the precoding matrices (table 12) used for 2 antennas transmission [20][21][25][27].

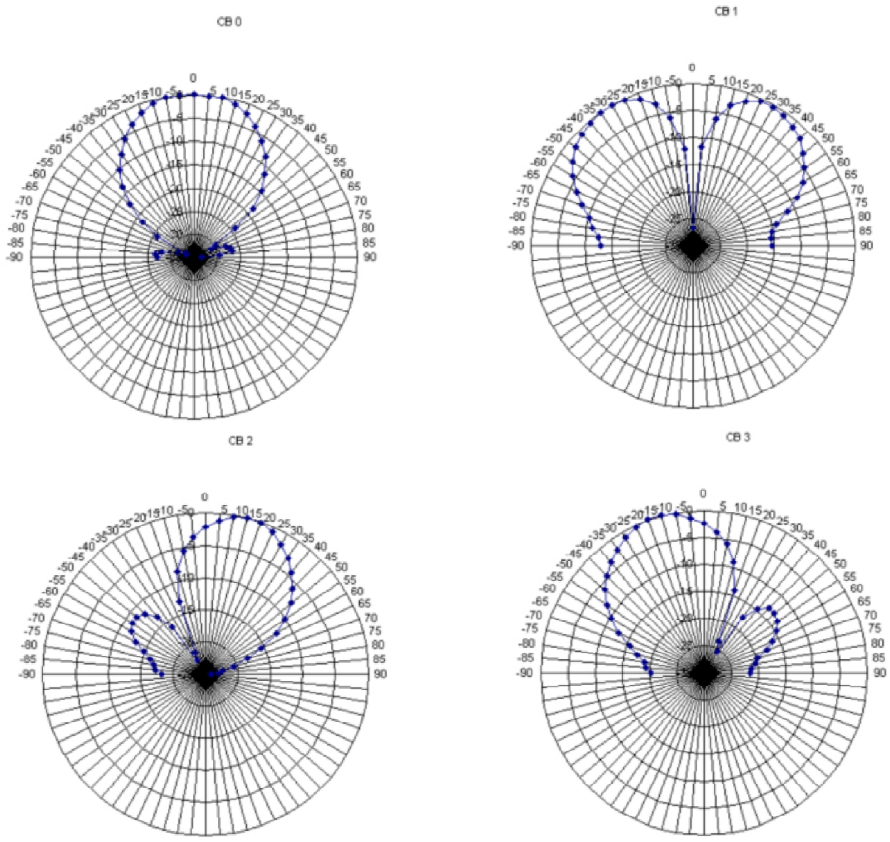

Figure 5. 10 - Horizontal beam diagrams performed by rank 1 codebook index 0, 1, 2, 3 matrices selected from 2 antennas book set [27]

5.7. TM7 - Single Layer MIMO Beamforming on Port 5

The LTE TM7 is a single layer beamforming mode suited to perform beam transmissions in the TDD variant of LTE system. As we said before, a beamforming transmission is used to increase coverage in order to reach UEs located at the cell edge, so in this case a beam pattern of a single layer is computed in order to direct the main lobe (constructive interference) in the direction of

the target UE. Contrarily at what happens in TM6, in this case the used precoding vector is not selected from the codebook set, instead BS directly perform channel estimation using reference signals received from the UE in the uplink (channel reciprocity in TDD). Then, using channel estimation, the BS can perform the desired precoding. After the precoding vector is computed, a UE specific reference signal (port 5) is coded and transmitted with the same weights used for data precoding (PDSCH). With the received UE-RS, the UE now has the information that needs to correctly demodulate the data transmitted in PDSCH.

Note that perform channel estimation at the BS using uplink reference signals is not achievable on FDD-LTE system, therefore one possible solution of use TM7 on FDD, is computing Angle of Arrive (AoA) and Direction of Arrive (DoA) at uplink. Using AoA and DoA is possible to get some information related with UE direction, and with that compute the beamforming weights.

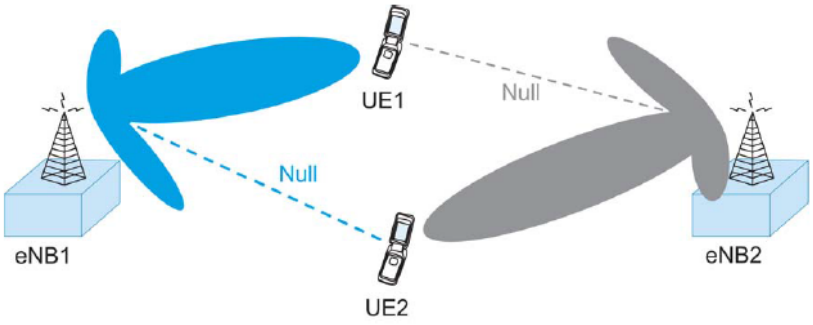

Figure 5. 11 - Single Layer Beamforming [13]

The precoding operation in a single layer MIMO beamforming mode in subcarrier i is the following,

$$\begin{bmatrix} y_0(i) \\ \cdot \\ \cdot \\ y_{N_T}(i) \end{bmatrix} = \begin{bmatrix} w^0(i) \\ \cdot \\ \cdot \\ w^{N_T}(i) \end{bmatrix} x^0(i) \qquad (5.\ 51)$$

Where $N_T$is the number of transmit antennas and i the subcarrier index.

Like it was said before, beamforming is done through repeating the same symbol with a phase shift difference across the transmit antennas. Looking above, we can see that in each antenna a phase shifted version of x^0 is applied, so the beam direction control is adapted changing the precoding weights in each antenna.

Comparing TM6 with TM7, we can see that more accurate UE tracking is achieved with TM7 for TDD mode. The reasons for this are explained by the feedback delays present in TM6, and also the use of more accurate channel coefficients in TM7 for precoding. See that BS in TM6 to acquire CSI needs to send the DW reference signals and wait that UE perform the necessary

computations to select and feedback the precoding matrix index, while in TM7 the BS just needs to receive the uplink reference signal to obtain the precise channel response. Note that the matrix selected from the codebook set is an approximation of the optimal precoding solution [20][21][25][27].

6. LTE MIMO Chain Implementation

6.1. Introduction

In this Chapter a simulation chain based on LTE MIMO transmission modes is implemented. Since it would not be realistic implement all the modes during this thesis work, we selected the mode 4 (TM4) discussed in the previous Chapter. This chain allows the simulation of several rank transmission modes using different LTE codebook indexes specified for 2 and 4 antennas. At the receiver side the data symbols are separated using defined multi-symbol equalizations such as, conventional ZF and MMSE, and the developed SIC-ZF and SIC MMSE equalizers.

As seen before, TM4 can be used with 2 or 4 transmit antennas, therefore a 2x2 and a 4x4 MIMO systems were developed in order to implement these 2 cases. In the 2x2 MIMO configuration, channel coding is not applied and the transmission is done using uncorrelated channels. For the case of 4x4 MIMO, 3 different simulation platforms were developed in order to evaluate system performance according channel correlation conditions. Therefore, the first and the second 4x4 MIMO platforms are implemented using uncorrelated and correlated channels respectively, and no channel coding is used for both; the third platform uses uncorrelated channels but now channel coding is applied.

In our chain we apply the same codebook index for the entire OFDM symbol, thus contrarily at what is done in LTE, we didn't use any SNR or correlation criterion to select the best precoding matrix per resource block.

6.2. LTE Implemented MIMO Mode Configurations

The chain used to simulate LTE TM4 is divided in 3 main parts, which are: transmission precoding, channel effect modeling, and receiver equalization. In the next section we present the overall modeling structure for both 2x2 MIMO and 4x4 MIMO configurations used in the development of LTE TM4 simulation model.

6.2.1. Closed Loop MIMO 2x2

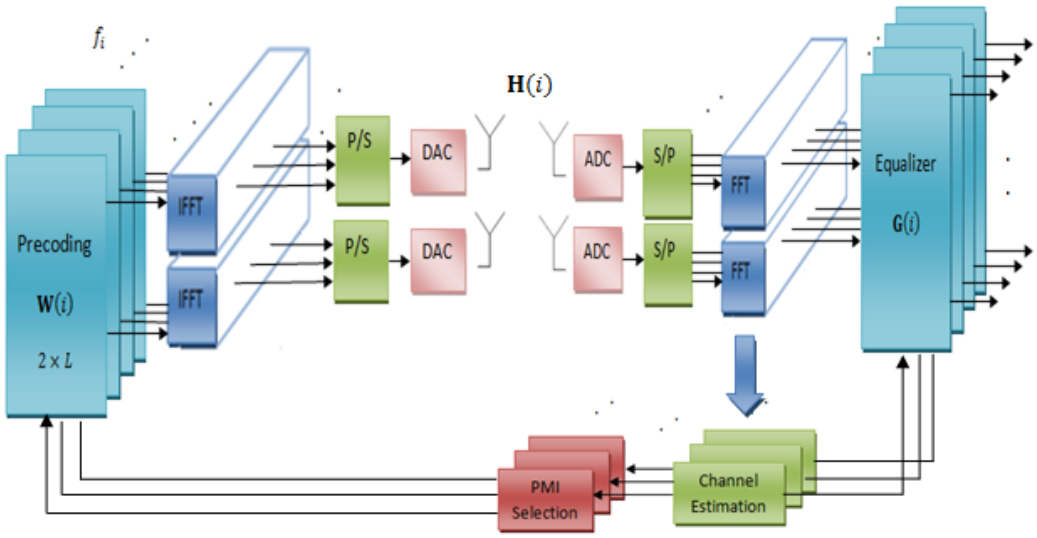

Figure 6. 1 - MIMO 2x2 configuration for LTE TM4

Let's use as reference Figure 6.1 where is presented the model of MIMO 2x2 simulation system for a rank L transmission.

In this simulation model a set of $L = 1, 2$ symbols are precoded in the frequency domain on each i subcarrier. After that, an IFFT operation is performed and a cyclic prefix is inserted to avoid ISI. At the receiver side, first the CP is removed and then a FFT operation is done, an estimate of the transited signal in frequency domain is obtained. Then, frequency domain equalization is performed in order to obtain an estimate of the L data symbols transmitted in each subcarrier.

In the implemented chain we assume perfect channels estimation, i.e., the channels estimation block of Figure 6.1 is not implemented, and the PMI selection is also not considered. We use the same precoding matrix for the entire OFDM signal, although in the LTE standard the precoding matrix selection should be done for some RE.

In Table 10 of Chapter 5.4 is presented the codebook used for 2 antennas at the transmitter. We can use the matrices in this codebook to adapt the transmission rank for 1 or 2 layers.

If we select codebook index 2 with 2 layers (rank 2), the transmitted signal is

$$\begin{bmatrix} y_0(i) \\ y_1(i) \end{bmatrix} = \frac{1}{2}\begin{bmatrix} 1 & 1 \\ j & -j \end{bmatrix}\begin{bmatrix} x^0(i) \\ x^1(i) \end{bmatrix} \quad (6.1)$$

Where $\mathbf{W} = \frac{1}{2}\begin{bmatrix} 1 & 1 \\ j & -j \end{bmatrix}$ is the precoder matrix and $x^0(i)$,$x^1(i)$ are the data symbols transmitted in parallel over subcarrier i.

The signals transmitted from antenna 1 and 2 are respectively,

$$y_0(i) = \frac{1}{2}(x^0(i) + x^1(i))$$
$$y_1(i) = \frac{1}{2}(jx^0(i) - jx^1(i))$$

If BS decides adapt to a rank 1 transmission, selecting codebook index 2 for 1 layer, the precoding operation is performed in the following form,

$$\begin{bmatrix} y_0(i) \\ y_1(i) \end{bmatrix} = \frac{1}{\sqrt{2}}\begin{bmatrix} 1 \\ j \end{bmatrix} x^0(i) \quad (6.2)$$

Where now $\mathbf{W} = \frac{1}{\sqrt{2}}\begin{bmatrix} 1 \\ j \end{bmatrix}$ and just $x^0(i)$ symbol is transmitted in subcarrier$i$.

The signals transmitted from antenna 1 and 2 are respectively,

$$y_0(i) = \frac{1}{\sqrt{2}}x^0(i)$$
$$y_1(i) = \frac{1}{\sqrt{2}}jx^0(i)$$

Note that while rank 1 just transmits 1 symbol in one OFDM subcarrier, in rank 2 case, 2 different symbols are transmitted in the same subcarrier of 2 parallel OFDM signals.
Considering the following MIMO 2x2 channel response $\mathbf{H}(i)$, the received signal $\mathbf{r}(i)$ will be the following,

$$\mathbf{r}(i) = \mathbf{H}(i)\mathbf{W}(i)\mathbf{x}(i) + \mathbf{n}(i) \quad (6.3)$$

With $\mathbf{H}(i)$ defined as,

$$\mathbf{H}(i) = \begin{bmatrix} h_{11}(i) & h_{21}(i) \\ h_{12}(i) & h_{22}(i) \end{bmatrix} \quad (6.4)$$

In order to simplify we will omit the subcarrier index i in the next expressions. The above equation can be expanded as,

$$r_0 = [h_{11} \quad h_{21}] \begin{bmatrix} y_0 \\ y_1 \end{bmatrix} + n_0 = h_{11}y_0 + h_{21}y_1 + n_0 \quad (6.5)$$

$$r_1 = [h_{12} \quad h_{22}] \begin{bmatrix} y_0 \\ y_1 \end{bmatrix} + n_1 = h_{12}y_0 + h_{22}y_1 + n_1$$

At the receiver, with channel knowledge available and knowing the precoding matrix index used, we will use 4 different types of equalizers to recover the symbols, which are: ZF, MMSE, SIC-ZF and SIC-MMSE. We will see in detail these equalizers in chapter 6.3 [2][8][20].

6.2.2. Closed Loop MIMO 4x4

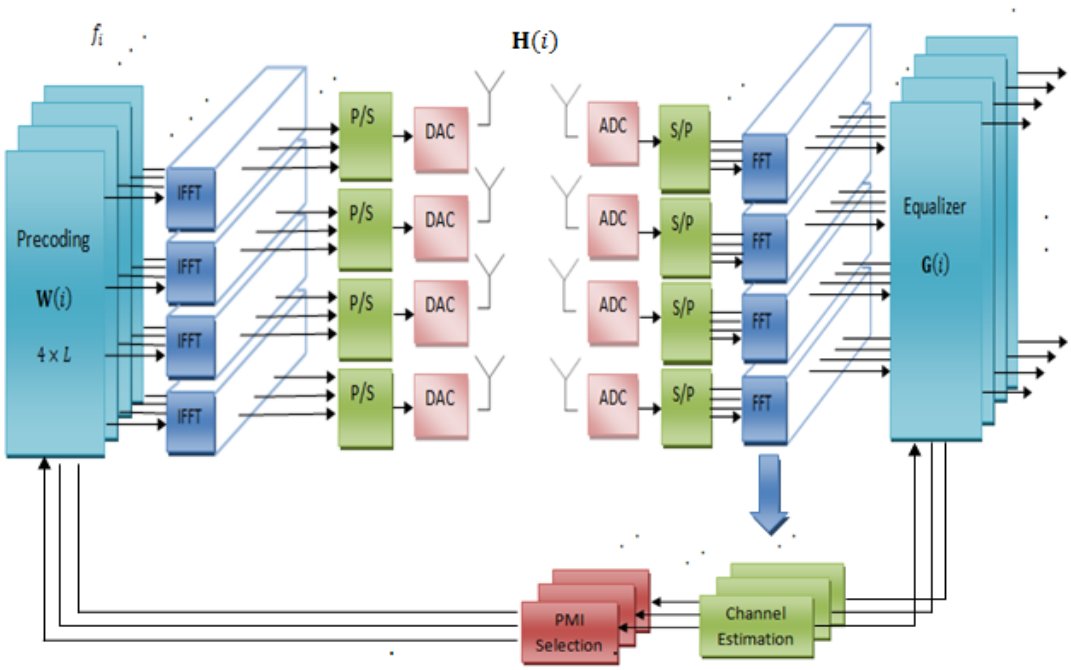

Figure 6. 2 - MIMO 4x4 configuration for LTE TM4

In 4x4 MIMO configuration the same principles discussed above are applied in here, the difference now is the possibility to transmit until 4 data symbols on each subcarrier. Looking to Figure 6.2 and considering the transmission of L data symbols on subcarrier i, we can see that now 4 OFDM signals are generated and transmitted in parallel.

In the Table 11 of Chapter 5 is presented the LTE codebook used to perform precoding with 4 transmit antennas. Like we refer before, each matrix presented in the codebook is computed based on a Householder transformation using the below expression [2][8][20].

$$\mathbf{W}_n = \mathbf{I} - 2\mathbf{u}_n\mathbf{u}_n^H / \mathbf{u}_n^H\mathbf{u}_n \tag{6. 6}$$

$$\mathbf{I} \rightarrow \text{4x4 Identity matrix}$$

The 4x4 precoding matrix is selected based on a vector $\mathbf{u}_n$, which is used by the Householder transformation to compute a 4x4 matrix. The rank adaptation is done making the concatenation of rank columns of the 4x4 matrix computed by the Householder transformation.

In order to understand the concatenation process, lets select for instance the codebook index 0.

$$\mathbf{u}_0 = [1 \ -1 \ -1 \ -1]^T \tag{6. 7}$$

Applying the Householder transformation in $\mathbf{u}_0$ we get the follow 4x4 matrix,

$$\mathbf{W_0} = \mathbf{I} - 2\mathbf{u}_0\mathbf{u}_0^H / \mathbf{u}_0^H\mathbf{u}_0 \tag{6. 8}$$

$$\mathbf{W}_0 = \frac{1}{2}\begin{bmatrix} 1 & 1 & 1 & 1 \\ 1 & 1 & -1 & -1 \\ 1 & -1 & 1 & -1 \\ 1 & -1 & -1 & 1 \end{bmatrix} \tag{6. 9}$$

Looking to the codebook table, the precoding matrix for codebook index 0 in rank 1 mode is the first column of $\mathbf{W}_0$.

$$\mathbf{W}_0^{\{1\}} = \frac{1}{2}\begin{bmatrix} 1 \\ 1 \\ 1 \\ 1 \end{bmatrix} \tag{6. 10}$$

In case of rank 2 transmission, columns 1 and 4 of $\mathbf{W}_0$ are concatenated.

$$\mathbf{W}_0^{\{1,4\}} = \frac{1}{2}\begin{bmatrix} 1 & 1 \\ 1 & -1 \\ 1 & -1 \\ 1 & 1 \end{bmatrix} \tag{6. 11}$$

For rank 3 transmission the process is the same

$$\mathbf{W}_0^{\{1,2,4\}} = \frac{1}{2}\begin{bmatrix} 1 & 1 & 1 \\ 1 & 1 & -1 \\ 1 & -1 & -1 \\ 1 & -1 & 1 \end{bmatrix} \quad (6.\ 12)$$

In the rank 4, $\mathbf{W}_0^{\{1,2,3,4\}} = \mathbf{W}_0$.

In order to present the precoding operation, let's assume that code index 0 in rank 3 mode is selected for transmission. The precoded transmitted signal **y** for each subcarrier is the following,

$$\begin{bmatrix} y_0(i) \\ y_1(i) \\ y_2(i) \\ y_3(i) \end{bmatrix} = \frac{1}{2\sqrt{3}}\begin{bmatrix} 1 & 1 & 1 \\ 1 & 1 & -1 \\ 1 & -1 & -1 \\ 1 & -1 & 1 \end{bmatrix}\begin{bmatrix} x^0(i) \\ x^1(i) \\ x^2(i) \end{bmatrix} \quad (6.\ 13)$$

$$y_0(i) = \frac{1}{2\sqrt{3}}(x^0(i) + x^1(i) + x^2(i))$$
$$y_1(i) = \frac{1}{2\sqrt{3}}(x^0(i) + x^1(i) - x^2(i))$$
$$y_2(i) = \frac{1}{2\sqrt{3}}(x^0(i) - x^1(i) - x^2(i))$$
$$y_3(i) = \frac{1}{2\sqrt{3}}(x^0(i) - x^1(i) + x^2(i))$$

Then, the following channel effect model is considered,

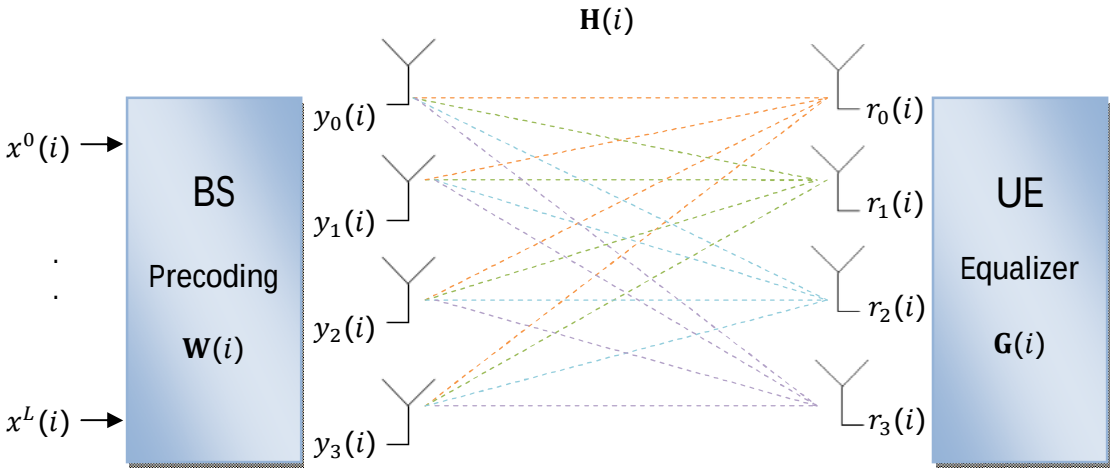

Figure 6. 3 - MIMO 4x4 signal model for a rank L transmission

Assume the following channel response in subcarrier i,

$$\mathbf{H}(i) = \begin{bmatrix} h_{11}(i) & h_{21}(i) & h_{31}(i) & h_{41}(i) \\ h_{12}(i) & h_{22}(i) & h_{32}(i) & h_{42}(i) \\ h_{13}(i) & h_{23}(i) & h_{33}(i) & h_{43}(i) \\ h_{14}(i) & h_{24}(i) & h_{34}(i) & h_{44}(i) \end{bmatrix} \quad (6.\ 14)$$

Hereinafter, we omit subcarrier index i. Considering a rank 3 transmission ($L = 3$), the received signal $\mathbf{r}$ for each subcarrier is modeled in the following way,

$$\begin{bmatrix} r_0 \\ r_1 \\ r_2 \\ r_3 \end{bmatrix} = \begin{bmatrix} h_{11} & h_{21} & h_{31} & h_{41} \\ h_{12} & h_{22} & h_{32} & h_{42} \\ h_{13} & h_{23} & h_{33} & h_{43} \\ h_{14} & h_{24} & h_{34} & h_{44} \end{bmatrix} \begin{bmatrix} y_0 \\ y_1 \\ y_2 \\ y_3 \end{bmatrix} + \begin{bmatrix} n_0 \\ n_1 \\ n_2 \\ n_3 \end{bmatrix} \quad (6.\ 15)$$

Finally at the receiver, like in MIMO 2x2 configuration, the ZF, MMSE, SIC-ZF and SIC-MMSE equalizers were used to recover the L symbols transmitted in each subcarrier.

6.3. Equalization Strategies

The aim of precoding operation in a SM MIMO system is reduce the correlation between the channels and thus allows designing more efficient equalizer in order to reduce the interference between the symbols, and also increase the signal strength at the receiver. For the case of single rank the diversity order can be increased. Note that to perform optimal precoding would be necessary at the BS full knowledge of the channel coefficients in order to anticipate the channel effect and thus adapt the signal. However, even optimal precoding may not be enough to ensure free inter- data symbol interference and good signal strength, is also necessary verify full decorrelation between the channel coefficient. For the case of full uncorrelated antenna channels the fixed LTE precoder matrices are useless.

In FDD mode, only the UE is able to perform DW channel estimation, thus the only way of BS acquire the channel is receiving the feedback from the UE. See that if UE, feedback individually each channel coefficient, the uplink overhead due feedback would be too high, so this is one of the reasons why LTE uses a codebook set (fixed orthogonal precoders) and feedback PMI indexes for precoding selection.

The received signal, after FFT operation and CP removal, is given by

$$\mathbf{r = HWx + n = Ax + n} \quad (6.\ 16)$$

Where $\mathbf{A} = \mathbf{HW}$ represents the equivalent channel. Considering a 4x4 MIMO system with rank 4, the equivalent channel is

$$\mathbf{A} = \begin{bmatrix} h_{11} & h_{21} & h_{31} & h_{41} \\ h_{12} & h_{22} & h_{32} & h_{42} \\ h_{13} & h_{23} & h_{33} & h_{43} \\ h_{14} & h_{24} & h_{34} & h_{44} \end{bmatrix} \begin{bmatrix} w_{11} & w_{21} & w_{31} & w_{41} \\ w_{12} & w_{22} & w_{32} & w_{42} \\ w_{13} & w_{23} & w_{33} & w_{43} \\ w_{14} & w_{24} & w_{34} & w_{44} \end{bmatrix} \quad \textbf{(6. 17)}$$

At the receiver (UE), and after the estimation of the matrix **H,** is performed a correlation between the estimated channel matrix and all precoding matrices **W**. The precoding matrix **W** reported to the BS via PMI feedback is the one that ensure less correlation between the coefficients of matrix **A**. As discussed this selection process was not implemented in the chain.
To separate the spatial data streams we implemented different multi-symbol equalizers. The aim of equalization is to eliminate the channel effect in the received signal, therefore with equalization we pretend separate the set of *L* symbols transmitted in the same subcarrier, and also maximize the strength in each symbol. The estimated symbols after equalization are given by

$$\hat{\mathbf{x}} = \mathbf{GAx} + \mathbf{Gn} \quad \textbf{(6. 18)}$$

Where **G** represents the equalization matrix. In this work we considered 4 different equalizers: the 2 conventional ones ZF and MMSE, and 2 interference cancelation based SIC-ZF and SIC-MMSE.

- **Multi-symbol Zero Forcing**

From equation (6.16) we can see that to the data streams the matrix **G** can be set as,

$$\mathbf{G}_{\mathrm{ZF}} = \left(\mathbf{A}^{\mathrm{H}}\mathbf{A}\right)^{-1}\mathbf{A}^{\mathrm{H}} \quad \textbf{(6. 19)}$$

Replacing this matrix in equation (6.18) we get

$$\hat{\mathbf{x}} = \mathbf{Ix} + \mathbf{G}_{\mathrm{ZF}}\mathbf{n} \quad \textbf{(6. 20)}$$

As can be seen the data stream can be separated. Note that if matrix **A** is full correlated, the inverse cannot exist and the data symbols cannot be separate, or even existing the matrix **A** can be close to singular and as consequence the noise is strongly enhanced. This is one the reasons to use the precoder **W** prior to transmission. May happened in some scenario that the elements of **H** are strongly correlated [2][8].

- **Multi-symbol MMSE**

The other conventional equalizer is MMSE, which basically does a trade-off between the noise enhancement and interference mitigation. It allows some level of interference between data symbols but the noise is not enhanced as in the ZF. The equalizer matrix is given by

$$\mathbf{G}_{\mathrm{MMSE}} = \left(\mathbf{A}^{\mathrm{H}}\mathbf{A} + \sigma^2\mathbf{I}_{rank}\right)^{-1}\mathbf{A}^{\mathrm{H}} \quad (6.\ 21)$$

When the noise tends to zero the performance of this equalizer tends to the one obtained with ZF. Thus, is expected that the MMSE achieves better performance in low and medium SNR regimes [2][8].

- **Interference Cancelation schemes**

In Successive Interference Cancelation (SIC) technique, after recover a data layer/codeword using ZF or MMSE equalization, we will use the recovered layer to cancel that layer from the overall received signal, so in the next iteration to recover a different layer, the equalizer doesn't need to deal with the interference of the first layer in the received signal, making easier the symbol separation.

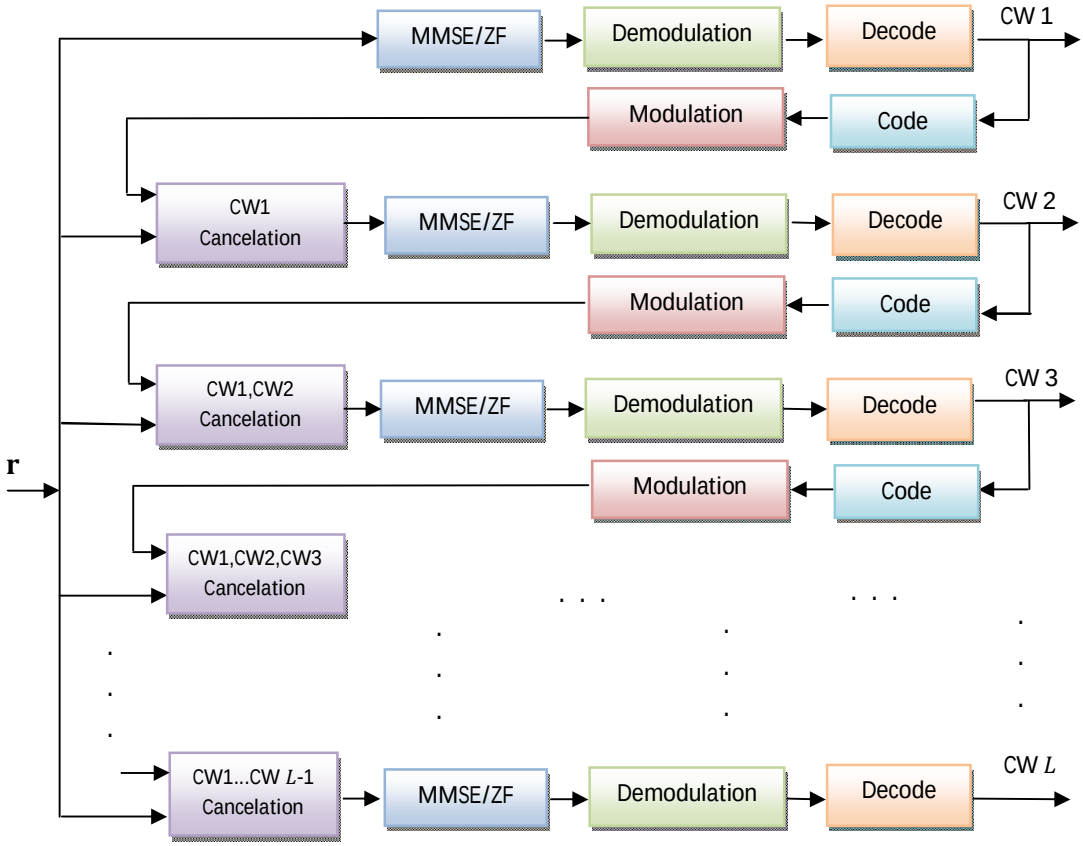

Figure 6. 4 - SIC equalizer

In Figure 6.4 is presented the working diagram structure of SIC equalization. We can see that a rank L transmission is received, so the SIC receiver will recover L layers or codeword's (assume that each CW is mapped in one layer) from the received signal.
In the first iteration to recover layer 1, the received signal is fully equalized, resulting in the achievement of all the layers. Then, we demodulate and decode only layer 1, and we code and modulate layer 1 again in order to correct some errors using FEC codes. After error correcting with FEC, we subtract layer 1 in the received signal, resulting in interference elimination of layer 1 in the overall signal, therefore in the next iteration the ZF/MMSE equalizer just need do separate $L - \mathbf{1}$ layers. We should refer that in Figure 6.4 is not present a precoding block after the modulation block; this precoding block put the layer symbols in the same form of how they were received, in order to perform subtraction. The subtract process referred above is repeated until the received signal just remains with 1 layer [2][8][9].

In order to present the mathematical treatment of SIC equalization, let's suppose a rank 3 transmission where $x^0(i), x^1(i)$ and $x^2(i)$ are the set of symbols sent in parallel on subcarrier$i$. Also assume that each one of the 3 parallel layers is composed by M_{Layer} complex symbols, therefore M_{Layer} subcarriers will be considered in OFDM modulation.

Also consider the following for the rank 3 transmission,

$$\mathbf{A}(i) = \mathbf{H}(i)\mathbf{W}(i) \tag{6. 22}$$

Note that in rank 3 transmission applied on a 4x4 MIMO system, the precoding matrix $\mathbf{W}$ has 4x3 size, like it was seen before. Therefore assume the following,

$$\mathbf{A}(i) = \begin{bmatrix} h_{11}(i) & h_{21}(i) & h_{31}(i) & h_{41}(i) \\ h_{12}(i) & h_{22}(i) & h_{32}(i) & h_{42}(i) \\ h_{13}(i) & h_{23}(i) & h_{33}(i) & h_{43}(i) \\ h_{14}(i) & h_{24}(i) & h_{34}(i) & h_{44}(i) \end{bmatrix} \begin{bmatrix} w_{11}(i) & w_{21}(i) & w_{31}(i) \\ w_{12}(i) & w_{22}(i) & w_{32}(i) \\ w_{13}(i) & w_{23}(i) & w_{33}(i) \\ w_{14}(i) & w_{24}(i) & w_{34}(i) \end{bmatrix} \tag{6. 23}$$

$$\mathbf{A}(i) = \begin{bmatrix} a_{11}(i) & a_{21}(i) & a_{31}(i) \\ a_{12}(i) & a_{22}(i) & a_{32}(i) \\ a_{13}(i) & a_{23}(i) & a_{33}(i) \\ a_{14}(i) & a_{24}(i) & a_{34}(i) \end{bmatrix}$$

As discussed, the received signal in subcarrier i will be,

$$\mathbf{r}(i) = \mathbf{A}(i)\mathbf{x}(i) + \mathbf{n}(i) \tag{6. 24}$$

We can expand the above expression in the following matrix form,

$$\begin{bmatrix} r_0(i) \\ r_1(i) \\ r_2(i) \\ r_3(i) \end{bmatrix} = \begin{bmatrix} a_{11}(i) & a_{21}(i) & a_{31}(i) \\ a_{12}(i) & a_{22}(i) & a_{32}(i) \\ a_{13}(i) & a_{23}(i) & a_{33}(i) \\ a_{14}(i) & a_{24}(i) & a_{34}(i) \end{bmatrix} \begin{bmatrix} x^0(i) \\ x^1(i) \\ x^2(i) \end{bmatrix} + \begin{bmatrix} n_0(i) \\ n_1(i) \\ n_2(i) \\ n_3(i) \end{bmatrix} \quad (6.\ 25)$$

$$r_0(i) = a_{11}(i)x^0(i) + a_{21}(i)x^1(i) + a_{31}(i)x^2(i) + n_0(i)$$

$$r_1(i) = a_{12}(i)x^0(i) + a_{22}(i)x^1(i) + a_{32}(i)x^2(i) + n_1(i)$$

$$r_2(i) = a_{13}(i)x^0(i) + a_{23}(i)x^1(i) + a_{33}(i)x^2(i) + n_2(i)$$

$$r_3(i) = a_{14}(i)x^0(i) + a_{24}(i)x^1(i) + a_{34}(i)x^2(i) + n_3(i)$$

Where $r_0(i)$,$r_1(i)$, $r_2(i)$ and $r_3(i)$are the signals received on antennas 0, 1, 2 and 3 respectively.

In this demonstration is considered SIC-ZF equalization, therefore the equalization matrix used in each iteration for subcarrier i is the following,

$$\mathbf{G}_{\mathrm{ZF}}(i) = \left(\mathbf{A}(i)^{\mathrm{H}}\mathbf{A}(i)\right)^{-1}\mathbf{A}(i)^{\mathrm{H}} \quad (6.\ 26)$$

In the first iteration we perform ZF equalization for all the subcarriers using the received signal $\mathbf{r}(i)$, therefore we obtain an estimative of all the symbols transmitted in the 3 layers. From the three estimated layers, only layer 1 is used as output in this first iteration, like is presented bellow.

$$\hat{\mathbf{x}}(i) = \mathbf{G}_{\mathrm{ZF}}(i)\mathbf{r}(i) \quad (6.\ 27)$$

After we perform the ZF equalization for all the M_{Layer} subcarriers, we get the estimative for the three transmitted layers, which will be $\hat{\mathbf{x}}_\mathbf{0}$, $\hat{\mathbf{x}}_\mathbf{1}$ and $\hat{\mathbf{x}}_\mathbf{2}$, as shown bellow. (6. 28)

$$\hat{\mathbf{x}}_\mathbf{0} = \left[\hat{x}^0(1) \quad \dots \quad \hat{x}^0\left(M_{Layer}\right)\right]$$

$$\hat{\mathbf{x}}_\mathbf{1} = \left[\hat{x}^1(1) \quad \dots \quad \hat{x}^1\left(M_{Layer}\right)\right] \quad (6.\ 29)$$

$$\hat{\mathbf{x}}_\mathbf{2} = \left[\hat{x}^2(1) \quad \dots \quad \hat{x}^2\left(M_{Layer}\right)\right] \quad (6.\ 30)$$

In this first iteration only $\hat{\mathbf{x}}_\mathbf{0}$ is used as output, therefore considering that channel coding is applied, we just demodulate and decode $\hat{\mathbf{x}}_\mathbf{0}$ symbols. From this point forward consider that $\hat{\mathbf{x}}_{\boldsymbol{LC}}$ are the equalized layer L symbols ($\hat{\mathbf{x}}_{\boldsymbol{L}}$) after being demodulated, decoded, coded and modulated again.

In the second iteration, firstly we will use $\hat{\mathbf{x}}_{\mathbf{0C}} = \left[\hat{x}_C^0(1) \quad \dots \quad \hat{x}_C^0(M_{Layer})\right]$ in order to cancel the interference of layer 0 in the overall received signal $\mathbf{r}(i)$, in all the subcarriers. Note that before we cancel layer 0 we must to perform precoding of $\hat{\mathbf{x}}_{\mathbf{0C}}$ symbols again. Thus for layer 0 cancelation we will use the following precoding vector,

$$\mathbf{a_0}(i) = [a_{11}(i) \quad a_{12}(i) \quad a_{13}(i) \quad a_{14}(i)]^T \tag{6. 31}$$

Then, we perform the following operation in order to cancel layer 0 interference of the overall received signal $\mathbf{r}(i)$,

$$\mathbf{r}'(i) = \mathbf{r}(i) - \hat{x}_C^0(i)\mathbf{a_0}(i) \tag{6. 32}$$

We can see the above expression in the matrix notation presented bellow,

$$\begin{bmatrix} r_0'(i) \\ r_1'(i) \\ r_2'(i) \\ r_3'(i) \end{bmatrix} = \begin{bmatrix} a_{11}(i) & a_{21}(i) & a_{31}(i) \\ a_{12}(i) & a_{22}(i) & a_{32}(i) \\ a_{13}(i) & a_{23}(i) & a_{33}(i) \\ a_{14}(i) & a_{24}(i) & a_{34}(i) \end{bmatrix} \begin{bmatrix} x^0(i) \\ x^1(i) \\ x^2(i) \end{bmatrix} - \hat{x}_C^0(i) \begin{bmatrix} a_{11}(i) \\ a_{12}(i) \\ a_{13}(i) \\ a_{14}(i) \end{bmatrix} + \begin{bmatrix} n_0(i) \\ n_1(i) \\ n_2(i) \\ n_3(i) \end{bmatrix}$$

Note that if the estimation of layer 0 symbols will be done correctly, $\mathbf{r}'(i)$ will be the following,

$$\begin{bmatrix} r_0'(i) \\ r_1'(i) \\ r_2'(i) \\ r_3'(i) \end{bmatrix} = \begin{bmatrix} a_{21}(i) & a_{31}(i) \\ a_{22}(i) & a_{32}(i) \\ a_{23}(i) & a_{33}(i) \\ a_{24}(i) & a_{34}(i) \end{bmatrix} \begin{bmatrix} x^1(i) \\ x^2(i) \end{bmatrix} + \begin{bmatrix} n_0(i) \\ n_1(i) \\ n_2(i) \\ n_3(i) \end{bmatrix}$$

Now, to equalize $\mathbf{r}'(i)$ a different equalization matrix must be computed, therefore the following matrix $\mathbf{G}_{\mathrm{ZF}}'(i)$ is used,

$$\mathbf{G}_{\mathrm{ZF}}'(i) = \left(\mathbf{A}'(i)^{\mathrm{H}}\mathbf{A}'(i)\right)^{-1}\mathbf{A}'(i)^{\mathrm{H}} \tag{6. 33}$$

With $\mathbf{A}'(i)$ being equal to,

$$\mathbf{A}'(i) = \begin{bmatrix} a_{21}(i) & a_{31}(i) \\ a_{22}(i) & a_{32}(i) \\ a_{23}(i) & a_{33}(i) \\ a_{24}(i) & a_{34}(i) \end{bmatrix} \tag{6. 34}$$

After cancel interference of layer 0, we will equalize signal $\mathbf{r}'(i)$ like is presented bellow,

$$\hat{\mathbf{x}}'(i) = \mathbf{G}_{\mathrm{ZF}}'(i)\mathbf{r}'(i) \tag{6. 35}$$

With the above equalization we obtain a new estimative for layer 1 and layer 2 symbols, like is shown bellow,

$$\hat{\mathbf{x}}_{\mathbf{1}}' = \left[\hat{x}^1(1) \quad \dots \quad \hat{x}^1\left(M_{Layer}\right)\right] \tag{6. 36}$$

$$\hat{\mathbf{x}}_{\mathbf{2}}' = \left[\hat{x}^2(1) \quad \dots \quad \hat{x}^2\left(M_{Layer}\right)\right] \tag{6. 37}$$

In this second iteration we will output $\hat{\mathbf{x}}_{\mathbf{1}}'$, therefore demodulation and channel decoding is performed over $\hat{\mathbf{x}}_{\mathbf{1}}'$symbols.

In the third iteration we will eliminate the interference of layer 1 in $\mathbf{r}'(i)$. Therefore like it was done in the first iteration we will demodulate, decode, code and modulate again $\hat{\mathbf{x}}_{\mathbf{1}}'$ in order to obtain $\hat{\mathbf{x}}_{\mathbf{1C}}' = \left[\hat{x}_C^1(1) \quad \dots \quad \hat{x}_C^1\left(M_{Layer}\right)\right]$, which will be used to eliminate the interference of layer 1 in $\mathbf{r}'(i)$.

The precoding vector used in this iteration is,

$$\mathbf{a_1}(i) = [a_{21}(i) \quad a_{22}(i) \quad a_{23}(i) \quad a_{24}(i)]^T \tag{6. 38}$$

Then, we perform the following operation in order to cancel layer 1 interference of the received signal $\mathbf{r}'(i)$,

$$\mathbf{r}''(i) = \mathbf{r'}(i) - \hat{x}_C^1(i)\mathbf{a_1}(i) \tag{6. 39}$$

In case of perfect symbol estimation, the following is obtained,

$$\begin{bmatrix} r_0''(i) \\ r_1''(i) \\ r_2''(i) \\ r_3''(i) \end{bmatrix} = \begin{bmatrix} a_{31}(i) \\ a_{32}(i) \\ a_{33}(i) \\ a_{34}(i) \end{bmatrix} x^2(i) + \begin{bmatrix} n_0(i) \\ n_1(i) \\ n_2(i) \\ n_3(i) \end{bmatrix}$$

Finally, we will equalize $\mathbf{r}''(i)$ without interference of any other layer. Performing again equalization over $\mathbf{r}''(i)$ we will obtain the layer 2 data symbols, which after demodulation and channel decoding, an output of layer 2 can be obtain.

6.4 Channel Correlation Model

In this work we also consider the effect of channel correlation for different rank values. So, we start to generate the uncorrelated channels using the LTE ETU model, then with the selected geometric spatial parameters used to simulate the different correlation scenarios, we will compute a correlation matrix using the Kronecker model. This matrix is used to correlate channels. In this chapter we assume as reference the geometrical configuration presented in 2.4.

- **Kronecker model**

According the spatial input parameters ($\bar{\Phi}_{AoD/AOA}, \sigma_{AoD/AoA}, N_R, N_T, d$) for the set of antennas at the receiver and transmitter, we will compute for each one a correlation matrix $\mathbf{R_{Rx}}$ and $\mathbf{R_{Tx}}$, where each matrix element ρ_{xy} is a coefficient that correlate antenna x with antenna$y$.

In the case of 4x4 MIMO, the matrices are the following,

$$\mathbf{R}_{\text{Tx}} = \begin{bmatrix} 1 & \rho_{12} & \rho_{13} & \rho_{14} \\ \rho_{21} & 1 & \rho_{23} & \rho_{24} \\ \rho_{31} & \rho_{32} & 1 & \rho_{34} \\ \rho_{41} & \rho_{42} & \rho_{43} & 1 \end{bmatrix} \qquad \mathbf{R}_{\text{Rx}} = \begin{bmatrix} 1 & \rho'_{12} & \rho'_{13} & \rho'_{14} \\ \rho'_{21} & 1 & \rho'_{23} & \rho'_{24} \\ \rho'_{31} & \rho'_{32} & 1 & \rho'_{34} \\ \rho'_{41} & \rho'_{42} & \rho'_{43} & 1 \end{bmatrix} \quad \text{(6. 40)}$$

The correlation coefficients for $\mathbf{R}_{\text{Tx}}$ are computed using the following expression,

$$\rho_{xy}(D) = \int_{\bar{\Phi}_{AoD}-\pi}^{\bar{\Phi}_{AoD}+\pi} e^{jDsin(\bar{\Phi}_{AoD})} PAS(\Phi) d\Phi \quad \text{(6. 41)}$$

$$\rho_{xy}(D) = \int_{\bar{\Phi}_{AoD}-\pi}^{\bar{\Phi}_{AoD}+\pi} e^{jDsin(\bar{\Phi}_{AoD})} ce^{\frac{-\sqrt{2}|\Phi-\bar{\Phi}_{AoD}|}{\sigma_{AoD}}} d\Phi$$

Where $PAS(\Phi)$ is the power azimuth spectrum, which has a Laplacian (Φ, σ) distribution around the mean$\bar{\Phi}$. The $PAS(\Phi)$ tell us the power distribution in the azimuth domain.

$$PAS(\Phi) = ce^{\frac{-\sqrt{2}|\Phi-\bar{\Phi}|}{\sigma}} \quad \text{(6. 42)}$$

$$D = \frac{2\pi d}{\lambda} \quad \text{(6. 43)}$$

In the above expressions, $\bar{\Phi}_{AoD/AoA}$ is the mean angle of departure/arrive, $\sigma_{AoD/AoA}$ is the angular spread for the angle of departure/arrive, c is a normalization factor, d is the distance between the antennas, N_T and N_R are the number of transmit and receive antennas respectively. In the case of $\mathbf{R}_{\mathrm{Rx}}$ we use the same expressions, but now with input parameters $\bar{\Phi}_{AoA}$, σ_{AoA} and the correct$d$. Note that correlation coefficients will depend of the distance between the antennas, and also will depend of $PAS(\Phi)$. The $PAS(\Phi)$ parameters (Φ, σ) used will model different scattering levels in propagation scenarios, which will result in different correlation effects in the MIMO channels.

Then, performing eigenvalues decomposition we will compute $\mathbf{R}_{\mathrm{Rx}}^{1/2}$and $\mathbf{R}_{\mathrm{Tx}}^{1/2}$, which are defined as $\mathbf{R}_{\mathrm{Rx/Tx}}^{1/2}(\mathbf{R}_{\mathrm{Rx/Tx}}^{1/2})^{\mathbf{H}} = \mathbf{R}_{\mathrm{Rx/Tx}}$.

$$[\mathbf{V}, \mathbf{D}] = \mathrm{eig}(\mathbf{R}_{\mathrm{Rx}}) \qquad [\mathbf{V}, \mathbf{D}] = \mathrm{eig}(\mathbf{R}_{\mathrm{Tx}}) \tag{6. 44}$$

$$\mathbf{R}_{\mathrm{Rx}}^{1/2} = \mathbf{V}\sqrt{\mathbf{D}} \qquad \mathbf{R}_{\mathrm{Tx}}^{1/2} = \mathbf{V}\sqrt{\mathbf{D}}$$

Finally using the Kronecker product we obtain the correlation matrix $\mathbf{R}_{\mathrm{H}}$, which will be used to correlate the input uncorrelated time domain channel coefficients of $\mathbf{H}_{\mathrm{i}}$.

$$\mathbf{R}_{\mathrm{H}} = \mathbf{R}_{\mathrm{Tx}}^{1/2} \otimes \mathbf{R}_{\mathrm{Rx}}^{1/2} \tag{6. 45}$$

In MIMO 4x4, $\mathbf{R}_{\mathrm{H}}$ is a 16x16 size matrix used to correlate the 16 independent channel coefficients in each sample time (tap). Note that the correlation operation only change the amplitude of the channel taps, making the number of taps and the respective positions remains the same defined in the LTE ETU model used to compute $\mathbf{H}_{\mathrm{i}}$.

The output correlated coefficients $\mathbf{H}_{\mathrm{corr}}$ for a sample time (tap), are computed multiplying $\mathbf{R}_{\mathrm{H}}$ by $\mathbf{H}_{\mathrm{i}}$.In the expression bellow, i is the tap index [32].

$$\mathbf{H}_{\mathrm{corr}} = \mathbf{R}_{\mathrm{H}}\mathbf{H}_{\mathrm{i}} \tag{6. 46}$$

$$\begin{bmatrix} h_{c11}(t_i) \\ h_{c12}(t_i) \\ h_{c13}(t_i) \\ h_{c14}(t_i) \\ h_{c21}(t_i) \\ h_{c22}(t_i) \\ \vdots \\ h_{c44}(t_i) \end{bmatrix} = \begin{bmatrix} R_{1,1} & \cdots & R_{1,16} \\ \vdots & \ddots & \vdots \\ R_{16,1} & \cdots & R_{16,16} \end{bmatrix} \begin{bmatrix} h_{11}(t_i) \\ h_{12}(t_i) \\ h_{13}(t_i) \\ h_{14}(t_i) \\ h_{21}(t_i) \\ h_{22}(t_i) \\ \vdots \\ h_{44}(t_i) \end{bmatrix}$$

6.5 Simulation Platform Structure

In this section we present the block diagram structure of the programs used to simulate the 2x2 MIMO and 4x4 MIMO configurations. In the next two pages is presented in landscape format the diagrams of 2x2 MIMO and 4x4 MIMO, which we now describe in detail.

In both configurations we start to generate and modulate a fixed set of random bits, which are reorganized in rank parallel layers using the layer map block. Therefore at the output of the layer map block, several vector columns are obtained, with each column being composed by rank complex symbols. Then, at the precoding block we use the columns of rank symbols in order to precode data using the matrix selected from the LTE codebook set. The output of precoding operation is composed by 2 (2x2 MIMO) or 4 (4x4 MIMO) parallel precoded signals, which are transmitted in parallel on the same frequency but in different antennas/OFDM signals. This precoding operation is done individually for each subcarrier. Next, each output of the precoding block is distributed in the frequency domain using the OFDM map block in each antenna branch. After we add noise and perform the correct matrix multiplication by the channel frequency response, we recover the symbols transmitted in the rank layers using 4 different types of equalizers: ZF, MMSE, SIC-ZF and SIC-MMSE. At the output of each equalizer we obtain rank layers with the data symbols transmitted, then, in the layer demap block we put the symbols of the rank layers in the correct serial sequence. Finally, after demodulation, we obtain the recover bits which are compared with the original bit sequence in order to compute the BER for each tested equalizer.

MIMO 2x2 Platform Simulation Structure

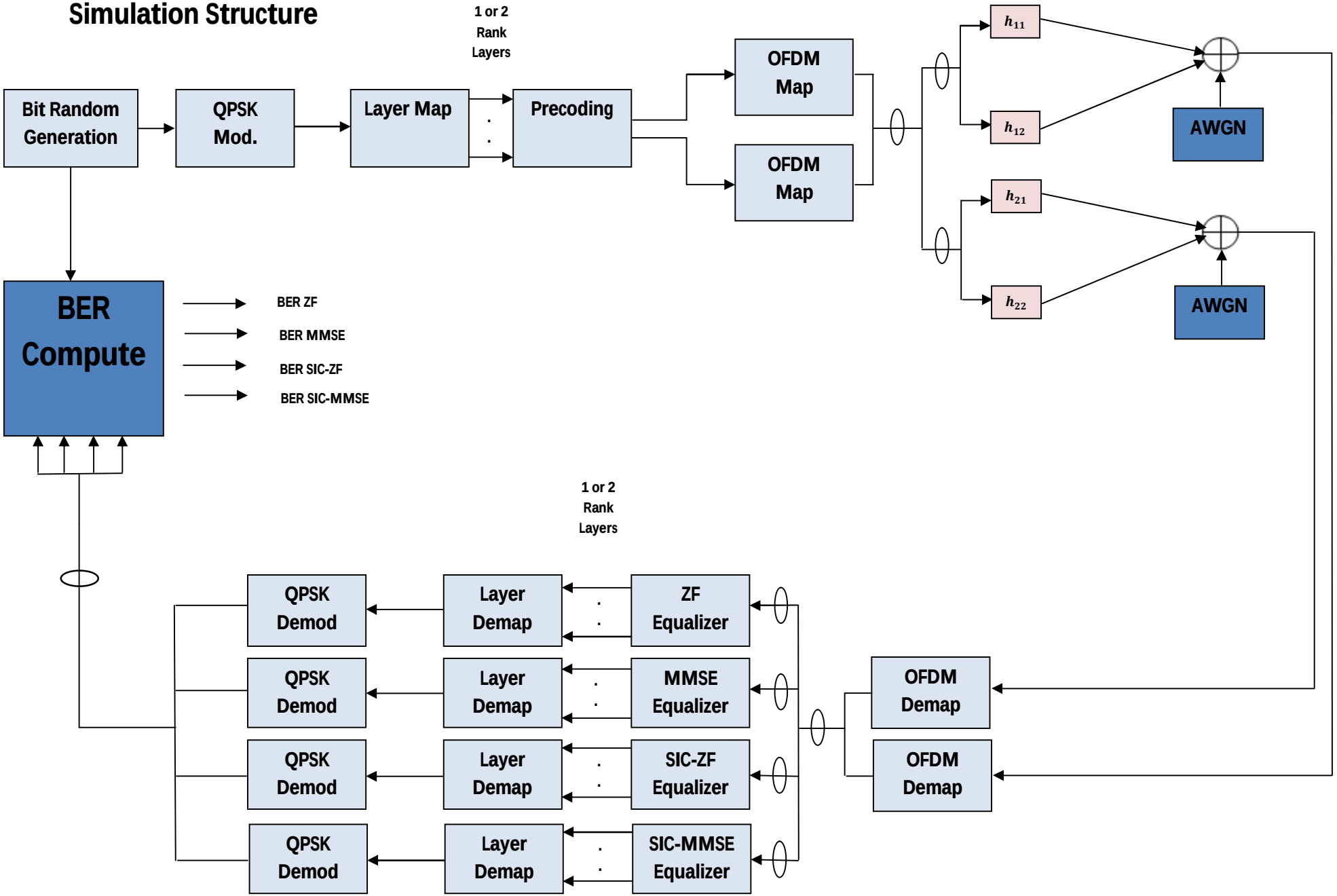

MIMO 4x4 Platform Simulation Structure

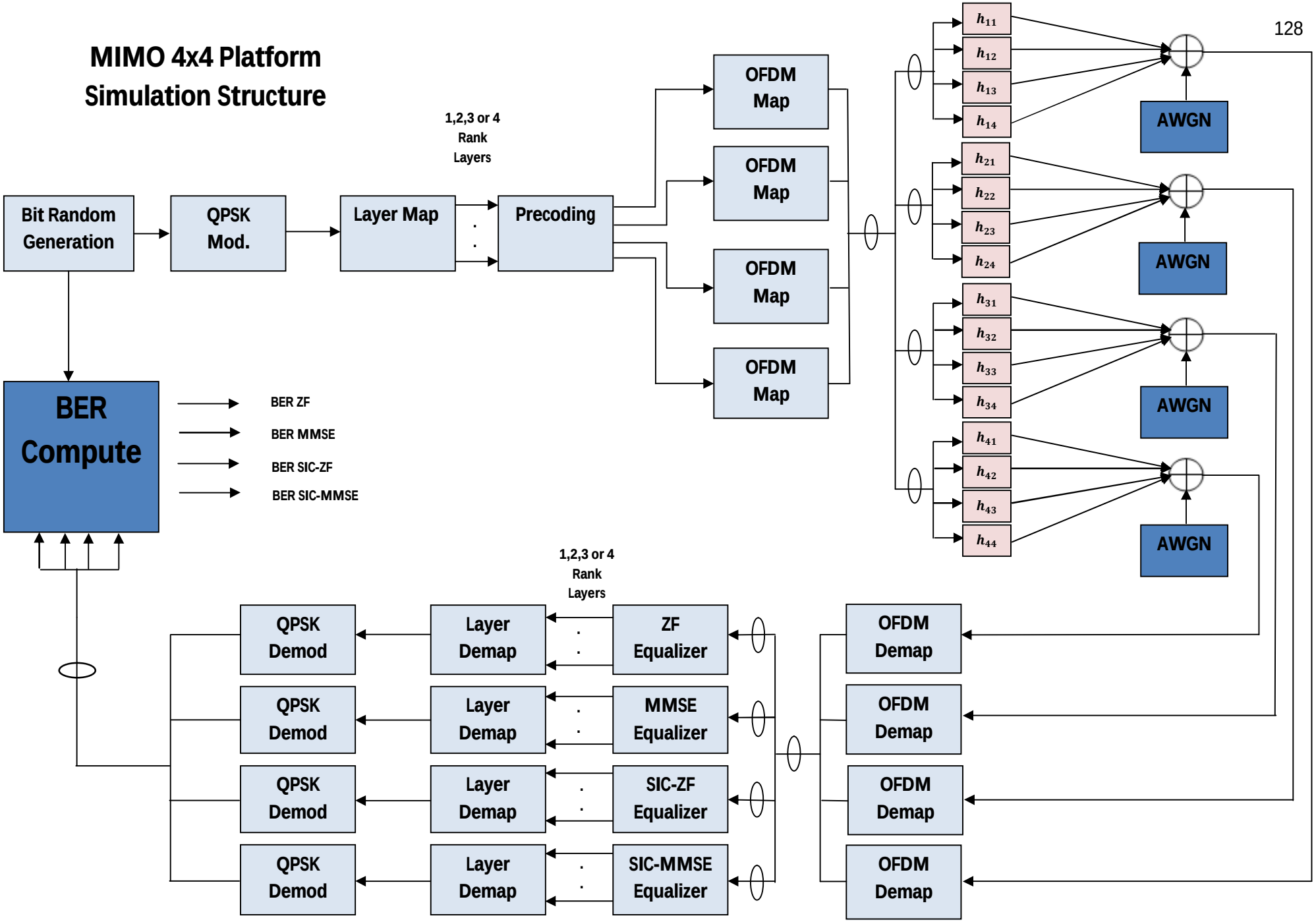

6.6 Simulation Results

In this section we present the results obtained for several configurations of the 2x2 and 4x4 MIMO systems implemented. The main simulation parameters are presented in Table13.

	Uncorrelated channels 4x4 and 2x2 MIMO	**Correlated channels 4x4 MIMO**	**Uncorrelated channels 4x4 MIMO with channel coding**
Modulation	QPSK		
Channel Model	LTE Extended Typical Urban Channel (ETU) Uncorrelated Rayleigh fading		
Angle of Arrive (mean/spread)	-	67.5°/68°	-
Angle of Departure (mean/spread)	-	50°/8°	-
Receiver/Transmitter Antenna Spacing (Wavelength)	-	0.5/0.5	-
Channel Coding	-	-	Turbo Coding Rate 1/3 (punctured to 1/2)

Table 13 - Simulation parameters

6.6.1 Results for 2x2 MIMO with uncorrelated channels

Starting by analyze the difference between the curves for code index 1 and code index 2 we can see that there are no big difference. Like we said before, these simulations were computed applying the same code index to the entire OFDM signal, which is not the exact method used by LTE. The LTE changes the precoding matrix along the OFDM subcarriers in order to select the

matrix which reduces channel correlation conditions in those subcarriers. Therefore, the performance is the same irrespective the precoding matrix considered.

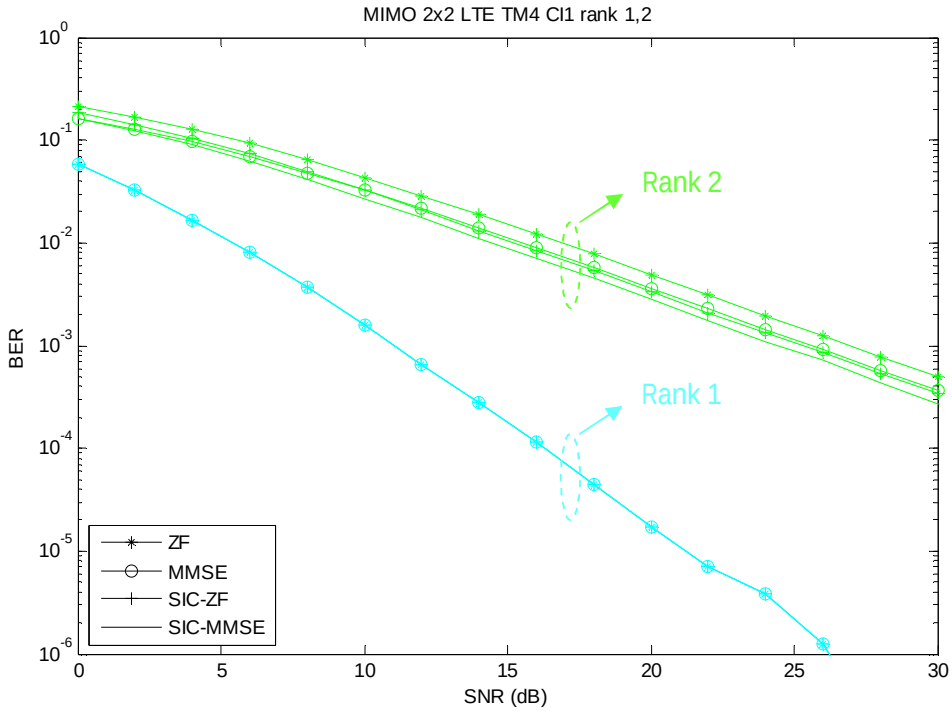

Figure 6. 5 - BER results in 2x2 MIMO for LTE TM4 code index 1

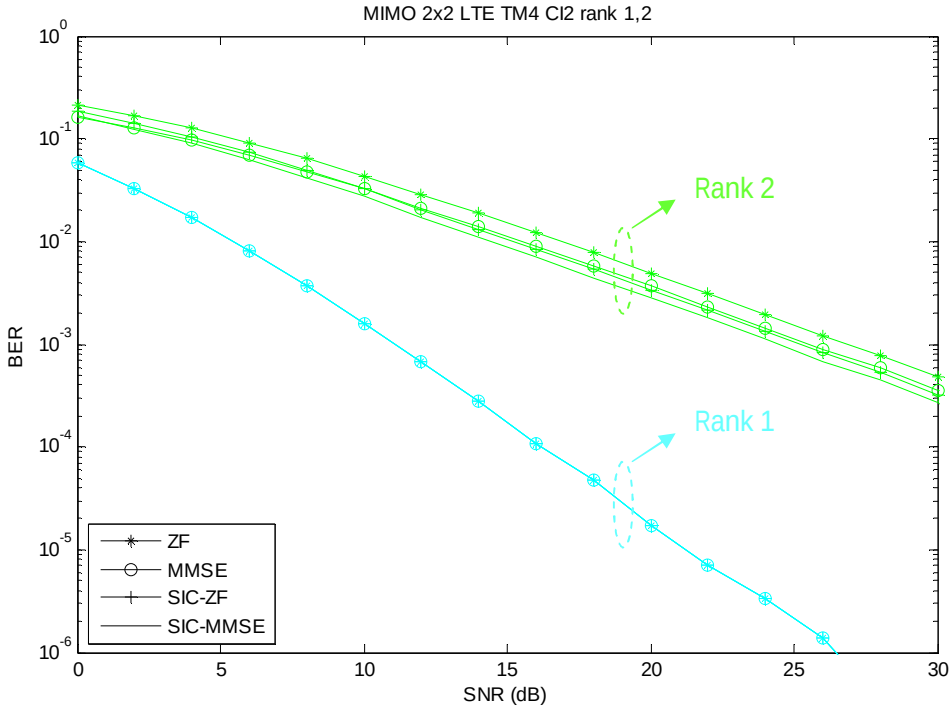

Figure 6. 6 - BER results in 2x2 MIMO for LTE TM4 code index 2

The compute of the matrix rank in the UE is done based on the singular values of the channel matrix (SVD). These singular values are indicators of the available capacity in each one of the parallel channels for a given subcarrier, therefore according the number of singular values which are under a given value, a rank indicator is selected avoiding the use of the bad pipes.
When we switch for a lower rank transmission, we are increasing diversity gain experimented by each layer, therefore lower BER results are achieved. The cost of this diversity gain increase is the reduction of multiplexing gain and consequently spectral efficiency; hence to maintain the same transmission rate, more bandwidth must be used.
Analyzing the equalizers, we can see that for rank 2 the SIC-MMSE outperforms the other ones. From the Figures we can observe the ZF has the worst performance, since it fully removes the interference at the cost of increasing the noise. However, the performance of all equalizers is similar since the interference level is not high in this 2x2 MIMO scenario with rank 2. For the rank 1, i.e., a scenario without any inter-symbol interference, both MMSE and ZF equalizer have approximately the same performance, as expected. Note that for rank 1, does not make sense to consider the SIC approaches.

6.6.2 Results for 4x4 MIMO

- **Results for Uncorrelated Channels**

Like we said before, in LTE TM4 for a 4x4 MIMO configuration, the BS can adapt the number of symbols transmitted in one subcarrier selecting a transmission rank mode that could range between 1 and 4. Starting to compare rank 1 and rank 2 curves between 2x2 MIMO and 4x4 MIMO for uncorrelated channels, we can see that for a given SNR the number of bits received correctly is significantly higher in 4x4 MIMO, hence for the same amount of data transmitted in the same bandwidth, we can verify that a more reliable transmission is achieved increasing the number of antennas at both sides of a MIMO system link. Therefore, increasing the number of antennas at both system sides, an improvement in diversity level is achieved keeping constant the SM gain.
Focusing now in 4x4 MIMO, as discussed in 2x2 MIMO, we can see that increasing rank transmission we improve spectral efficiency using higher SM modes, but with lower diversity level experimented by each layer, which results in lower transmission reliability (high BER results). In order to improve diversity, lower rank transmissions must be used. We should refer that in a MIMO channel there is a trade-off between achieve SM and diversity gains, therefore

is not possible use the spatial dimensions in MIMO channel to achieve maximum SM and diversity gains simultaneously.

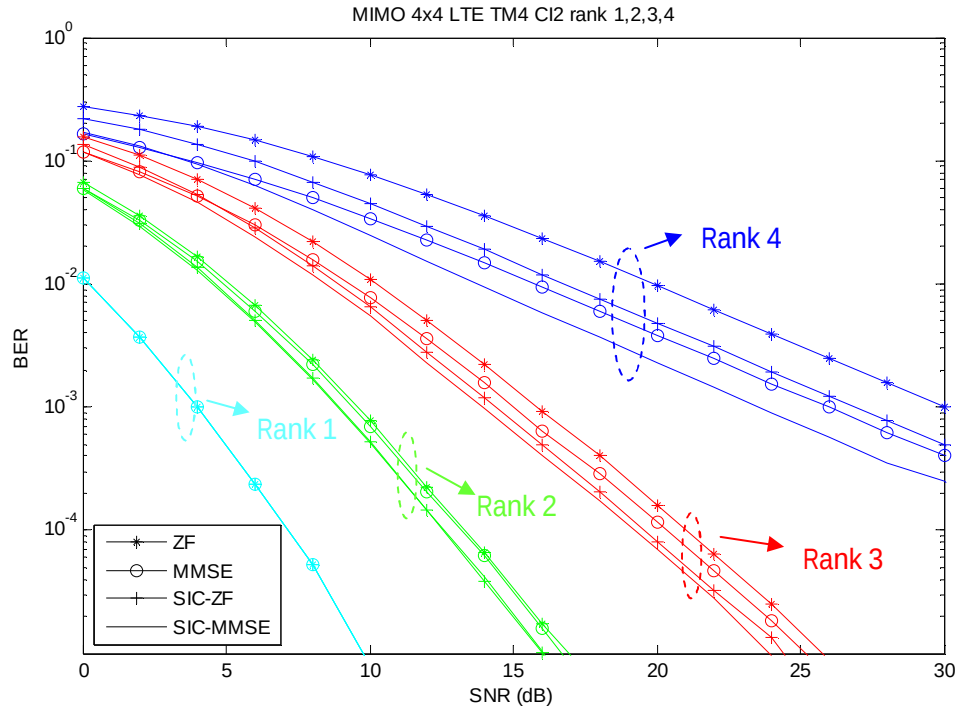

Figure 6. 7- BER results in normal 4x4 MIMO for LTE TM4 code index 2

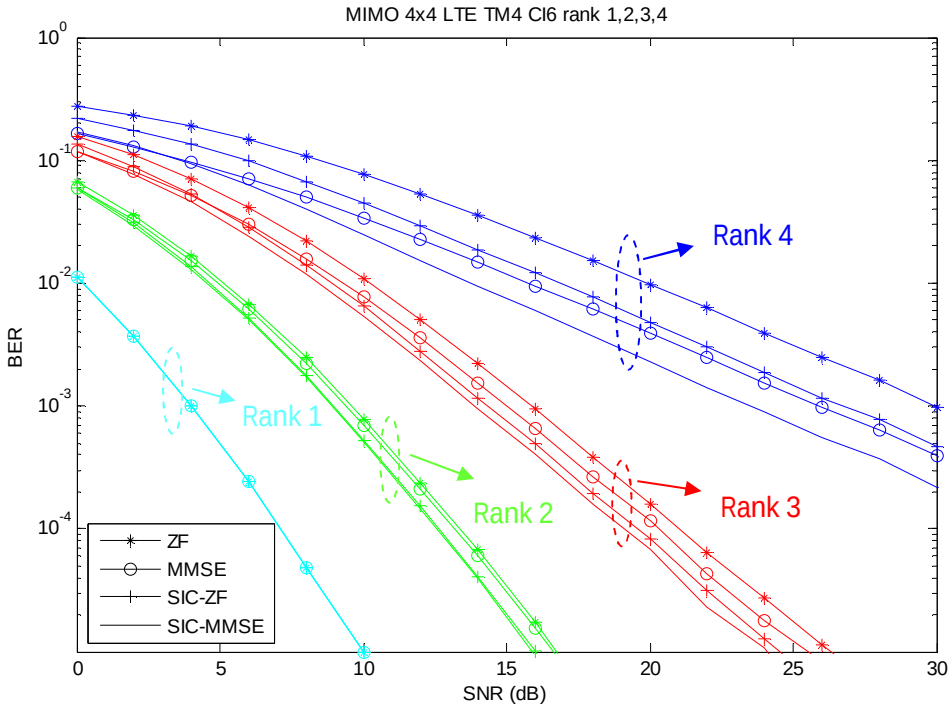

Figure 6. 8- BER results in normal 4x4 MIMO for LTE TM4 code index 6

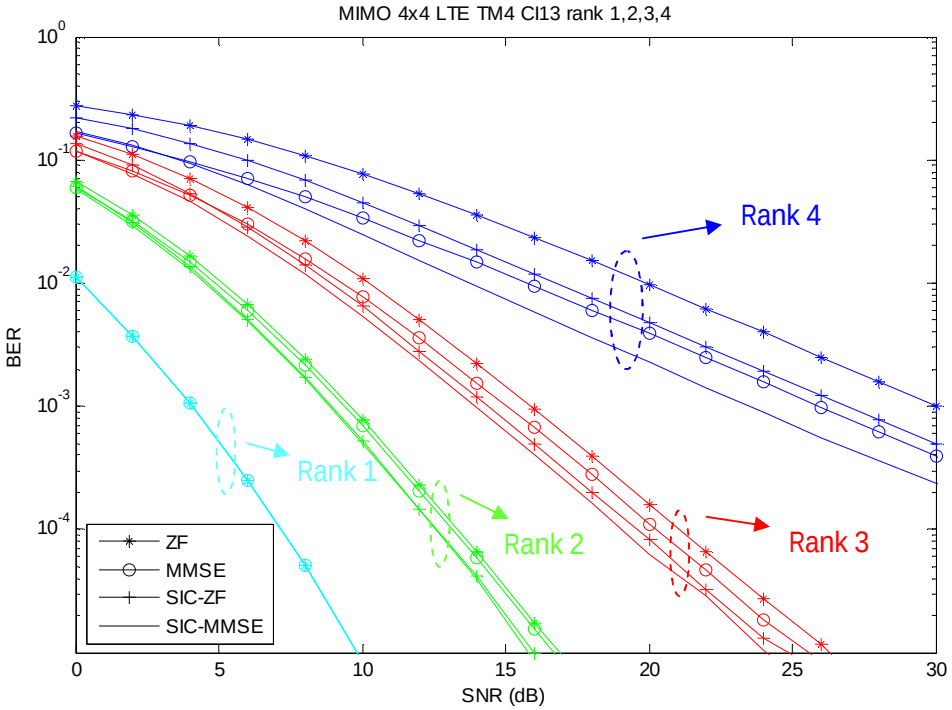

Figure 6. 9- BER results in normal 4x4 MIMO for LTE TM4 code index 13

Analyzing the equalizers, we can see that for rank 4 the SIC-MMSE outperforms the other ones. Note that rank 4, represents the scenario where the equalizers must deal with higher interference level, and thus should be efficient to remove it. From the Figures we can observe that the ZF has the worst performance, since it fully removes the interference at the cost of increasing the noise. This noise enhancement drawback is mitigated by using the MMSE equalizer, and thus the performance is improved when compared with ZF. Considering the SIC based equalizers, we can see that they clearly outperform the MMSE and ZF ones, since they are more efficient to remove the overall interference. Other important issue is that decreasing the rank, which means that the inherent systems diversity is increased; the performance of all equalizers is quite similar. For rank 2 we can see a minor gain of the SIC based approaches regarding MMSE and ZF ones. Also, it can be shown that for rank 1 (the SIC approaches not considered) both equalizers MMSE and ZF have the same performance. Note that ZF tends to MMSE when SNR tends to infinite or when the diversity order increases.

- **Results for Correlated Channels**

In figures 6.10, 6.11 and 6.12 is used the same system configuration of the previous 4x4 MIMO, but now simulating a transmission under high channel correlation conditions.

When we perform a transmission under high correlation conditions, the capacity of the several channel pipes decrease strongly, and we can verify that analyzing the low results obtained for the singular values (SVD) of the correlated channel, which results in low values for the rank computation performed over channel matrix estimation. Therefore, in this case the only chance of transmit the data, is reducing the spatial multiplexing gain using lower rank transmissions. Another aspect that we should notice from the curves in Figures 6.10, 6.11 and 6.12 is that, although the similar BER results obtained for the 3 codebook indexes, we can see a performance difference in rank 2 curves between CI6 and the other codebook matrices used, therefore as discussed before, we can conclude that the transmission is not indifferent to the selected precoding matrix, especially in the case of high channel correlation conditions. Note that the selection of the precoding matrix which maximizes channel decorrelation for a given subcarrier is crucial to improve transmission performance under this type of conditions.

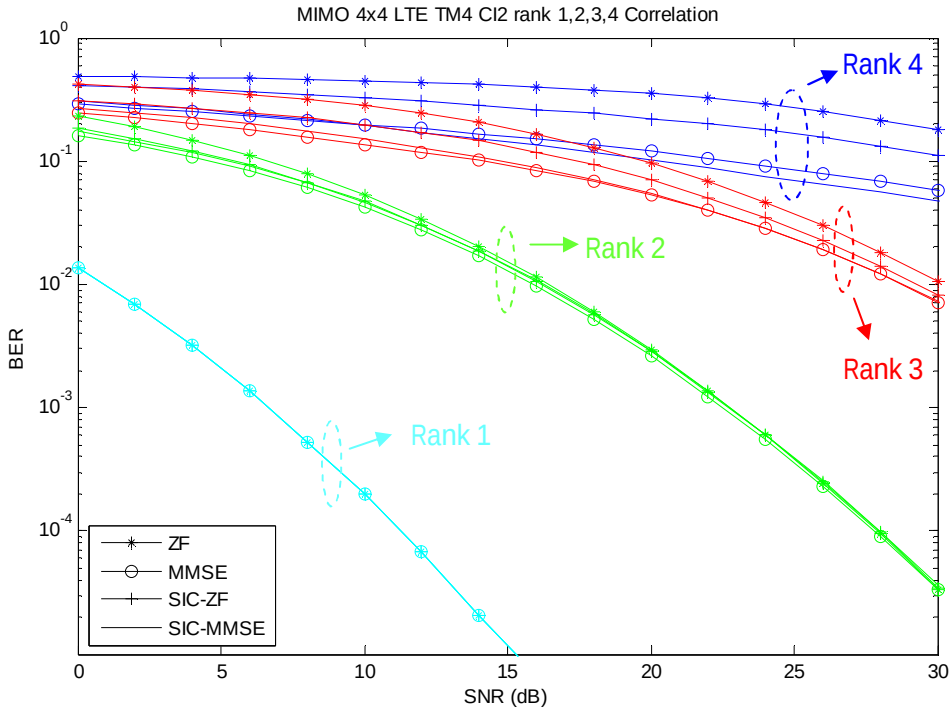

Figure 6. 10 - BER results with channel correlation in 4x4 MIMO for LTE TM4 code index 2

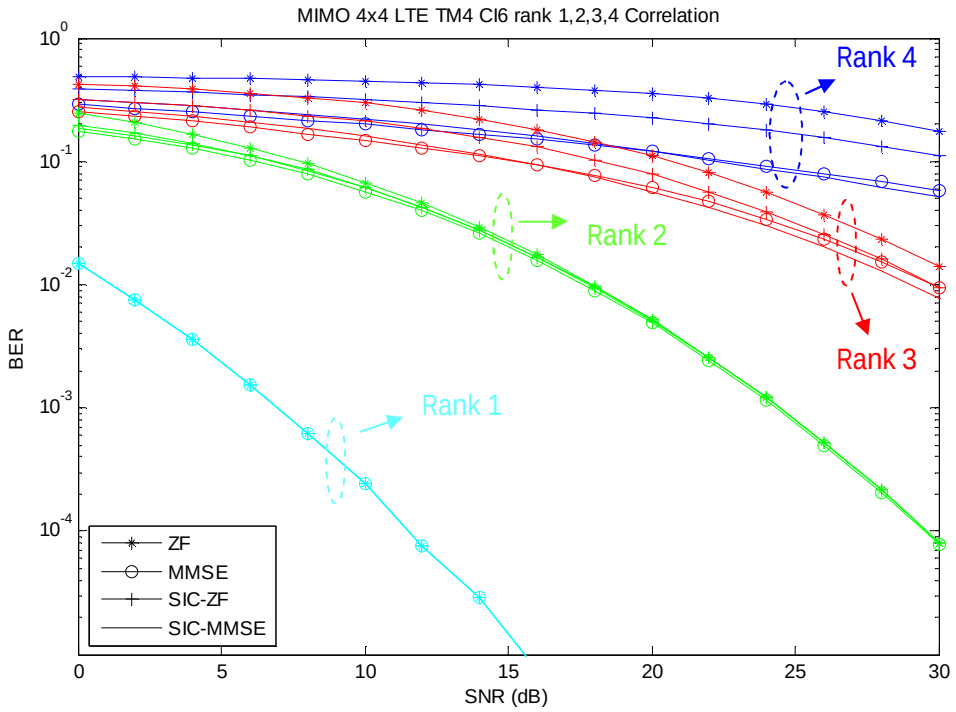

Figure 6. 11 - BER results with channel correlation in 4x4 MIMO for LTE TM4 code index 6

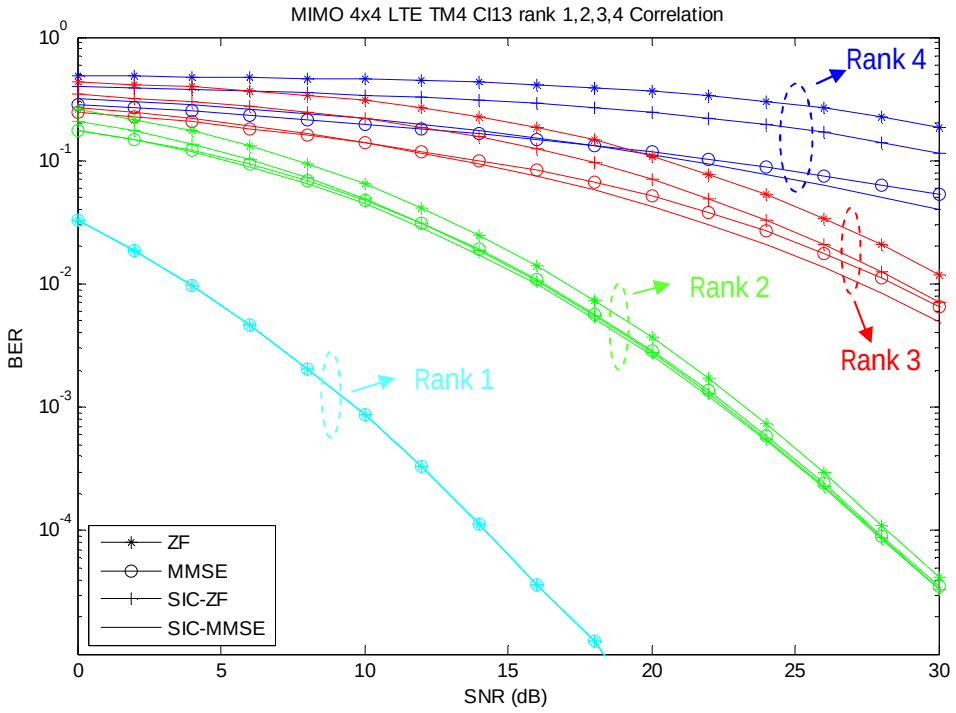

Figure 6. 12 - BER results with channel correlation in 4x4 MIMO for LTE TM4 code index 13

- **Results for 4x4 MIMO Uncorrelated with Channel Coding**

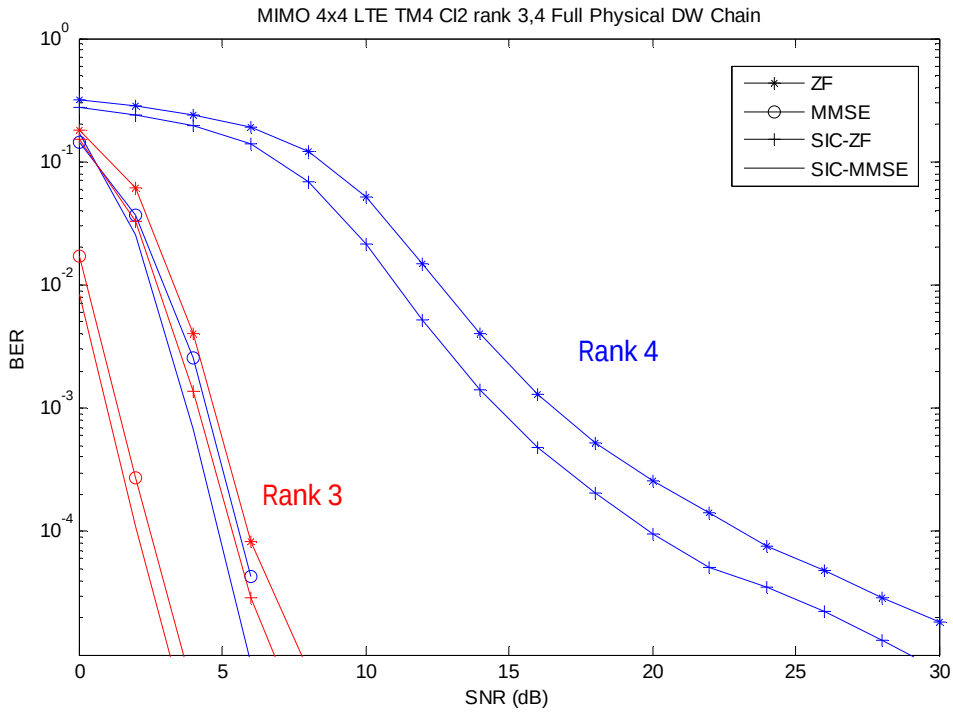

Figure 6. 13 - BER results with channel coding in 4x4 MIMO for LTE TM4 code index 2

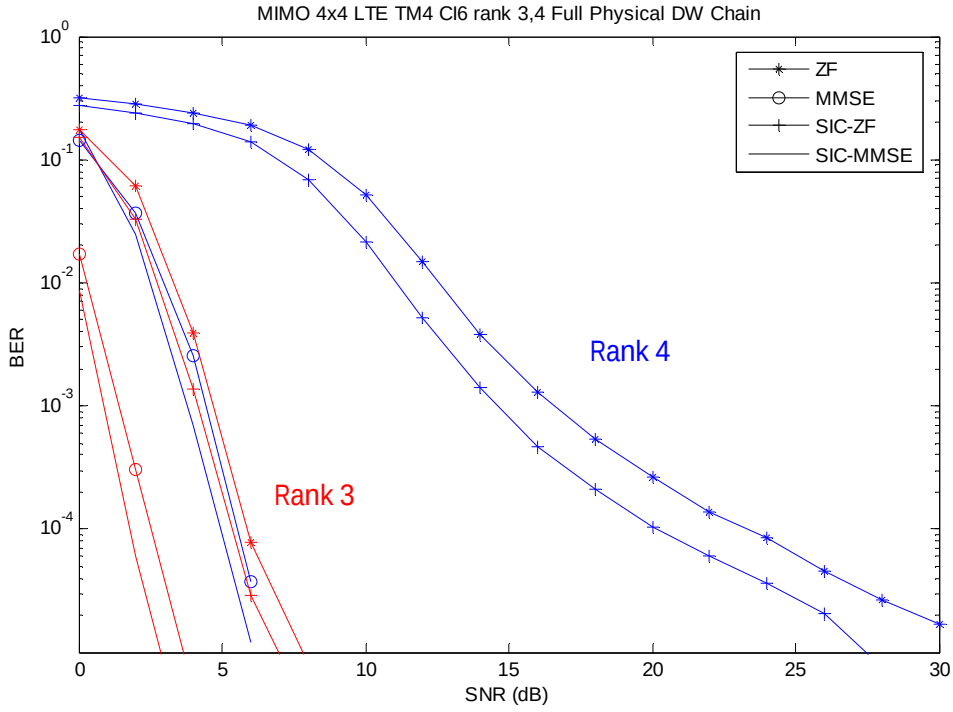

Figure 6. 14 - BER results with channel coding in 4x4 MIMO for LTE TM4 code index 6

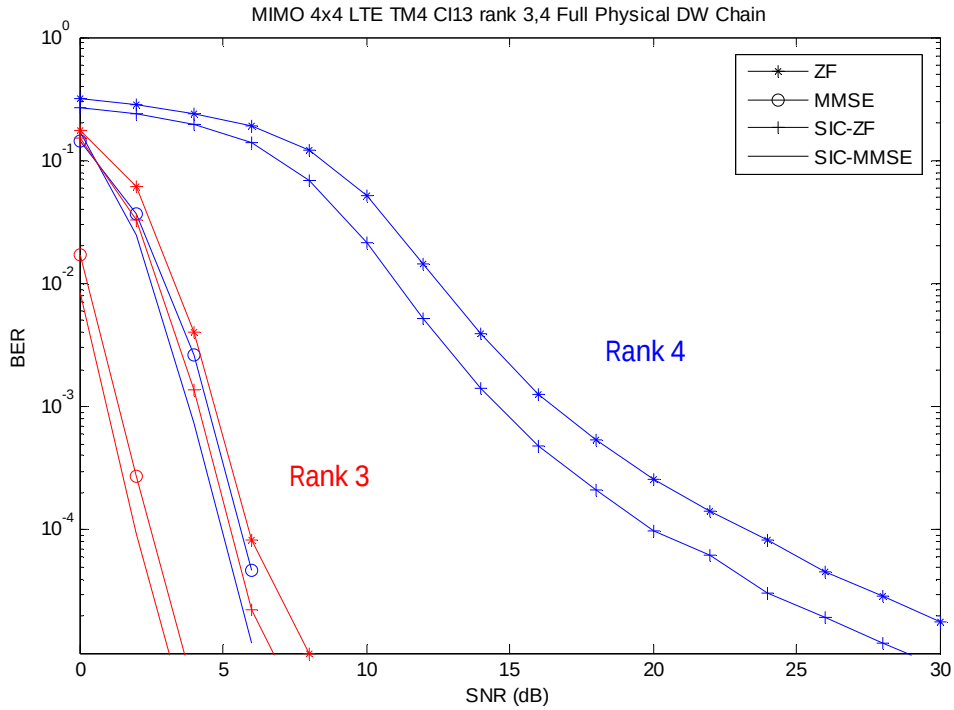

Figure 6. 15 - BER results with channel coding in 4x4 MIMO for LTE TM4 code index 13

The last simulation results were computed using channel coding; therefore error correction capacity was integrated in our simulation platform. Looking to Figures 6.13, 6.14 and 6.15, we can see a significant improvement in the BER results. The main reason for this difference was precisely the use of the 1/3 Turbo FEC code, which allows error correction at the receiver.

We should say that the number of OFDM simulation symbols was not enough to verify errors for rank 1 and rank 2, therefore in all SNR points the BER was 0.

7. Conclusion and Future Work

7.1. Conclusion

In this master thesis we start to see that the most difficult physical phenomena to deal when we perform a wireless transmission over a urban radio channel is the multipath characteristic of the channel, which results in frequency selectivity fading. Note, that while path loss and shadowing can be override controlling the transmission power, in the case of multipath fading we need to consider complex signal processing techniques to improve the communication for a given transmission scenario. Then, we saw that one of the solutions to improve several communication metrics over this type of channel is adding a new spatial dimension using multiple antennas at both transmitter and receiver, which is defined as MIMO systems. Considering the spatial dimension, we can use 3 types of MIMO mechanisms, which are spatial-multiplexing, diversity and beamforming. With spatial-multiplexing we can increase transmission throughput; using diversity mechanism we can improve transmission reliability using SFBC/STBC block codes; and with beamforming, cell coverage increase could be achieved. This can be achieved without the use of additional time-frequency resources, which make MIMO technology very attractive for practical wireless systems. The performance of these 3 mechanisms is strongly influenced by the spatial channel correlation conditions, and also by the capacity in acquires with accuracy the channels parameters in both sides of the communication link. In terms of correlation requirements, we saw that while SM and diversity mechanisms needs of low spatial correlation between the channels to separate the symbols without interference and with good strength, beamforming can also be implemented with higher

spatial correlation conditions. Regarding CSI availability, we saw that for diversity mechanisms CSI must be available at the receiver, in the case of SM mode CSI must be known at least in one side of the link, and in beamforming mechanism CSI must be available at the transmitter. Giving particular attention to SM modes, we saw that if CSI is available in both sides of the link we can perform SVD technique to separate with power allocation control, the set of symbols transmitted in the same subcarrier; otherwise if CSI is available at just one side of the link, a equalization technique like ZF, MMSE or SIC must be computed at the side where CSI is available.

In the second part of the work we presented the LTE MIMO transmission modes in order to show how the MIMO mechanisms are adapted to be implemented in a practical cellular standard (LTE), where system practical constraints must be taken in account in the design of the MIMO transmission schemes. We saw that diversity in LTE is performed using SFBC mapping for 2 antennas transmission, and a specific type of SFBC-FSTD mapping is used to 4 antennas. In the case of SM, LTE uses an open-loop mode for high mobility, a closed-loop mode for low mobility and a MU-MIMO mode to serve several UEs in the same frequency. For beamforming, LTE uses a codebook based beamforming mode for FDD variant, and 2 modes suited for TDD variant, being one of them a hybrid beamforming-SM mode (not presented), where a 2 layer beam transmission is performed.

In the last part of the work we analyze in detail the work structure and the performance of LTE closed-loop mode. About the work structure we saw that due the FDD impossibility of channel estimation at the uplink, LTE performs channel estimation at the UE. After estimate the channel, the UE seeks in the codebook which precoding matrix will minimize the correlation between the channels, so that the correct PMI index is reported to the BS. Another important reported index is the RI, which is selected based on rank computation of the channel matrix estimation. This rank value defines the number of layers that can be transmitted over the estimated channel conditions. In the analyzes of the results obtained with the developed simulation platform, we showed that under high correlation channel conditions is very difficult to achieve high multiplexing gains using any kind of equalizer. We also saw that with the increase of transmission rank in LTE TM4, reduced diversity levels are experimented by each transmitted layer. Regarding the equalizers used, the SIC-MMSE was the one with the better performance, particularly for high rank transmissions. For low rank the performance of the studied equalizer is basically the same. Also, it was shown that for uncorrelated channels the use of fixed precoding is useless.

As final conclusion, the results have clearly shown the system performance improvement when multiple antennas are employed and thus this technology plays an important role in the current and future cellular systems.

7.2. Future Work and Trends

In terms of MIMO future trends, the path is continue increasing the number of antennas at both transmitter and receiver in order to allow high diversity and SM gains, being already verified in LTE-Advanced, where a 8 layer SM transmission mode is available. The other trend is the use of hybrid modes, where the advantages of beamforming and SM are combined in a single mode, like it happens in LTE R9 TM8.

Concerning the future work to improve the simulation platform developed we suggest the following:

- Implement the PMI index mechanism to select the best precoder and thus improve the performance when correlated channels are considered.
- Implement the channels estimation block to evaluate the discussed equalizers under imperfect CSI.
- Implement precoding algorithms based on the knowledge of CSI at the transmitter side and compare the results with the fixed precoding matrix considered in the LTE.

Bibliography

[1] Gameiro, A. (2012). Slides of Wireless Networks subject, Aveiro University, Departament of Electronic, Telecommunications and Informatics, Aveiro, Portugal.

[2] Stefania Sesia; Issam Toufik; Matthew Baker. (2009). *LTE - The UMTS Long Term Evolution.* Chicago: John Wiley & Sons Ltd.

[3] Erik Dahlman, Stefan Parkvall, Johan Sköld and Per Beming. (2008). *3G Evolution.* Oxford: Elsevier Ltd.

[4] Kevin Linehan, Julius Robson. (2012). *What base station antenna configuration is best for LTE-Advanced?* White Paper, Commscope.

[5] Harri Holma; Antti Toskala. (2009). *LTE for UMTS – OFDMA and SC-FDMA Based Radio Access.* Chichester, West Sussex, United Kingdom: John Wiley & Sons Ltd.

[6] (2010). *MIMO Channel Modeling and Emulation Test Challenges.* Application Note, Agilent Technologies.

[7] Schwartz, M. (2004). *Mobile Wireless Communications.* Cambridge: Cambridge University Press.

[8] Atilio Gameiro, Adão Silva. (2013). Slides Wireless Communications subject, Aveiro University, Departament of Electronic, Telecommunications and Informatics, Aveiro, Portugal.

[9] Khan, F. (2009). *LTE for 4G Mobile Broadband.* Cambridge: Cambridge University Press.

[10] Silva, A. P. (2007). *Pré-Filtragem no Espaço-Frequência para o Sistema MC-CDMA.*PhD Thesis, Aveiro University, Aveiro.

[11] (2011). *Correlation-based Spatial Channel Modeling.* White Paper, Spirent.

[12] (2012). *TD-LTE and MIMO Beamforming Principles and Test Challenges.* White Paper, Spirent.

[13] (2012). *Verify and Visualize Your TD-LTE Beamforming Signals.* Application Note, Agilent Technologies.

[14] Greenpacket. (2010). *Antenna Technology*. Obtido em 2013, de greenpacket: http://www.greenpacket.com/technology_Devices_Antenna_Technology.html

[15] Ian F. Akyildiz, David M. Gutierrez-Estevez, Elias Chavarria Reyes. (2010). *The evolution to 4G cellular systems: LTE-Advanced.* Elseiver.

[16] (2009). *The LTE Network Architecture.* White Paper, Alcatel Lucent.

[17] *LTE Layers Data Flow.* (2013). Obtido em 2013, de tutorialspoint: http://www.tutorialspoint.com/lte/lte_layers_data_flow.htm

[18] Technologies, A. (2009). *LTE and the Evolution to 4G Wireless.* (M. Rumney, Ed.) Agilent Technologies.

[19] (2010). *LTE in a Nutshell: The Physical Layer*. White Paper, Telesystem Innovations.

[20] (2010). *TS 36.211 v9.1.0 Release 9, LTE Evolved Universal Terrestrial Radio Access (E-UTRA) Physical Channels and Modulation.* Technical Specification, 3GPP.

[21] (2009). *MIMO in LTE and LTE-Advanced.* White Paper, Ericsson, Ericsson Research.

[22] (2010). *TS 36.212 v9.2.0 Release 9, LTE Evolved Universal Terrestrial Radio Access (E-UTRA) Multiplexing and Channel Coding.* Technical Specification, 3GPP.

[23] Hongyan. (6 de August de 2009). *CQI Reporting in LTE*. Obtido em 18 de November de 2013, de LTE University: http://lteuniversity.com/get_trained/expert_opinion1/b/hongyanlei/archive/2009/08/06/cqi-reporting-in-lte.aspx

[24] (2010). *TS 36.213 v9.2.0 Release 9, Evolved Universal Terrestrial Radio Access (E-UTRA) Physical Layer Procedures.* Technical Specification, 3GPP.

[25] (2009). *The Seven Modes of MIMO in LTE.* White Paper, Telesystem Innovations.

[26] Hidekazu Taoka; Satoshi Nagata; Kazuaki Takeda; Yuichi Kakishima; Xiaoming She; Katsutoshi Kusume. *MIMO and CoMP in LTE-Advanced.* Beijing: NTT DOCOMO Technical Journal.

[27] (2011). *LTE Transmission Modes and Beamforming*. White Paper, Rohde & Schwarz.

[28] Jonathan Duplicy, Biljana Badic, Rajarajan Balraj, Rizwan Ghaffa, Péter Horváth, Florian Kaltenberger, Raymond Knopp, István Z. Kovács, Hung T. Nguyen, Deepaknath Tandur, and Guillaume Vivier. (2011). MU-MIMO in LTE Systems. *EURASIP Journal onWireless Communications and Networking* .

[29] Rohde & Schwarz, W. P. (2011). *LTE Transmission Modes and Beamforming.*

[30] Juho Lee, Jin-Kyu Han, Jianzhong (Charlie) Zhang. (2009). MIMO Technologies in 3GPP LTE and LTE-Advanced. *EURASIP Journal onWireless Communications and Networking* .

[31] Sankar, K. (2 de 11 de 2009). *MIMO*. Obtido em 2013, de Dsplog Signal Processing for Communication: http://www.dsplog.com/category/mimo/

[32] Guy Nuhamovich, Doron Ezri, Eli Sofer, Atilio Gameiro, Adão Silva, Ramiro, Sobles, Quiliano Pérez , Óscar Moreno, Damien Castelain, Loïc Brunel, M. Santos, Jean-Benoît Pierrot, Valentin Savin, Jaouhar Ayadi, Vasile Bota, Mihaly Varga. *System definition and criteria to select the schemes.* Research Project, CODIV Project.

[33] Dimitra Zarbouti, George Tsoulos, Dimitra Kaklamani. (2006). Theory and Practice of MIMO Wireless Communication Systems. In G. V. Tsoulos, *MIMO System Technology for Wireless Communications* (p. 378).

[34] IAF GmbH. (2010). *MIMO OFDM Testbed for future mobile networks*. Obtido em 2013, de IAF: http://alt.iaf-bs.de/projects/3GLTE-mimo-ofdm-testbed.en.html.

[35] Larouche, J.-B. (2013, 06 13). *Alamouti Space-Time Block Coding*. Retrieved 2013, from nutaq: http://nutaq.com/en/blog/alamouti-space-time-block-coding.